Hybrid Multi-Access Protocols for Real-Time Transmission and Power Conservation in Wireless Networks

by

Zi-Tsan Chou©

Advisor: Professor **Ching-Chi Hsu**

Professors **Ferng-Ching Lin** and **Tei-Wei Kuo**

DISSERTATION

Submitted in partial fulfillment of the requirements for

the degree of Doctor of Philosophy in

Department of Computer Science and Information Engineering at

National Taiwan University, Taipei, Taiwan

July 4, 2003

Abstract

In this dissertation, we propose several novel hybrid medium access control (MAC) protocols for infrastructure and ad hoc wireless networks. The first part presents real-time MAC protocols and the second part presents the energy-conserving MAC designs.

For topology-transparent deterministic broadcast in a TDMA-based MANET, we have the following results. (i) We first present the dimension-combination broadcasting (DCB) algorithm for a single-channel MANET, which achieves an exponential order improvement in terms of broadcast completion time, as compared with the polylogarithmic broadcast algorithm. (ii) On the basis of DCB, we then propose several different multi-channel broadcast algorithms for different network environments. In contrast with single channel systems, the frame length is significantly reduced in multi-channel systems. With the additional support of GPS and the transceivers with tunable transmission range, the maximum tolerable network degree is also highly promoted. (iii) All our proposed algorithms are simple and easily implementable in a fully distributed manner. Most importantly, we guarantee that, for all our proposed protocols, there are no redundant transmission rounds in a frame. It implies that, in terms of bandwidth and energy consumption, our solutions reach the efficient performance.

For MAC-level reliable broadcast in a multi-channel MANET, we have the following results. (i) We propose an adaptive location-aware broadcast (ALAB) protocol which supports reliable unicast, multicast, and broadcast transmission services in an integrated manner. (ii) ALAB is scalable and topology-transparent since both the time to broadcast a packet and the number of channels required are independent of the network topology. (iii) In ALAB, all the deadlock, starvation, hidden and exposed terminal problems are completely eliminated. (iv) ALAB is a merger of condensed TDMA and tree-splitting algorithms. At high traffic or density, it outperforms the pure TDMA because of spatial reuse and dynamic slot management.

At low traffic or density, it outperforms the pure CSMA/CA because of its embedded stable tree-splitting algorithm. Above all, even under the fixed-total-bandwidth model, ALAB delivers superior performance than IEEE 802.11, ADAPT, and ABROAD.

For polling-based MAC protocol in a wireless multimedia LAN, we have the following results. (i) We tailor the IEEE 802.11 PCF operation so that our new protocol, named Q-PCF (quality-of-service PCF), can coexist with IEEE 802.11 DCF, while providing QoS guarantees to real-time multimedia applications. (ii) Q-PCF supports multiple priority levels and guarantees that high-priority stations always join the polling list earlier than low-priority stations. (iii) Q-PCF provides fast reservation scheme such that real-time stations can get on the polling list in bounded time. (iv) Q-PCF employs dynamic bandwidth allocation scheme to support CBR/VBR transportation and provide per-flow probabilistic performance assurances. (v) Q-PCF adopts the novel mobile-assisted admission control technique so that the access point can admit as many newly flows as possible, while not violating admitted flows' guarantees. (vi) We believe that the Q-PCF protocol can be easily applied to the current IEEE 802.11 products without major modifications.

For power-saving MAC protocols in an asynchronous MANET, we have the following results. (i) We propose a new beacon transfer procedure, which is scalable and insensitive to the number of contending stations. (ii) Three proposed randomized power saving protocols achieve correct neighbor maintenance in asynchronous environments with high probability. Especially, our solutions offer the network designers full flexibility in trading energy, latency, and accuracy accuracy versus each other by appropriately tuning the protocol parameters. (iii) Compared with the grid quorum-based protocol, the interleaving cyclic finite projective plane-based protocol always guarantees a 100% neighbor discovery probability while obtaining a nearly 75% reduction in radio active ratio under about the same energy-delay product. Therefore, it is suitable for energy-limited applications. (iv) We believe that our protocols can be applied to the current IEEE 802.11-based wireless LAN cards with little modification.

Contents

List of Figures

List of Tables

Chapter 1

Introduction

1.1 Background

1.1.1 Network Architecture

With the progress of wideband radio technologies and the proliferation of portable computers, wireless networks are emerging as an attractive alternative or complementary to wired networks because of cost effectiveness, ease of installation, and tether-free access to the Internet. Based on the network architecture, wireless networks can be approximately divided into two classes: ad hoc networks and infrastructure networks [48].

- *Ad hoc networks*: A mobile ad-hoc network (MANET) is an autonomous system of mobile hosts capable of communicating with each other by wireless links without the assistance of base stations. The applications of the MANET are getting more and more important, especially in the emergency, military, entertainment, and outdoor business environments, in which instant fixed infrastructure or centralized administration is difficult or too expensive to establish.

- *Infrastructure networks*: An infrastructure network typically consists of a central base station, also known as an access point, and a finite set of associated mobile stations. Through the access point, mobile users can easily access the Internet resources. Moreover, by allocating a number of adjacent access points in a limited area, the extended infrastructure network can provide the seamless roaming service for mobile users.

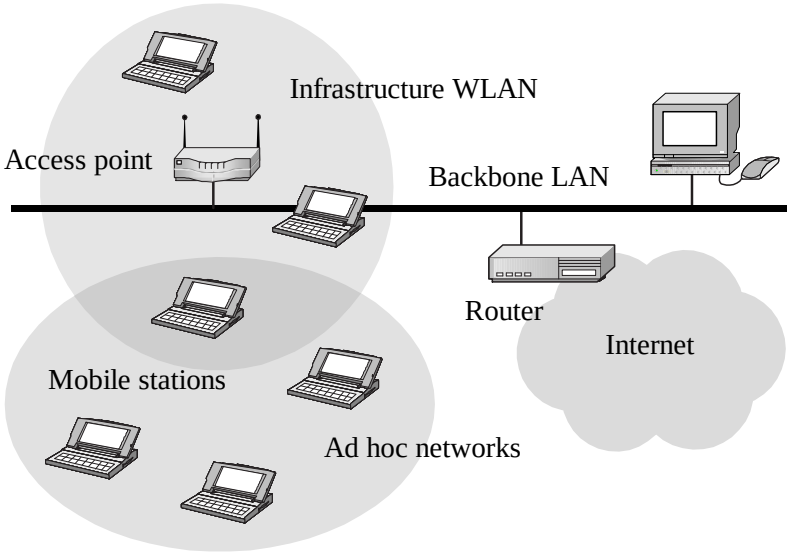

Figure 1.1: Example of infrastructure and ad hoc networks.

Figure 1.1 shows a common wireless network deployment which includes infrastructure and ad hoc networks.

1.1.2 Multiplexing

In wireless network environments, medium is basically shared; and multiple simultaneous transmissions will result in garbled data, making communication impossible. Multiplexing specifies how several stations can share a medium without interference. For wireless communication, multiplexing can be carried out in three dimensions: time, channel, and space. The definitions of these multiplexing schemes are described as follows.

- *Time Division Multiple Access* (TDMA): In TDMA, all stations usually transmit data on the same channel, but their transmissions are separated in time. Further, time is divided into frames of fixed duration, and each frame is divided into a fixed number of time slots. Each station limits its transmission to a single slot. Since two transmission overlapping in time will result in co-channel interference, TDMA requires clock synchronization and the guard time between two frames.

- *Channel Division Multiple Access*: The concept of this scheme is to divide the available bandwidth of a single medium into a number of orthogonal or independent chan-

nels. Physically, wireless channels can be realized by different carrier frequencies or by different orthogonal codes. Thus in our definition, channel division multiple access includes FDMA (frequency division multiple access) and CDMA (code division multiple access). In FDMA/CDMA, each station is allocated its own channel spectrum, and these channels shall be separated by guard channel to avoid adjacent channel interference.

- *Space Division Multiple Access* (SDMA): Due to transceiver hardware capacity, battery power conservation, and network capacity enhancement, mobile stations have limited transmission ranges. If pair of mobile stations using the same channel are located far enough, then their transmissions can be initiated simultaneously without suffering collisions. Hence in SDMA, distant stations are allowed to send data on the same channel at the time. Note that the space between the interference range is called the guard space.

1.1.3 Wireless MAC Issues

On the basis of multiplexing, the media access control (MAC) protocol specifies how and when stations coordinately access to the shared medium such that they can communicate with each other in an orderly and efficient manner. Although wireless networks offer mobile users greater flexibility and convenience than wired counterparts, they also introduce several new technological challenges/constraints [8, 13, 18, 19, 65].

- *Scarce Resources*: In wireless systems, two key resources–bandwidth and energy–are more severely limited as compared with wired networks. Due to technology limitations, the radio bandwidth and battery capacity may not be dramatically promoted in the not-so-distant future.

- *Half-Duplex Operation*: In wireless networks, a radio unit cannot transmit and receive simultaneously since when transmitting, a large fraction of the signal energy leaks into the receive path. The leakage signal typically has much higher power than the received signal, which makes it impossible to detect a collision event while transmitting data.

- *Location-Dependent Carrier Sensing*: In the wireless medium, because of multipath propagation, signal strength decays according to a power law with distance, carrier sensing is a function of the position of the receiver relative to the transmitter. Therefore, all carrier sense multiple access (CSMA)-based protocols will face four problems [65]: capture effect, hidden terminal, exposed terminal, and near-far problems.

- *Timing synchronization*: In an infrastructure WLAN, the base station or access point can periodically broadcast beacon frames to realize clock synchronization. However, in a large-scale MANET, it is extremely difficult (if not impossible) for all nodes to keep synchronized at all times because of severe beacon contention, unpredictable node mobility, and heavy traffic of timing information exchange.

Undoubtedly, designing a practical MAC protocol for wireless networks shall seriously take the above-mentioned constraints into consideration. Although the primary objective of a MAC protocol is to maximize the throughput while minimizing the access delay, a decent wireless MAC protocol shall also possess the following advanced features [8, 13, 18, 19, 20].

- *Topology Transparency*: This metric is especially important for ad hoc networks. A MAC protocol relying on correct neighborhood knowledge requires to gather and maintain link state information. However, the ability to maintain link state information hinges on the operation of the MAC protocol itself. Since the network topology may change quickly, frequently, and unpredictably, a topology-dependent MAC protocol is thus not stable and completely unsuitable for ad hoc networks.

- *Reliable Broadcast*: Obviously, a single reliable MAC broadcast can be implemented by sending one or more reliable unicast messages. However, this approach is not scalable since the time to complete a broadcast increases with the number of neighbors. On the other hand, a MAC protocol with reliable broadcast support will be of great benefit to the routing function, multicasting applications, cluster management, and real-time applications.

- *Real-Time Transmission*: With the convergence of voice, video, and data networks, it is now necessary for MAC protocols to provide quality-of-service (QoS) guarantees for real-time traffic support. A priority MAC protocol can support real-time transmission

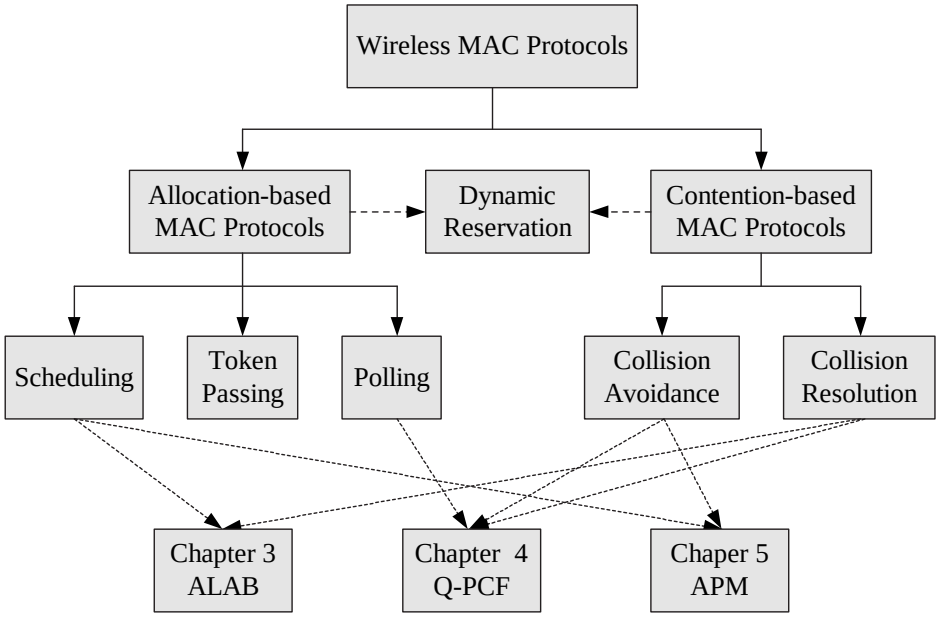

Figure 1.2: Classification of wireless MAC protocols.

by allowing the highest-priority station to seize the medium earlier than lower-priority stations.

- *Energy Conservation*: It is well known that, due to technology limitations, the battery capacity will not be dramatically improved in the not-so-distant future. Therefore, it is essential to investigate power saving MAC protocols to prolong the lifetime of both individual nodes and the network.

1.1.4 MAC Protocol Classification

As shown in Figure 1.2, wireless MAC protocols proposed so far can be approximately classified into two categories [8, 18, 44]. One is allocation-based protocols, and the other is contention-based protocols. Allocation-based protocols, such as TDMA and polling, are primarily designed to support bounded access delay and scheduled bandwidth utilization. Nevertheless, these protocols are insensitive to variations in network loads or topology connectivity. As to the contention-based protocols, such as CSMA-based and ALOHA-based protocols, they are primarily designed to support asynchronous data transfer. However, these protocols may not be stable especially when contending traffic is heavy. We believe that a hy-

brid (reservation-based) MAC protocol that merges both of the advantages of the allocation- and contention-based protocols and overcomes their individual drawbacks is a better candidate for wireless networks. Figure 1.2 indicates that several hybrid protocols are proposed in this dissertation. In Chapter 3, we propose the ALAB protocol which combines the condensed TDMA and tree-splitting (collision resolution) algorithm. In Chapter 4, we propose the Q-PCF protocol which combines DCF (collision avoidance), tree-splitting algorithm, and polling-based protocol. In Chapter 5, we propose the ASP (asynchronous power management) protocols which combines DCF and awake/sleep pattern scheduling algorithm. Importantly, these hybrid protocols significantly improve the functions and performance of the IEEE 802.11.

1.1.5 IEEE 802.11 Overview

Since November 1999, the IEEE 802.11 task group have defined two international wireless MAC standards [48]: the distributed coordination function (DCF) for ad hoc networks and the point coordination function (PCF) for infrastructure WLANs. In what follows, we briefly review the DCF and PCF. For a more complete and detailed presentation, please refer to the IEEE 802.11 standard [48].

- *Distributed Coordination Function* (DCF): The DCF employs *carrier sense multiple access with collision avoidance* (CSMA/CA) strategy to provide asynchronous data service. When a station desiring to access the medium shall first sense the channel to determine whether the medium is busy. If the medium is busy, that station shall first defer until the medium is determined to be idle for an interval equal to DIFS (Distributed InterFrame Space) and then perform the *binary exponential backoff* procedure. This is because just after the medium becomes idle following a busy medium is when the highest probability of a collision exists. By standard, the backoff time is defined as

$$\mathrm{BackoffTime} = \mathrm{SlotTime} \times \mathcal{U}[\,0,\,(\mathrm{CW}_{min}+1)\times 2^{NumAtt}-1\,], \qquad (1.1)$$

  where CW_{min} denotes the minimum contention window and $NumAtt$ denotes the number of retransmission attempts. Note that the function $\mathcal{U}[0,\,\mathrm{CW}]$ returns an integer drawn from a uniform distribution over the set $\{0, 1, \cdots, \mathrm{CW}\}$, where $\mathrm{CW}_{min} \leq$

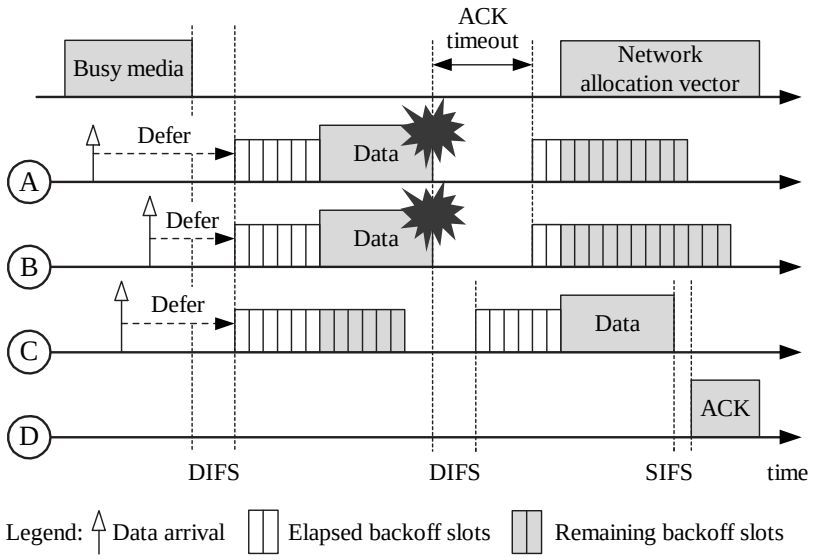

Figure 1.3: Example of DCF operation. Since the medium is determined busy, stations A, B, C defer until the end of the current transmission. Unluckily, stations A and B select the same backoff time, their transmissions thus collide; and their backoff procedure can restart only after the end of the ACK timeout interval. As soon as C's backoff timer expires, station C sends the data frame to station D. Luckily, no collision occurs at this time. Hence station D acknowledges its receipt after an elapsed SIFS.

$\mathrm{CW} \leq \mathrm{CW}_{max}$. The backoff timer is decremented as long as the channel is sensed idle. To ensure fairness among DCF stations, if the medium is determined busy at any time during a backoff slot, then the backoff timer shall be *frozen*. When the channel is sensed idle again for more than a DIFS, the backoff timer can be reactivated. Whenever the backoff timer reaches zero, transmission shall commence. The effect of this procedure is that when multiple stations enter the backoff stage at the same time, then the station choosing the minimum backoff time will win the contention. To ensure reliability, the directed data frame will announce the *network allocation vector* (NAV) through the Duration field to reserve the channel. Any contending stations hearing the NAV shall suppress its transmitting activity until the NAV decreases to zero or is reset via the ACK frame. Upon reception of the data frame, the destination station shall reply the ACK frame after an elapsed SIFS (Short InterFrame Space). Note that $\mathrm{SIFS} < \mathrm{DIFS}$. If the sending station does not hear the ACK signal, it shall resend the data frame after waiting at least an ACK timeout interval or drops that frame when the

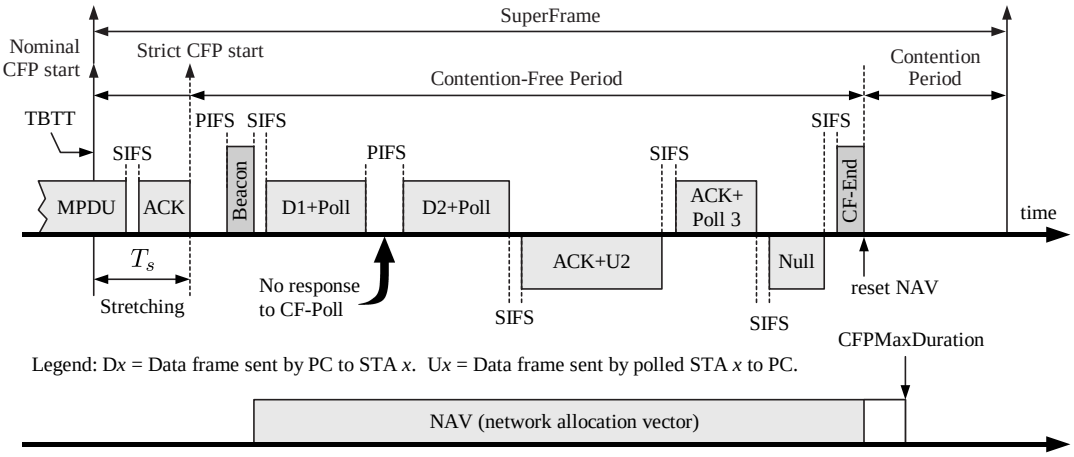

Figure 1.4: Example of PCF operation. To bandwidth efficiency, the PC utilizes a single frame to send data and CF-Poll to station 1. However, station 1 makes no response. After an elapsed PIFS, the PC polls the next station. Finally, when station 3 polled by the PC, it perceives that time is not enough to send its queued MPDU before the end of the CFP. Thus station 3 responds a *Null* frame and set the *more data* bit to 1 to allow the PC to distinguish between an empty queue and a response due to insufficient time to transfer an MPDU.

DCF retry limit is reached. Figure 1.3 illustrates the DCF operation.

- *Point Coordination Function* (PCF): As shown in Figure 1.4, when a *point coordinator* (PC) is operating in a WLAN, the two coordination functions alternate with each other. The contention-free period (CFP), during which the PCF is active, and the following contention period (CP), during which the DCF is active, are together referred to as a *contention-free repetition interval* or *superframe*. The minimum length of the contention period (CP) must be long enough for the delivery of one maximum-size MAC protocol data unit (MPDU) and its associated ACK. At the nominal start of each CFP (also known as *TBTT*), the PC shall sense the medium. After waiting a PIFS (Priority InterFrame Space) medium idle time, the PC seizes control of the medium by broadcasting a beacon frame and announcing the NAV. Note that $\mathrm{SIFS} < \mathrm{PIFS} < \mathrm{DIFS}$. On the other hand, it is possible for contention-based service runs past the TBTT. In the case of a busy medium due to DCF traffic, the CFP is *foreshortened* and the beacon should be delayed for the time (T_s) required to complete the existing DCF frame exchange. Such a phenomenon is called *stretching* and we depict the stretching event

in Figure 4.3. To lock out DCF-based access, all stations receiving the beacon shall update their NAV to the maximum duration, CFPMaxDuration. After gaining control of the medium, the PC polls associated stations on the *polling list* in a round-robin manner. The CFP may either last until the CFPMaxDuration has elapsed since TBTT, or be ended prematurely by the PC broadcasting a CF-End frame, if all stations on the polling list have been polled. To improve efficiency, acknowledgements (CF-ACK) and polls (CF-Poll) may be *piggybacked* on data frames. Note that, during the CFP, if a polled station makes no response to the CF-Poll, then the PC polls the next station on its polling list after an elapsed PIFS. By this way, the PC ensures that it retains control of the medium and resists the DCF-based interference. Figure 1.4 illustrates the PCF operation.

1.2 Our Contributions

This dissertation presents novel energy conserving designs and real-time multi-access protocols for infrastructure and ad hoc wireless networks. Specifically, we focus our attention to the following issues. (i) Topology-transparent deterministic broadcasting for multi-hop ad hoc networks. (ii) Adaptive location-aware MAC protocols for reliable broadcast support in multi-channel ad hoc networks. (iii) The polling-based MAC protocol with priority reservation and dynamic bandwidth allocation mechanisms to support multimedia applications with QoS requirements. (iv) Randomized power management protocols with flexible neighbor maintenance for asynchronous ad hoc networks.

For topology-transparent deterministic broadcast in a TDMA-based MANET, we have the following results [17]. (i) We first present the dimension-combination broadcasting (DCB) algorithm for a single-channel MANET, which achieves an exponential order improvement in terms of broadcast completion time, as compared with the polylogarithmic broadcast algorithm [4]. (ii) On the basis of DCB, we then propose several different multi-channel broadcast algorithms for different network environments. In contrast with single channel systems, the frame length is significantly reduced in multi-channel systems. With the additional support of GPS and the transceivers with tunable transmission range, the maximum tolerable network degree is also highly promoted. (iii) All our proposed algorithms

are simple and easily implementable in a fully distributed manner. (iv) Most importantly, we guarantee that, for all our proposed protocols, there are no redundant transmission rounds in a frame. It implies that, in terms of bandwidth and energy consumption, our solutions reach the efficient performance.

For MAC-level reliable broadcast in a multi-channel MANET, we have the following results [18]. (i) We propose an adaptive location-aware broadcast (ALAB) protocol which supports reliable unicast, multicast, and broadcast transmission services in an integrated manner. (ii) ALAB is scalable and topology-transparent since both the time to broadcast a packet and the number of channels required are independent of the network topology. (iii) In ALAB, all the deadlock, starvation, hidden and exposed terminal problems are completely eliminated. (iv) ALAB is a merger of condensed TDMA and tree-splitting algorithms. At high traffic or density, it outperforms the pure TDMA because of spatial reuse and dynamic slot management. At low traffic or density, it outperforms the pure CSMA/CA because of its embedded stable tree-splitting algorithm. Above all, even under the fixed-total-bandwidth model, ALAB delivers superior performance than IEEE 802.11, ADAPT [11], and ABROAD [13].

For polling-based MAC protocol in a wireless multimedia LAN, we have the following results [20]. (i) We tailor the PCF operation so that our new protocol, named Q-PCF (quality-of-service PCF), can coexist with IEEE 802.11 DCF [48], while providing QoS guarantees to real-time multimedia applications. (ii) Q-PCF supports multiple priority levels and guarantees that high-priority stations always join the polling list earlier than low-priority stations. (iii) Q-PCF provides fast reservation scheme such that real-time stations can get on the polling list in bounded time. (iv) Q-PCF employs dynamic bandwidth allocation scheme to support CBR/VBR transportation and provide per-flow probabilistic performance assurances. (v) Q-PCF adopts the novel mobile-assisted admission control technique so that the access point can admit as many newly flows as possible, while not violating admitted flows' guarantees. (vi) We believe that the Q-PCF protocol can be easily applied to the current IEEE 802.11 products without major modifications.

For power-saving MAC protocols in an asynchronous MANET, we have the following results [19]. (i) We propose a new beacon transfer procedure, which is scalable and insensitive to the number of contending stations. (ii) Three proposed randomized power saving protocols achieve correct neighbor maintenance in asynchronous environments with high

Feature	Theme	Core Technique	Environment
Real-Time Transmission	Chapter 2: Topology-Transparent TDMA-based Broadcast	Dimension-Combination Splitting Tree	Multi-Hop MANET
	Chapter3: Location-Aware MAC Protocols for Reliable Broadcast	First-Success Dimension Splitting Tree	Multi-Channel MANET
	Chapter 4: Quality-of-Service Point Coordination Function	Depth-First-Traversal Dimension Splitting Tree	Infrastructure WLAN
Power Conservation	Chapter 5: Power Management Protocols	Cyclic Finite Projective Plane	Asynchronous MANET

Figure 1.5: The relationships among each chapters. The first part (Chapter 2 $\sim$ Chapter 4) deals with the real-time transmission issues. The second part presents energy-conserving designs.

probability. More specifically, our solutions offer the network designers full flexibility in trading energy, latency, and accuracy accuracy versus each other by appropriately tuning the protocol parameters. (iii) Compared with the grid quorum-based protocol [78], the interleaving cyclic finite projective plane-based protocol always guarantees a 100% neighbor discovery probability while obtaining a nearly 75% reduction in radio active ratio under about the same energy-delay product. Therefore, it is suitable for energy-limited applications. (iv) We believe that our protocols can be applied to the current IEEE 802.11-based wireless LAN cards with little modification.

1.3 Dissertation Organization

The remainder of this dissertation is organized as follows. The first part (Chapter 2 $\sim$ Chapter 4) deals with the real-time transmission issues and the second part (Chapter 5) presents energy-conserving designs. We can see that from Figure 1.5 that the core techniques used to achieve real-time transmission support are the constructions of various *dimension splitting trees*. Chapter 2 employs the dimension-combination tree splitting technique to develop

deterministic topology-transparent broadcast algorithms for multi-hop MANETs. Chapter 3 employs the first-success dimension-tree splitting technique to develop location-aware MAC protocols with reliable broadcast support for multi-channel MANETs. Chapter 4 employs the depth-first-traversal dimension-tree splitting technique to develop the Q-PCF protocol for IEEE 802.11 wireless multimedia LANs. Chapter 5 employs the cyclic finite projective plane technique to develop asynchronous power management protocols for IEEE 802.11 ad hoc networks. Chapter 6 concludes the dissertation results and points out possible future research directions.

Chapter 2

Topology-Transparent Broadcast for Multi-Hop MANET

2.1 Introduction

A mobile ad-hoc network (MANET) is an autonomous system of mobile hosts capable of communicating with each other by wireless links without the assistance of base stations. For the sake of battery power conservation and network capacity enhancement, a host may not be able to communicate directly with others in a single-hop manner. In this case, all message communication between them must pass through one or more intermediate hosts that double as routers. Since a MANET is characterized by energy-constrained mobile nodes, bandwidth-constrained links and unpredictably dynamic topology, every algorithm and protocol developed on it will face many great challenges. In this chapter, we are specially interested in a *broadcast* problem for ad-hoc networks in TDMA (*time-division multiple-access*) systems with multiple frequency channels.

Broadcast is the task of delivering a single identical message $\mathcal{M}$ from a particular source node to all the other nodes in the network. Several broadcast protocols for ad-hoc networks have been proposed, including centralized solutions [14, 28] and randomized solutions [3, 47, 51]. Although centralized protocols are deterministic and optimal in terms of time complexity, it is extremely difficult (if not impossible) that every nodes in the MANET must know and maintain the entire network topology information. As to the randomized pro-

tocols, they are not preferable if a prior known bound on the maximum delay is the necessary requirement for real-time systems or multimedia applications [4]. Broadcast protocols working with the partial network knowledge can be found in [12, 45, 61]. However, the efficiency, robustness, and stability of these protocols will become questionable when mobility is high and topology changes quickly and frequently, due to heavy loads on updated broadcast spanning trees or clusters information maintenance.

The authors in [4] proposed the first distributed *mobility-transparent deterministic* broadcast algorithm for TDMA-based ad-hoc networks. Their broadcast protocol called the *poly-logarithmic broadcast* (PB, for short) algorithm has many attractive properties. First, the accuracy of their broadcast protocol is always guaranteed independently of the current node's neighbors and of their rates of mobility. Each node computes its own transmission schedule depending only on the network size and the maximum degree, not depending on any knowledge of the network topology or the identity of the neighbors. Each node can deterministically specify the slots of the frame, in which the node is allowed to transmit a message. Therefore, no computational overhead is associated with the transmission of a message and no periodical recomputation of the transmission schedule is needed. In addition, a prior known bound on the maximum delay for broadcast completion time can be determined in advance. These make it attractive and suitable for multimedia applications in high mobility environments. Certainly, the shorter the frame length, the more efficient the protocol.

However, the PB algorithm still suffers some drawbacks. First, given an ad-hoc network with n nodes and the maximum degree Δ, it generates $(h! - 1)2^h\binom{\log n}{h} \in \Omega((\log n - h)^h)$ unnecessarily redundant transmission rounds in each frame, where $h = \lfloor \log \Delta \rfloor$. All these redundant transmissions not only severely waste battery power and increase the broadcast time, but also consume scarce bandwidth in wireless radio links. Besides, they may bring on hot spots, contention, and congestion in communications [60]. Second, it is only suitable in a very sparse network; that is, even the network degree Δ is very small, the PB algorithm will be compelled to switch to the *linear broadcast* (LB, for short) algorithm [4], which is the worst case choice. Finally, in order to compute the allowable transmission rounds in a frame, every nodes need to execute functions $Find\_Rounds$ and Get_The_Rounds [4]; however, the time complexity of them are about $\Theta(h!)$ times that of ours.

Motivated by these reasons, we propose the *dimension-combination broadcast* (DCB,

for short) algorithm. Compared with the PB algorithm [4], the DCB algorithm completely solves the serious redundant transmission problem. It implies that our broadcast algorithm is faster and consumes less energy and bandwidth resources. The frame length is dramatically reduced from $L = h!2^h\binom{\log n}{h}$ (by their PB protocol) to $\frac{L}{h!} = 2^h\binom{\log n}{h}$ (by our DCB protocol), where n is the total number of nodes. As far as the frame length is concerned, DCB achieves an *exponential* order improvement over PB. Finally, even their PB algorithm fails when the network degree exceeds the threshold $2^{\lfloor \log n/\log\log n+1\rfloor+1} - 1$, our algorithm still works well. The maximum tolerable network degree by the DCB algorithm is approximately two to eight times that by their PB algorithm for $n \leq 2^{29}$.

We also notice that the existing works have focused only on single channel systems. In literature [10, 25, 41, 80], we know that a multi-channel system outperforms a single channel system in many aspects, including throughput, reliability, bandwidth utilization, network scalability, synchronization implementation, admission control, and QoS support. Physically, these channels can be realized by different carrier frequencies in FDMA systems or by different orthogonal codes in CDMA systems. Importantly, if the algorithm [4] for a single channel system does not design carefully, it may not be an easy task to extend the work to solve a multi-channel problem. In this chapter, on the basis of DCB, we then propose several different multi-channel broadcast algorithms with multiple reception capacity for different network system environments. In contrast with single channel systems, the frame length is significantly reduced in multi-channel systems. With the additional support of GPS and the transceivers with tunable transmission power/range ability, the maximum tolerable network degree is also highly promoted. Location information has been exploited in several issues in the MANET such as routing [40] and random media access control [62, 80], but none of any previous works explore for the broadcast problem in TDMA networks. All our proposed algorithms are simple and easily implementable in a distributed way. Network designers can decide which of the algorithms is preferred according to the network equipment and global parameters such as the network size, the channel number, and the maximum degree. Finally, we guarantee that, for all our proposed protocols, there are no redundant transmissions in a frame. It implies that, in terms of energy and bandwidth consumption, our solutions reach the efficient performance.

The remainder of this chapter is organized as follows. In Section 2, the necessary prelim-

inaries are given. In Section 3, we present and analyze the DCB algorithm for single channel systems. Based on the DCB algorithm, three non-location-aware multi-channel broadcast algorithms are proposed in Section 4. In Section 5, we present two location-aware multi-channel broadcast algorithms. In Section 6, we summarize our results and conclude the chapter.

2.2 Preliminaries

2.2.1 Definitions and The Model

A multihop mobile radio network used to pass messages containing data and control information can be modelled as an undirected graph $G = (V, E)$ in which V, $|V| = n$, is the set of mobile hosts and there is an edge $(u, v) \in E$ if and only if u and v are in the transmission range of each other. In this case, we say that u and v are neighbors. The edge set may *vary* over time because of nodal mobility. The set of the neighbors of a node v is $N(v) = \{u|(u, v) \in E\}$ and $|N(v)|$ is the degree of v. The degree of the network G is denoted by $\Delta = \max\{|N(v)| \mid v \in V\}$. The distance $d(u, v)$ between u and v is defined as the minimum number of hops between u and v. The maximum distance between any two vertices of G is called the diameter D of the network. Given the source s of a message, all the nodes v such that $d(s, v) = \ell \leq D$ are said to belong to the ℓth layer of the network, where $0 \leq \ell \leq D$. We assign each node v in the network a unique identifer (ID) by a number in $\aleph = \{0, 1, \ldots, n-1\}$, where $|\aleph| = n$. Each channel is uniquely assigned by a number in $\mathcal{H} = \{0, 1, \ldots, \rho - 1\}$, where $1 \leq \rho < n$.

In this chapter, the multi-channel TDMA network model is assumed by following the same model as defined in [41]. The transmission time on each channel is divided into time slots (or *rounds*), which are in turn grouped into *frames*. Nodes in the network are assumed to be synchronized and that the round length is the same for each node. Each mobile radio host in a multi-channel network is equipped with the transceivers (a single transmitter and multiple receivers). Depending on the ability of the transceivers, each node can communicate with others either in the full-duplex mode or in the half-duplex mode. In the full-duplex mode, each host can transmit only one packet on one channel but receive multiple packets

on all channels in one slot simultaneously [41]. However, in the half-duplex mode, each host cannot transmit and receive at the same time [3, 10]. On a single channel, two types of communication collisions will arise [10, 25, 41]. The primary collision occurs when a node transmitting in a given slot is receiving in the same slot on the same channel. This also implies the converse: a receiving node cannot be transmitting on the same channel at the same time. The secondary collision occurs when node receives more than one packet in a slot on the same channel. In both cases, all packets are rendered useless. All these facts imply that only the half-duplex mode is allowed in single channel systems. To this end, we assume that if more than one nodes is transmitting on the same channel such that the packets overlap in time, then collision occurs on that channel. On the other hand, simultaneous reception of packets on other channels is not affected.

To deal with the broadcast problem, we need the following definitions and assumptions relative to the *conflicting set*. They are already established in [4], but we include them here for completeness.

Definition 2.2.1. [4] During the broadcast process, the nodes that in a given round have received a message $\mathcal{M}$ are said to be *covered* by the broadcast. The nodes that have not received $\mathcal{M}$ are said to be *uncovered*. Given a node v, $N_{\mathcal{C}}(v)$ denotes its covered neighbors and $N_{\mathcal{U}}(v)$ indicates its uncovered neighbors.

Definition 2.2.2. [4] A set R of covered nodes is a *conflicting set* when there is at least a neighbor common to all the nodes in R that has not received a message from them yet; namely, $\cap_{v \in R} N_{\mathcal{U}}(v) \neq \emptyset$.

We also comply with the following assumptions made in [4]. (1) At least one node in the MANET from a conflicting set remains in the transmission range of any neighboring uncovered node. (2) During the entire broadcast process, the network is required always to be *connected*. In other words, each uncovered node in the network must be able to receive a message.

The authors in [4] have proposed the deterministic distributed broadcast protocol for single channel multihop networks. Here we only slightly adjust their protocol description such that it can be adapted in multi-channel environments. The multi-channel protocol Π executed at each node in the network is in the following way.

1) The broadcast starts from the source's initiation at round 0 and is completed at round t if all nodes have correctly received the message $\mathcal{M}$ at one of the round $0, 1, 2, ..., t$.

2) Depending on the transceivers and the requirements of the protocols, every nodes communicate either in the half-duplex mode or in the full-duplex mode. However, in multi-channel systems, we assume every nodes work in the full-duplex mode unless additional statements. A node receives a message $\mathcal{M}$ in a specific round, if and only if, $\mathcal{M}$ is transmitted by *any* one of its neighbors on a channel without collision.

3) The action of a node in a specific round is deterministically established by its initial input; namely, its own ID my_ID, the total number of channels ρ, the total number of nodes n, and the degree of the network Δ. With the support of GPS, input of the location-aware protocols may include additionally updated location information $(x, y) \in \Re^2$.

4) Every node in the MANET during the entire broadcast process that has moved from an uncovered neighbors to a covered one must at some time be the neighbor of a node which has already received the broadcasted message $\mathcal{M}$, and will receive $\mathcal{M}$ from it [4] using a failsafe recovery procedure such as in [58, 69].

The broadcast thus proceeds according to a two-dimensional transmission schedule $L_\Pi = \langle T_1, T_2, \ldots, T_t \rangle$. Each transmission set $T_i = \{(v, j) | v \in \aleph \text{ and } j \in \mathcal{H}\}$ is composed of the set of two-tuples. Each element $(v, j) \in T_i$ specifies that the node $v \in \aleph$ acts as a (potential) transmitter on channel $j \in \mathcal{H}$ in round i, where $1 \leq i \leq t$.

2.2.2 General Broadcast Scheme

We slightly revise the general broadcast scheme proposed in [4] to make it suitable for multi-channel systems. Table 2.1 shows the scheme It is noteworthy that, by this scheme, multiple concurrent broadcasts are allowed [4]. Each node that either generated or received a message $\mathcal{M}$ is allowed to transmit it on a channel only in certain rounds in a frame. The node calculates these slots (at the set up of the network, or any time the number of the nodes in the network changes) by means of the $Round\_Numbers$ procedure. The set

Table 2.1: General multi-channel broadcast scheme.

PROCEDURE $Round\_Numbers(n, \Delta, \rho)$;
begin
$Transm = Get\_The\_Rounds(n, \Delta, \rho)$;
end;

$Transm = \{(i, j)|1 \leq i \leq L$ and $j \in \mathcal{H}\}$ is composed of the set of two-tuples. Each element $(i, j) \in Transm$ indicates that in round i, the node is allowed to transmit a message on channel j. The set $Transm$ is obtained by scheduling, in a deterministic way, the transmissions of the covered nodes to guarantee the correct delivery of the message independently of the possibility of collisions. Furthermore, it remains unchanged in each frame, regardless of changes in the network topology. Therefore, no computational overhead is associated with a message and no periodical recommputation of transmission schedule is needed.

It has been shown [4] that this scheme fulfills the broadcast of the message $\mathcal{M}$ in a layer by layer fashion. In other words, each node v such that $d(s, v) = \ell$ transmits $\mathcal{M}$ issued by the source node s after $\mathcal{M}$ has been transmitted by all the nodes in the layer $\ell - 1$ and before each node in the layer $\ell + 1$ will transmit it, $0 \leq \ell \leq D$. The broadcast completion time is thus bounded by $t \leq DL$ rounds as long as the function *Get_The_Rounds* can correctly forward the message from a given layer to the subsequent one in the L rounds of a frame.

2.2.3 Multichannel Linear Broadcast

In this subsection, we propose a simple broadcast algorithm called the *multi-channel linear broadcast* (MLB, for short) algorithm that achieves the above-mentioned requirements and properties. The detailed description is shown in Table 2.2. The node $i \in \aleph$ is allowed to transmit in round $1 + \lfloor i/\rho \rfloor$ using channel i mod ρ. For each channel, at most one node is allowed to transmit in each round in a frame, thus no collision can ever occur. When $\rho = 1$, MLB is reduced to the linear broadcast algorithm [4]. Consider a multihop network with n

Table 2.2: Multichannel linear broadcast algorithm.

FUNCTION $Get\_The\_Rounds(n, \Delta, \rho)$: $(round, channel)$;
begin
    output ($1 + \lfloor \text{my\_ID}/\rho \rfloor$, my_ID mod ρ);
end;

nodes, the frame length of the MLB protocol is $L_1 = \lceil n/\rho \rceil$. The broadcast completion time is hence bounded by $D\lceil n/\rho \rceil$.

In many normal circumstances, for some channels, by allowing more than one node to transmit in a round, we can still guarantee the mobility independence property while correctly forwarding the message. The broadcast time can therefore be shorten. It is clear that, unless the network is too dense, the MLB algorithm is the worst case choice. We can attain this goal by designing the combinatorial algorithms such that the *hitting* requirements are satisfied. That is, given a transmission schedule $\langle T_1, T_2, \ldots, T_L \rangle$ of a frame and any nonempty conflicting set R, there exists at least a transmission set $T = \{(v, j) | v \in \aleph, j \in \mathcal{H}\} \in \langle T_1, \ldots, T_L \rangle$ such that either one of the following conditions is true: (1) $|R \cap V(T)| = 1$, where $V(T) = \{v | (v, j) \in T\}$. (2) $|R \cap V(T)| > 1$; however, there is only one node $v^* \in R \cap V(T)$ using the channel j^* for transmission, where $j^* \in C(T) = \{j | (v, j) \in T\}$. In this chapter, we will present novel algorithms that, given two nonempty sets of integers $\aleph$ and $\mathcal{H}$, distribute the elements of any nonempty set $R \subseteq \aleph$ in a family $\mathcal{F}$ of L subsets of $(\aleph, \mathcal{H})$ pairs, so that the hitting requirements are satisfied. In this case, we say that $\mathcal{F}$ *hits* R. This family can be regarded as the transmission sets of nodes allowed to transmit in a specific round on some specific channels, so as to always guarantee the correct delivery of a message.

Clearly, different broadcast transmission scheduling (Get_The_Rounds functions) will result in different broadcast protocols. Our chief concern in this chapter is the bandwidth-efficient Get_The_Rounds functions' design and the main objective is to minimize the frame

length constrained to given network resources.

2.3 Dimension-Combination Broadcast

In single channel networks, the authors in [4] proposed the mobility-transparent deterministic broadcast algorithm, called the polylogarithmic broadcast (PB) algorithm, for sparse network topologies. They first assign each node a unique number from the set $P = \{1, 2, \ldots, n-1, n\}$ as its ID. In order to satisfy the hitting property, they develop the combinatorial algorithm $Divide$ to partition the set of integers optimally at the bottom. Then they use the function $Smash$ from the top to divide the set P recursively. According to the degree of the network Δ, they derive the appropriate depth of the recursion to generate all transmission sets. Thereafter, they use two functions Get_The_Rounds and $Find\_Rounds$ to compute the allowable transmission rounds in a frame for each network node. However, the solution combining both of the functions $Divide$ and $Smash$ to obtain the transmission schedule in a bottom-up manner only achieves the local optimum. Because of the recursion, there are $(h! - 1)2^h\binom{\log n}{h} \in \Omega((\log n - h)^h)$ redundant transmission rounds in each frame, where $h = \lfloor \log \Delta \rfloor$. Owing to this reason, we adopt the top-down approach to develop the *dimension-combination broadcast*(DCB, for short) algorithm and elaborate on it in the sequel.

2.3.1 Definitions

Initially, each of the n stations in the MANET can be assigned a distinct ID number in the range from 0 to $n - 1$ [59]. We consider $|\aleph| = n = 2^k$ and all logarithms are assumed to be base 2. The reader will not fail to see that they are assumed for simplicity only and the general case is similar. Given an integer $v \in \aleph$, let $Binary(v) = (v_k v_{k-1} \ldots v_2 v_1)$ denote its binary string. Thus every integer in $\aleph$ can be represented by a unique binary k-tuples $(v_k v_{k-1} \ldots v_2 v_1)$, where $v_i \in \{0, 1\}$. The ith bit corresponds to the ith *dimension*. For example, $\aleph = \{0, 1, \ldots, 14, 15\}$, $v = 13 \in \aleph$, and $Binary(13) = (1101)$. We can partition the set $\aleph$ along the ith dimension into two subsets according to the value of the ith bit. For example, let $\aleph = \{0, 1, 2, 3\} = \{00, 01, 10, 11\}$. We can partition the set $\aleph$ along the first

dimension into two subsets $\{00, 10\}$ and $\{01, 11\}$.

Definition 2.3.1. Let $\mathcal{R}$ be any nonempty set of integers whose maximum element $\gamma \leq 2^k - 1$. The set $\mathcal{R}\left(\begin{smallmatrix} b_i & b_{i-1} & \cdots & b_2 & b_1 \\ p_i & p_{i-1} & \cdots & p_2 & p_1 \end{smallmatrix}\right) \subseteq \mathcal{R}$ is defined as the set in which all the p_jth bit values of the integers are equal to b_j, for all $1 \leq j \leq i \leq k$ and $b_j \in \{0, 1\}$. In other words, $\mathcal{R}\left(\begin{smallmatrix} b_i & b_{i-1} & \cdots & b_2 & b_1 \\ p_i & p_{i-1} & \cdots & p_2 & p_1 \end{smallmatrix}\right) = \{(v_k v_{k-1} \ldots v_2 v_1) \in \mathcal{R} | v_{p_i} = b_i, v_{p_{i-1}} = b_{i-1}, \ldots, v_{p_1} = b_1\}$.

For example, let $\aleph = \{0, 1, \ldots, 15\}$, then $\aleph\left(\begin{smallmatrix} 1 & 0 \\ 3 & 2 \end{smallmatrix}\right) = \{(v_4 v_3 v_2 v_1) \in \aleph | v_3 = 1, v_2 = 0\} = \{*10*\} = \{$0100, 0101, 1100, 1101$\} = \{4, 5, 12, 13\}$, where "$*$" means "*don't care*". We can partition $\aleph$ along dimensions 2 and 3 into four subsets $\aleph\left(\begin{smallmatrix} 0 & 0 \\ 3 & 2 \end{smallmatrix}\right)$, $\aleph\left(\begin{smallmatrix} 0 & 1 \\ 3 & 2 \end{smallmatrix}\right)$, $\aleph\left(\begin{smallmatrix} 1 & 0 \\ 3 & 2 \end{smallmatrix}\right)$, and $\aleph\left(\begin{smallmatrix} 1 & 1 \\ 3 & 2 \end{smallmatrix}\right)$. Given the set $\aleph = \{0, 1, \ldots, 2^k - 1\}$, it is easy to show that we can divide it along any h different dimensions into 2^h subsets and each size will be equal to 2^{k-h}, $0 \leq h \leq k$.

Definition 2.3.2. Given a nonempty set $R \subseteq \aleph$, the *feasible partition dimension set* $\mathcal{D} = \{d_1, d_2, \ldots\}$ over R is defined as the set where the bit values of the d_ith dimension of the integers in R are not all equal, for all $d_i \in \mathcal{D}$.

For example, $R = \{8, 12\} = \{$1000, 1100$\}$, then $\mathcal{D} = \{3\}$. $R = \{32, 33, 36, 37, 49, 53, 54\} = \{$100000, 100001, 100100, 100101, 110001, 110100, 110101$\}$, then $\mathcal{D} = \{1, 3, 5\}$. Note that $\mathcal{D} = \emptyset$ when $|R| = 1$.

2.3.2 Basic Idea

The idea[1] behind our broadcast protocol is to construct a full binary tree, called the *dimension partition tree*, whose root is the nonempty conflicting set R such that at least one leaf contains only one node. The internal nodes of the dimension partition tree are associated with groups of two or more nodes. According to the bit values of the binary expansion of node IDs on a specific dimension of $\mathcal{D}$, those nodes of the same height will be assigned to the left or right subtree rooted at that node. Consider $\aleph = \{0, 1, \ldots, 63\}$ and the set $R = \{32, 33, 36, 37, 49, 53, 54\} = \{$100000, 100001, 100100, 100101, 110001, 110100, 110101$\}$. In order to construct the dimension partition tree, R is first partitioned along the first dimension into two subsets $R\left(\begin{smallmatrix} 0 \\ 1 \end{smallmatrix}\right)$ and $R\left(\begin{smallmatrix} 1 \\ 1 \end{smallmatrix}\right)$, where $R\left(\begin{smallmatrix} 0 \\ 1 \end{smallmatrix}\right) = \{100000, 100100, 110100\}$

[1]This subsection is the joint work of Zi-Tsan Chou and Young-Ching Deng. See [23].

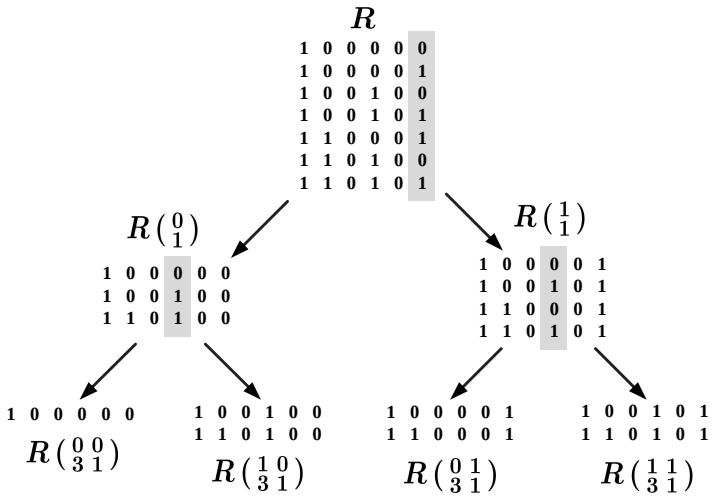

Figure 2.1: A dimension partition tree whose root is R and whose height is $\lfloor \log |R| \rfloor$.

and $R(\begin{smallmatrix}1\\1\end{smallmatrix}) = \{100001, 100101, 110001, 110101\}$. Because none of them is singleton, partition process need continue. Both of $R(\begin{smallmatrix}0\\1\end{smallmatrix})$ and $R(\begin{smallmatrix}1\\1\end{smallmatrix})$ are further divided via the third dimension. Since the size of $R(\begin{smallmatrix}0&0\\3&1\end{smallmatrix}) = \{100000\}$ is equal to one, the partition process can stop. Figure 2.1 shows the detailed partition process and its corresponding dimension partition tree of height $\lfloor \log |R| \rfloor = 2$. By observing the construction process of the dimension partition tree, we have the following lemma[2].

Lemma 2.3.1. Let $R \subseteq \aleph$ and $2^h \leq |R| < 2^{h+1}$. For each h, $0 \leq h < \log n$, we have the following results. (1) $|\mathcal{D}| \geq h$. (2) We can partition R via at most some h different dimensions from $\mathcal{D}$ into $m = 2^h$ subsets $R_1, R_2, \ldots, R_m$ such that there exists at least one set $R^* \in \{R_1, R_2, \ldots, R_m\}$ and $|R^*| = 1$.

On the basis of the dimension partition tree, we implement our *division* (partition) method by the function $Divide$ shown in Table 2.3. The job of the function $Divide(\aleph, h)$ is to partition the set $\aleph$ along all the possible h-combinations of the dimensions in the lexicographic order. Given the degree of the network Δ, the function call $Divide(\aleph, h)$ with the parameter $h = \lfloor \log \Delta \rfloor$ will return $L_2 = 2^h \binom{\log n}{h}$ subsets of $\aleph$. All these sets are composed of the transmission sets $\{T_1, T_2, \ldots, T_{L_2}\}$ of a frame. Given any nonempty conflicting set R, since $1 \leq |R| \leq \Delta$, by Lemma 3.3, the total number of dimensions used

[2]This lemma has been proven by Young-Ching Deng.

to partition R to construct its corresponding dimension partition tree will never exceed $h = \lfloor \log \Delta \rfloor$. Therefore, we can expect that after partitioning the set $\aleph$ along all the possible h-combinations of the dimensions to generate a family $\mathcal{F} \subseteq 2^{\aleph}$, there will exist at least one set, say $T \in \mathcal{F}$, such that $|T \cap R| = |R^*| = 1$. In this case, $\mathcal{F}$ hits R. For example, $\aleph = \{0, 1, \ldots, 63\}$, $R = \{32, 33, 36, 37, 49, 53, 54\}$, and $\mathcal{D} = \{1, 3, 5\}$. Let $4 \leq \Delta < 8$ and $h = \lfloor \log \Delta \rfloor = 2$. Table 2.5 shows the transmission sets $\{T_1, T_2, \ldots, T_{60}\}$ generated by $Divide(\aleph, 2)$ and their corresponding rounds. Compared with Figure 2.1 and Table 2.5, we can find that $T_5 \cap R = R \left(\begin{smallmatrix} 0 & 0 \\ 3 & 1 \end{smallmatrix}\right) = \{32\}$; namely, T_5 hits R.

2.3.3 The Algorithm

Once we have a constructive way to generate all transmission sets, the final step for the DCB algorithm is to develop the function Get_The_Rounds, through which each node can derive its allowable transmission rounds in a frame by only its ID. One advantage of our division method is that it allows us to develop Get_The_Rounds easily without explicitly computing and counting every transmission sets. Thus the algorithm time complexity can be reduced and the broadcast protocol can achieve a fully distributed way. Indeed, the DCB algorithm shown in Table 2.4 attains this goal. On the whole, we have the following theorem [23].

Theorem 2.3.1. Consider a single channel TDMA-based ad-hoc network with n nodes and the maximum degree $\Delta = 2^{h+1} - 1$, $1 \leq h < \log n$, in which each node v executes the DCB algorithm. First, the function $Divide(\aleph, h)$ returns no redundant transmission sets. Second, in a frame of length $L = 2^h \binom{\log n}{h}$, the message $\mathcal{M}$ can be correctly forwarded between any two consecutive layers. Finally, the DCB algorithm completes the broadcast within $t \leq D2^h \binom{\log n}{h}$ rounds in multihop networks with the diameter D.

In order that all nodes could be in agreement with the maximum degree Δ, the authors in [4] suggest that a separate, dedicated, out-of-band signaling is used to disseminate the information on the current network degree. Consider a multihop networks with n nodes and the maximum degree $\Delta = 2^{h+1} - 1$, $1 \leq h < \log n$. For each integer h, if the frame length $L_2 = 2^h \binom{\log n}{h}$ exceeds n, then the DCB protocol will be compelled to switch to the linear broadcast (LB, for short) algorithm. In other words, given the network size n, the maximum value of h satisfying the inequality $2^h \binom{\log n}{h} < n$ indicates *the range of the*

Table 2.3: The $Divide(\aleph, h)$ function.

FUNCTION $Divide(\aleph, h)$: Set of Transmission Sets;
begin
  for ($i = 0$; $i < h$; i++)
    set[i] = $i + 1$;
  position = $h - 1$; count=1;
  $k = \lceil \log |\aleph| \rceil$;
  while (count $\leq \binom{k}{h}$)
    begin
      for ($i = 0$; $i < 2^h$; i++)
        begin
          $b_h b_{h-1} \ldots b_2 b_1 = Binary(i)$;
          output $T_{2^h \times (\text{count}-1)+i+1} = \aleph \begin{pmatrix} b_h & b_{h-1} & \cdots & b_2 & b_1 \\ \text{set}[h-1] & \text{set}[h-2] & \cdots & \text{set}[1] & \text{set}[0] \end{pmatrix}$;
        end
      if (set[$h - 1$]==k)
        position$--$;
      else
        position = $h - 1$;
      set[position]++;
      for (i=position+1; $i < h$; i++)
        set[i] = set[$i - 1$] + 1;
      count++;
    end
end;

Table 2.4: The dimension-combination broadcast algorithm.

FUNCTION $Get\_The\_Rounds(n, \Delta)$: Set of integers;
begin
  $k = \lceil \log n \rceil$;
  $b_k b_{k-1} \ldots b_2 b_1 = Binary(\text{my\_ID})$;
  $h = \lfloor \log \Delta \rfloor$;
  for ($i = 0$; $i < h$; i++)
    set[i] = $i + 1$;
  position = $h - 1$; count=1;
  rank=0; subrank=0;
  $Transm = \emptyset$;
  while (count $\leq \binom{k}{h}$)
    begin
      for ($i = 0$; $i < h$; i++)
        subrank = subrank + $b_{\text{set}[i]} \times 2^i$;
      $round = 2^h \times$ rank + subrank + 1;
      $Transm = Transm \cup round$;
      rank++; subrank = 0;
      if (set[$h - 1$]==k)
        position$--$;
      else
        position = $h - 1$;
      set[position]++;
      for (i=position+1; $i < h$; i++)
        set[i] = set[$i - 1$] + 1;
      count++;
    end
  output $Transm$;
end;

Table 2.5: Consider an ad-hoc network with $\aleph = \{0, 1, \ldots, 63\}$ and $h = \lfloor \log \Delta \rfloor = 2$ ($4 \leq \Delta < 8$). The function $Divide(\aleph, 2)$ will generate 60 transmission sets $\{T_1, T_2, \ldots, T_{60}\}$. The following table shows the transmission sets and their corresponding rounds.

rank	subrank	transmission set	round	rank	subrank	transmission set	round
0	0	****00	1	7	2	*1**0*	31
	1	****01	2		3	*1**1*	32
	2	****10	3	8	0	0***0*	33
	3	****11	4		1	0***1*	34
1	0	***0*0	5		2	1***0*	35
	1	***0*1	6		3	1***1*	36
	2	***1*0	7	9	0	**00**	37
	3	***1*1	8		1	**01**	38
2	0	**0**0	9		2	**10**	39
	1	**0**1	10		3	**11**	40
	2	**1**0	11	10	0	*0*0**	41
	3	**1**1	12		1	*0*1**	42
3	0	*0***0	13		2	*1*0**	43
	1	*0***1	14		3	*1*1**	44
	2	*1***0	15	11	0	0**0**	45
	3	*1***1	16		1	0**1**	46
4	0	0****0	17		2	1**0**	47
	1	0****1	18		3	1**1**	48
	2	1****0	19	12	0	*00***	49
	3	1****1	20		1	*01***	50
5	0	***00*	21		2	*10***	51
	1	***01*	22		3	*11***	52
	2	***10*	23	13	0	0*0***	53
	3	***11*	24		1	0*1***	54

rank	subrank	transmission set	round	rank	subrank	transmission set	round
6	0	**0*0*	25		2	1*0***	55
	1	**0*1*	26		3	1*1***	56
	2	**1*0*	27	14	0	00****	57
	3	**1*1*	28		1	01****	58
7	0	*0**0*	29		2	10****	59
	1	*0**1*	30		3	11****	60

tolerable network degrees $2^h \leq \Delta \leq 2^{h+1} - 1$, in which the DCB outperforms the LB. The range of the tolerable network degrees by the PB algorithm can be derived in a similar way. From Figure 2.2, we can find that the maximum tolerable network degree by the DCB algorithm is approximately two to eight times that by the PB algorithm for $n \leq 2^{29}$.

2.4 Multichannel Broadcast

On the basis of the DCB algorithm, in this section, we propose three deterministic broadcast algorithms for multi-channel systems with multiple reception capacity. In contrast with single channel systems, we hope that the frame length can be significantly reduced in multi-channel systems. Clearly, given ρ channels and the optimal frame length L^* for signal channel systems, the best performance that we can hope to attain is roughly L^*/ρ.

2.4.1 Channel-Modulo Dimension-Combination Broadcast

The simplest way to extend the DCB algorithm to multi-channel systems is using the modulo operation. Initially, we assign uniformly the n nodes to the ρ channels by the modulo operation; that is, node $i \in \aleph$ chooses the channel $i \mod \rho$. Then we proceed to perform the DCB algorithm on the group of nodes assigned to each of the channels individually. Table 2.6 shows the *channel-modulo dimension-combination broadcast* (CMDCB, for short) algorithm. By Theorem 2.3.1, nodes associated with the same channel can correctly forward the message between any two consecutive layers by the DCB algorithm. In addition, simultane-

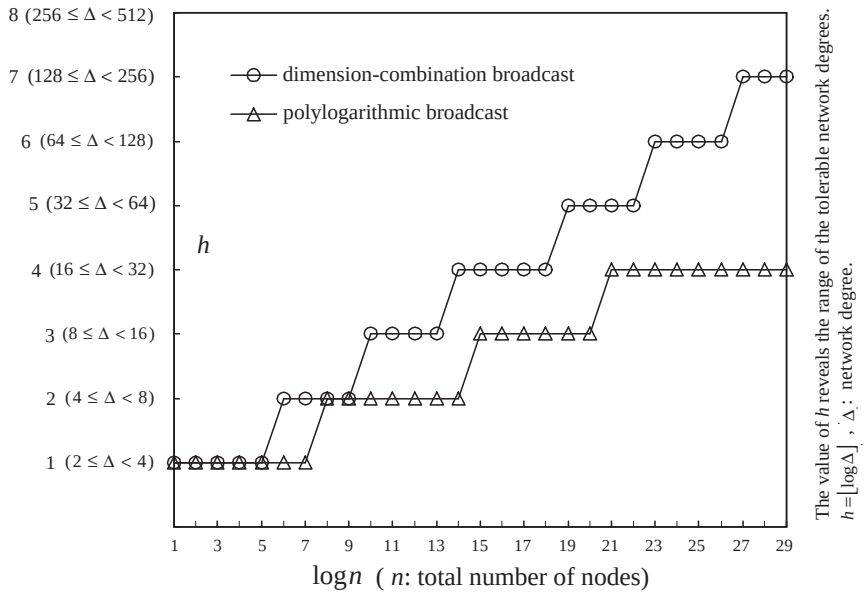

Figure 2.2: The range of the tolerable network degrees vs. network size for DCB and PB.

ous reception of packets on other channels is not affected. The correctness of the CMDCB algorithm for multi-channel systems is thus evident. Consider a multihop network with n nodes and maximum degree $\Delta = 2^{h+1} - 1$, $1 \leq h < \log n$, the frame length of the CMDCB protocol is $L_3 = 2^h \binom{\lceil \log \lceil n/\rho \rceil \rceil}{h}$. The broadcast completion time is hence bounded by DL_3. Obviously, the more the number of channels, the shorter the frame length. However, to ensure the formula L_3 meaningful, the value of ρ should satisfy the constraint $h \leq \lceil \log \lceil n/\rho \rceil \rceil$; namely, $\rho \leq n/2^h$. To sum up, when $\rho = n/2^h$, the frame length L_3 leads to the minimum.

2.4.2 Parallel-Transmission Dimension-Combination Broadcast

The basic idea behind the *parallel-transmission dimension-combination broadcast* (PTDCB, for short) algorithm is that if we allow more than one transmission sets for single channel systems to transmit in a slot by different channels, the broadcast time can thus be shorten. Observing Tables 2.3, 2.4, and 2.5, we can find that the transmission sets which are mutually disjoint can concurrently transmit messages without violating the hitting requirements, if we assign different channels to these sets. In other words, if $T_a \cap T_b = \emptyset$ in single channel systems, then both T_a and T_b can transmit messages in the same slot using different channels in multi-channel systems. Let $\mathcal{P}_i = \{T_{i\times 2^h+1}, T_{i\times 2^h+2}, \ldots, T_{(i+1)\times 2^h}\}$, where $T_j \in \mathcal{P}_i$ is one

Table 2.6: The channel-modulo dimension-combination broadcast algorithm.

FUNCTION $Get\_The\_Rounds(n, \Delta, \rho)$;
begin
$channel = \text{my\_ID} \mod \rho$;
$my\_new\_ID = 1 + \lfloor \text{my\_ID}/\rho \rfloor$;
execute the $DCB\_Algorithm$ by my_new_ID
to compute the allowable transmission rounds;
end;

of the transmission sets generated by $Divide(\aleph, h)$ and $i \times 2^h + 1 \leq j \leq (i+1) \times 2^h$. We have the following theorem.

Theorem 2.4.1. Given any two transmission sets T_a and T_b, if $a \neq b$ and $T_a, T_b \in \mathcal{P}_i$, then $T_a \cap T_b = \emptyset$ for all $i \times 2^h + 1 \leq a, b \leq (i+1) \times 2^h$ and $0 \leq i \leq \binom{\log n}{h} - 1$.

Proof. According to the function $Divide(\aleph, h)$, any two transmission sets T_a and T_b belonging to the same $\mathcal{P}_i$ have the form of $T_a = \aleph \left(\begin{smallmatrix} a_h & a_{h-1} & \cdots & a_1 \\ p_h & p_{h-1} & \cdots & p_1 \end{smallmatrix} \right)$ and $T_b = \aleph \left(\begin{smallmatrix} b_h & b_{h-1} & \cdots & b_1 \\ p_h & p_{h-1} & \cdots & p_1 \end{smallmatrix} \right)$, where $(a_h a_{h-1} \ldots a_1) = Binary(a)$ and $(b_h b_{h-1} \ldots b_1) = Binary(b)$. Since $a \neq b$, there must exist at least one element $p_\ell \in \{p_1, p_2, \ldots, p_h\}$ such that $a_\ell \neq b_\ell$, where $1 \leq \ell \leq h$. The bit values of the p_ℓth dimension of all the integers in T_a are equal to a_ℓ, whereas those in T_b are equal to b_ℓ. Hence $T_a \cap T_b = \emptyset$. The theorem thus follows. □

By Theorem 4.1, we know that at most $\min\{\rho, 2^h\}$ transmission sets can use different channels for concurrent transmission. Following this strategy, we can obtain the PTDCB algorithm by replacing the following instructions in the DCB algorithm

$round = 2^h \times$ rank + subrank + 1;
$Transm = Transm \cup round$;

by the instructions below.

$channel = \text{subrank} \mod \rho$;
$round = \lceil 2^h / \min\{\rho, 2^h\} \rceil \times \text{rank} + \lfloor \text{sunrank}/\rho \rfloor + 1$;
$Transm = Transm \cup (round, channel)$;

Similar to the arguments in the previous subsection, the correctness of the PTDCB algorithm for multi-channel systems can be easily proved. Consider a multihop network with n nodes and maximum degree $\Delta = 2^{h+1} - 1$, $1 \leq h < \log n$, the frame length of the PTDCB protocol is $L_4 = \lceil 2^h / \min\{\rho, 2^h\} \rceil \binom{\log n}{h}$. The broadcast completion time is hence bounded by DL_4. Clearly, when $\rho = 2^h$, L_4 achieves the minimum.

2.4.3 Color-Hit Dimension-Combination Broadcast

Again, consider the same example shown in Figure 2.1. Given the conflicting set $R = \{32, 33, 36, 37, 49, 53, 54\} = \{100000, 100001, 100100, 100101, 110001, 110100, 110101\}$, if the sets $R\left(\begin{smallmatrix} 0 & 0 \\ 3 & 1 \end{smallmatrix}\right)$, $R\left(\begin{smallmatrix} 0 & 1 \\ 3 & 1 \end{smallmatrix}\right)$, $R\left(\begin{smallmatrix} 1 & 0 \\ 3 & 1 \end{smallmatrix}\right)$, and $R\left(\begin{smallmatrix} 1 & 1 \\ 3 & 1 \end{smallmatrix}\right)$ concurrently transmit messages using channels 0, 1, 2, and 3 respectively, then $R\left(\begin{smallmatrix} 0 & 0 \\ 3 & 1 \end{smallmatrix}\right) = \{100000\}$ can successfully delivery the message since only one node in R uses the channel 0. On the basis of the dimension partition tree, we propose the *color-hit dimension-combination broadcast* (CTDCB, for short) algorithm, in which the hitting requirements are satisfied by the scheduled channel usage. The detailed description is shown in Table 2.7. The correctness for the CTDCB algorithm is similar to the arguments in Section 3.2 and thus can be easily proved. To ensure that the CTDCB algorithm can work functionally, the total number of channels ρ should be no less than $2^{\lfloor \log \Delta \rfloor}$. Consider a multihop network with n nodes and the maximum degree $\Delta = 2^{h+1} - 1$, $1 \leq h < \log n$, the frame length of the CTDCB protocol is $L_5 = \binom{\log n}{\lfloor \log \rho \rfloor}$. The broadcast completion time is hence bounded by DL_5. Even though $\rho \geq 2^h$, the worthier occasion to run the CTDCB algorithm rather than the PTDCB algorithm is when $L_5 \leq L_4$. Put these together, the CTDCB protocol is adoptable when $\lfloor \frac{\log n}{2} \rfloor \leq h \leq \lfloor \log \rho \rfloor$.

2.4.4 Remark

Up to the present, we have proposed four distributed deterministic broadcast algorithms for multi-channel systems including MLB, CMDCB, PTDCB, and CTDCB. Obviously, unless

Table 2.7: The color-hit dimension-combination broadcast algorithm.

FUNCTION $Get\_The\_Rounds(n, \Delta, \rho)$: Set of $(round, channel)$ pairs;
begin
  $k = \lceil \log n \rceil$;
  $b_k b_{k-1} \ldots b_2 b_1 = Binary(\text{my\_ID})$;
  $\delta = \lfloor \log \rho \rfloor$;
  for ($i = 0$; $i < \delta$; i++)
    set[i] = $i + 1$;
  position = $\delta - 1$; $Transm = \emptyset$;
  $round = 1$; $channel = 0$;
  while ($round \leq \binom{k}{\delta}$)
    begin
      for ($i = 0$; $i < \delta$; i++)
        $channel$ = $channel$ + $b_{\text{set}[i]} \times 2^i$;
      $Transm = Transm \cup (round, channel)$;
      $round$++; $channel$= 0;
      if (set[$\delta - 1$]==k)
        position$--$;
      else
        position = $\delta - 1$;
      set[position]++;
      for (i=position+1; $i < \delta$; i++)
        set[i] = set[$i - 1$] + 1;
    end
  output $Transm$;
end;

Table 2.8: General location-aware multi-channel broadcast scheme.

PROCEDURE $Location\_Aware\_Broadcast(n, \Delta, \rho)$;
begin
  while (broadcast is unfinished)
    if (at the beginning of a frame)
      update its current location $(x, y) \in \Re^2$ via a GPS receiver;
      $Transm = Get\_The\_Rounds((x, y), n, \Delta, \rho)$;
    end_if;
  end_while;
end;

the network is too dense, the MLB protocol is not preferred. Consider a multihop networks with n nodes and the maximum degree $\Delta = 2^{h+1} - 1$, $1 \leq h < \log n$. For each integer h, if the value of $\min\{L_3, L_4, L_5\}$ exceeds $\lceil n/\rho \rceil$, then all these algorithms will be compelled to switch to the MLB algorithm.

In general, when the total number of channels is few, the PTDCB performs best among all because of its shortest frame length. However, an algorithm (PTDCB) may appear attractive because of shorter frame length, but may indeed perform poorly for larger number of channels because of limited degree of transmission concurrency. In MLB and CMDCB, the whole channels are fully utilizable even ρ is large. In other words, MLB and CMDCB offer better channel scalability.

2.5 Location-Aware Multichannel Broadcast

Almost all the above-mentioned algorithms are only suitable in a sparse network. In contrast with single channel systems, we hope that, in multi-channel systems, the maximum tolerable network degree can be also highly promoted. Fortunately, with the auxiliary of GPS and the

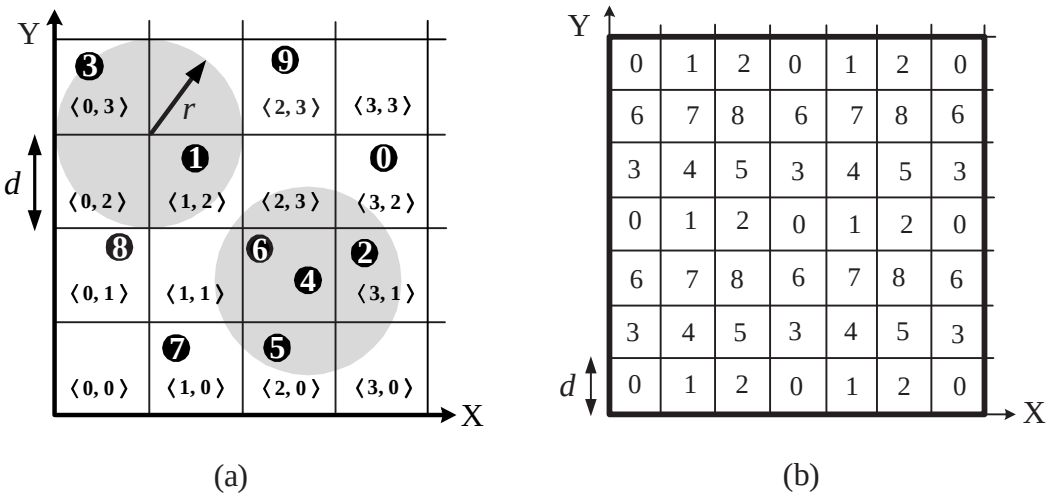

Figure 2.3: The GDCB model. Part (a) shows the relation between maximum transmission range r and the side length d of grids. That is, $d = r$. In addition, ten mobile hosts ⓪ $\sim$ ⑨ are dispersed randomly over the 2D geographic region. The integer pairs are the grid coordinate. In this figure, we can find that, with the help of GPS, the number of (potential) interfering neighbors of the node ④ is reduced from 3 to 1. Part (b) shows one possible channel assignment for the grid configuration. The integer within in the grid is the channel number.

transceivers with tunable transmission power/range ability, we can attain this goal. Table 2.8 shows the general location-aware deterministic multi-channel broadcast protocol $\overrightarrow{\Pi}$. Compared with Table 2.1, we can find that reducing the influence of the maximum degree on the frame length is achieved at the expense of the periodical recomputation of the transmission schedule by its updated location information at the beginning of each frame. By the protocol $\overrightarrow{\Pi}$, correct forwarding a message $\mathcal{M}$ between any two consecutive layers is still guaranteed within a deterministically bounded frame length and without depending either on the knowledge of current neighbors or on the rate of their mobility. Therefore, the protocol $\overrightarrow{\Pi}$ is still topology-independent. Again, by specifying the function $Get\_The\_Rounds((x, y), n, \Delta, \rho)$, we can obtain different location-aware broadcast protocols.

2.5.1 Grid Dimension-Combination Broadcast

The basic idea behind the *grid dimension-combination broadcast* (GDCB, for short) algorithm is very simple; in brief, we just imitate the organization of cellular/cluster networks.

This approach is widely adopted in many issues for the MANET [18, 40, 62, 80]. In our model of the ad-hoc network, nodes are dispersed randomly over a two-dimensional pre-defined geographic region. Each node is assumed to know its own position by virtue of its GPS receiver but not the position of any other nodes in the network. The pre-defined geographic region is partitioned into logical grids as illustrated in Figure 2.3(a). Each grid is a square of size $d \times d$. Let $\aleph_\infty = \{0, 1, 2, 3, \ldots\}$. Grids are numbered $\langle x, y\rangle \in \langle \aleph_\infty, \aleph_\infty \rangle$ following the conventional xy-coordinate. Each node must know how to map its physical location $(x, y) \in \Re^2$ to the corresponding grid coordinate $\langle x', y'\rangle$. As illustrated in Figure 2.3(a), we assign $\langle x', y'\rangle = \langle \lfloor \frac{x}{d} \rfloor, \lfloor \frac{y}{d} \rfloor \rangle$ throughout this chapter.

The GDCB algorithm is composed of two parts. One is the channel assignment and the other is the transmission scheduling. As to the channel assignment, for each grid, we assign a channel to it. When a node is located in a grid $\langle x, y\rangle$, it will use the channel $c\langle x, y\rangle \in \mathcal{H} = \{0, 1, \ldots, \rho - 1\}$ assigned to $\langle x, y\rangle$ for transmission. Let r_i be the transmission range of the node i and $r = \max\{r_i | i \in \aleph\}$. Determining the optimal values of r and d is not an easy task. Here we restrict the value of r to be no more than d. In our design, both of the node A located in $\langle x_1, y_1\rangle$ and the node B located in $\langle x_2, y_2\rangle$, where $x_1 \neq x_2$ or $y_1 \neq y_2$, that satisfy the inequality $\max\{|x_1 - x_2|, |y_1 - y_2|\} \leq 2$ are forbidden to use the same channel to prevent co-channel interference. To attain this goal, we can simply apply the distance-2 coloring algorithms [70, 80] for cellular or packet radio networks to assign the channel for each grid herein. Since $r \leq d$, the lower bound of ρ can be easily determined. Let $|G|$ denote the total number of grids in the pre-defined geographic region. The lower bound of ρ is 9 when $|G| \geq 9$. Figure 2.3(b) shows one possible channel assignment. Besides, in our design, by means of tuning the transmission power/range, we accommodate up to U users per grid where U is a design parameter. Thus, the maximum number of (potential) interfering nodes which are bounded within a grid is no more than $U - 1$. Let $\mathcal{A}$ denote the area of the pre-defined geographic region. If nodes are uniformly distributed over the area $\mathcal{A}$, U is on average equal to $\frac{n \times d^2}{\mathcal{A}}$. Let $\tilde{h} = \lfloor \log(U - 1) \rfloor$. Given the network degree Δ, the value of $\tilde{h}$ is much smaller than $h = \lfloor \log \Delta \rfloor$. Evidently, through the grid channel assignment, frequency reuse can be maximized and the the number of interfering nodes can be reduced. Consequently, the maximum tolerable network degree can be highly promoted.

As to the transmission scheduling part of the GDCB algorithm, it works the same as the

Table 2.9: The grid color-hit dimension-combination broadcast algorithm.

PROCEDURE $GCHDCB\_Algorithm(n, \Delta, \rho)$;
begin
  while (broadcast is unfinished) // $round\_number \leq D\binom{\log n}{\lfloor \log(U-1) \rfloor}$
    if (at the beginning of a frame)
      update its current location $(x, y) \in \Re^2$ via a GPS receiver;
      determine the set of allowable transmission channels $\Phi(x, y)$;
      compute the transmission schedule $Transm = \{(round, channel)\}$,
      where $channel \in \Phi\langle x, y\rangle$, by the $CTDCB\_Algorithm(n, \Delta, \beta)$;
    end_if;
  end_while;
end;

DCB algorithm. Consider a multihop network with n nodes, the frame length of the GDCB protocol is $L_6 = 2^{\tilde{h}}\binom{\log n}{\tilde{h}}$. The broadcast completion time is hence bounded by DL_6. Notice that it is the only approach in this chapter to support the ***half-duplex*** mode for multi-channel systems.

2.5.2 Grid Color-Hit Dimension-Combination Broadcast

With the support of GPS, the maximum tolerable network degree is successfully promoted. However, as we mentioned above, the GDCB algorithm does not make use of the power of full-duplex transceivers at all. On the other hand, the non-location-aware CHDCB algorithm works well only when the condition $\lfloor \frac{\log n}{2} \rfloor \leq h \leq \lfloor \log \rho \rfloor$ is satisfied. These motivate us to propose a hybrid algorithm which combines both of the advantages of GDCB and CHDCB and overcomes their individual drawbacks.

The *grid color-hit dimension-combination broadcast* (GCHDCB, for short) algorithm consists of two parts. One is the grid channel set assignment and the other is the node

Table 2.10: Comparison of existing mobility-transparent deterministic broadcast protocols.

protocol	channel no.	frame length	density cond.	location info.	duplex
LB [4]	1	n	dense	no	half
PB [4]	1	$h! \times 2^h \binom{\log n}{h}$	sparse	no	half
DCB	1	$2^h \binom{\log n}{h}$	sparse	no	half
MLB	ρ	$\lceil \frac{n}{\rho} \rceil$	dense	no	full
CMDCB	$\rho \leq \frac{n}{2^h}$	$2^h \binom{\lceil \log \lceil \frac{n}{\rho} \rceil \rceil}{h}$	sparse	no	full
PTDCB	ρ	$\lceil \frac{2^h}{\min\{\rho, 2^h\}} \rceil \binom{\log n}{h}$	sparse	no	full
CHDCB	$\rho \geq 2^h$	$\binom{\log n}{\lfloor \log \rho \rfloor}$	dense	no	full
GDCB	$\rho \geq 9$	$2^{\tilde{h}} \binom{\log n}{\tilde{h}}$	dense	yes	half
GCHDCB	$\rho \geq 9 \times 2^{\lfloor \log U \rfloor}$	$\binom{\log n}{\lfloor \log U \rfloor}$	dense	yes	full

transmission scheduling. The grid channel set assignment part of the GCHDCB algorithm works as follows. The pre-defined geographic region is partitioned into logical grids following the same way as we described above. We accommodate up to U users per grid where U is a design parameter. A grid $\langle x, y \rangle$ is assigned a set of channels $\Phi\langle x, y \rangle = \{c_1\langle x, y \rangle, c_2\langle x, y \rangle, \ldots, c_\beta\langle x, y \rangle\}$, where $\beta = 2^{\lfloor \log U \rfloor}$. Given two channel sets Φ_1 and Φ_2, they are *disjoint* if $\Phi_1 \cap \Phi_2 = \emptyset$. In our design, the node A located in $\langle x_1, y_1 \rangle$ and the node B located in $\langle x_2, y_2 \rangle$, where $\langle x_1, y_1 \rangle \neq \langle x_2, y_2 \rangle$, that satisfy the inequality $\max\{|x_1 - x_2|, |y_1 - y_2|\} \leq 2$ should use the disjoint channel sets for transmission; namely, $\Phi\langle x_1, y_1 \rangle \cap \Phi\langle x_2, y_2 \rangle = \emptyset$. Therefore, the co-channel interference between any adjacent grids can be avoid. Again, how to assign the channel sets to grids relies on the distance-2 coloring algorithms [70]. It is evident that the total number of assigned channels should be no more than ρ. In other words,

$$\bigcup_{(x,y) \in \mathcal{A}} \Phi\langle x, y \rangle \subseteq \mathcal{H} = \{0, 1, \ldots, \rho - 1\}.$$

The lower bound of ρ is $9 \times 2^{\lfloor \log U \rfloor}$ when $|G| \geq 9$.

As to the node transmission scheduling part of the GCHDCB algorithm, it works as follows. At the beginning of each frame, each node updates its current location information

(x, y) via a GPS receiver. Then it determines the corresponding channel set $\Phi\langle x, y\rangle$ via $\langle x, y\rangle$. Every nodes within the grid $\langle x, y\rangle$ can use only channels in $\Phi\langle x, y\rangle$ for transmission. Finally, each node computes its own transmission schedule by the CHDCB algorithm with the parameters n, Δ, and β. Table 2.9 shows the GCHDCB algorithm. Even though $\beta \leq U$, correct forwarding a message $\mathcal{M}$ between any two consecutive layers within a grid is guaranteed by the correctness of the CHDCB protocol. Thus the success of the entire broadcast process is also guaranteed. Consider a multihop network with n nodes, the frame length of the GCHDCB protocol is $L_7 = \binom{\log n}{\lfloor \log U \rfloor}$. The broadcast completion time is hence bounded by DL_7. With the assistance of GPS and the transceivers with tunable transmission power/range ability, the value of U can be confined to a small number. Consequently, the GCHDCB protocol becomes very efficient. We summarize the results of this chapter in Table 2.10.

2.6 Summary

Many broadcast algorithms have been proposed for mobile ad-hoc networks [3, 4, 12, 14, 23, 28, 45, 47, 60, 61]. Almost all existing algorithms assume the partial/entire network topology information and require heavy maintenance costs when the network topology changes quickly, frequently, and unpredictably. A broadcast algorithm which is deterministic mobility-transparent is particularly desirable for real-time systems and multimedia applications, especially in highly mobile environments. In this chapter, following the layer-by-layer broadcasting approach in [4] but with a whole different transmission scheduling strategy, we have proposed the dimension-combination broadcast (DCB) algorithm for single channel time-slotted networks. Compared with the PB algorithm [4], DCB completely eliminates the serious redundant transmission problem. As a consequence, DCB dramatically reduces the broadcast completion time, achieving an exponential order improvement over PB. Moreover, the maximum tolerable network degree by the DCB algorithm is approximately two to eight times that by the PB algorithm.

On the basis of DCB, we then propose several different multi-channel broadcast algorithms with multiple reception capacity for different network system environments. In contrast with single channel systems, the frame length is significantly reduced in multi-channel

systems. With the additional support of GPS and the transceivers with tunable transmission power/range ability, the maximum tolerable network degree is also highly promoted. If the total number of channels is few, PTDCB is the best choice. If the GPS receivers are available, GCHDCB is highly recommended. All our proposed algorithms are simple and easily implementable in a fully distributed manner. Network designers can decide which of the algorithms is preferred according to the given network resources. Most importantly, we guarantee that, for all our proposed protocols, there are no redundant transmission rounds in a frame. It implies that, in terms of bandwidth and energy consumption, our solutions reach the efficient performance.

Chapter 3

Location-Aware Multi-Access Protocols for Reliable Broadcast

3.1 Introduction

With the revolutionary advances of wireless technology, the applications of the MANET (mobile ad-hoc network) are getting more and more important, especially in the emergency, military, and outdoor business environments, in which instant fixed infrastructure or centralized administration is difficult or too expensive to establish. In the MANET, pair of nodes communicates by sending packets either over a direct wireless link or through a sequences of wireless links including some intermediate nodes. Due to the broadcast nature of the radio medium and the rapidly dynamic topology changes in the MANET, every algorithms and protocols developed on it will face many great challenges. In this chapter, we are specially interested in a *medium access control* (MAC) protocol for multihop networks with multiple frequency channels.

A MAC protocol is to address how to allocate the multi-access medium and resolve potential contention/collision among various stations. MAC protocols proposed so far can be approximately classified into two categories [5, 13]. One is allocation-based protocols, and the other is contention-based protocols. Deterministic allocation-based protocols, such as TDMA (time-division multiple-access) and its variants [41], are primarily designed to support bounded delay topology-independent transmissions by scheduled slot assignments.

Nevertheless, these protocols are insensitive to variations in network loads or station connectivity. Although dynamic topology-dependent transmission scheduling protocols [76, 83] can adjust themselves to station connectivity, they are not suitable for highly mobility environments due to heavy loads on updated link state information maintenance. As to the contention-based protocols, such as CSMA/CA and it variants [48, 80, 82], they are primarily designed to support asynchronized transmissions and bursty traffic. However, CSMA/CA is inherently unstable [31]. Because of this reason, the CARMA protocol based on the deterministic tree-splitting algorithm [31] and its multi-channel counterpart, CARMA-MC [32], were proposed. In CARMA, in order to maintain a consistent channel view for all stations in a multihop wireless network, a base station should be set up to govern this task. Hence it is not suitable for the large-scale MANET. Additionally, CARMA-MC can work correctly only with the help of the *code assignment* algorithm [33], through which the network system may spend long time and massive update messages in getting convergence when topology changes quickly and frequently. Further, the number of channels required by the code assignment algorithm is an order of the square of the maximum degree of the network. So it is inappropriate for a crowded environment [80, 82].

The authors in [13] define a *reliable* packet transmission as the successful delivery of the same packet from a source station to each neighbor in the destination set. Most previous works on MAC protocols including IEEE 802.11 [48], ADAPT [11], CARMA [31], GRID [80], and DCA [82] are designed to support only reliable unicast transmission. As indicated in [13, 37, 46, 54], reliable broadcast support at the MAC layer will be of great benefit to the routing function, multicasting applications, cluster management, and real-time systems. Obviously, a single reliable broadcast can be implemented by sending one or more reliable unicast messages. However, this approach is not scalable since the time to complete a broadcast increases with the number of neighbors. Besides, MAC protocols typically do not maintain link state information [13]. Recently, several link-level reliable broadcast protocols have been proposed, including FPRP [83], CATA [76], TPMA [37], ABROAD [13], and RBRP [54]. All of them work correctly only in time-slotted environments and depend on the collision detection capacity. In TPMA and RBRP, stations with bad luck in their elimination phase or reservation request phase may lead to starvation. To make matters worse, all of these protocols may lead to deadlocks. A *deadlock* [37, 54, 83] is said to occur if

two conflicting broadcasts are scheduled in the same slot and the senders do not realize this conflict. We also notice that all the above-mentioned protocols have focused only on single channel systems. From many literatures [32, 41, 59, 80, 82], we know that a multi-channel system outperforms a single channel system in many aspects, including throughput, reliability, bandwidth utilization, network scalability, synchronization implementation, and QoS support. Physically, these channels can be realized by different carrier frequencies in FDMA systems or by different orthogonal codes in CDMA systems.

The authors in [13] developed a simple hybrid MAC protocol, called ABROAD, for reliable broadcast in single channel environments. ABROAD is a merger of TDMA and MACA (Multiple Access with Collision Avoidance). Importantly, they try to combine both of the advantages of the allocation- and contention-based protocols and overcomes their individual drawbacks. Therefore, ABROAD can dynamically self-adjust its behavior according to the prevailing network conditions [11, 13]. Following their hybrid approach, but with a whole different design strategy, we propose novel multi-channel location-aware MAC protocols for link-level broadcast support in a multihop MANET. We call the resulting distributed protocol "Adaptive Location-Aware Broadcast" (ALAB) protocol. Since a MANET should operate in a physical area, it is very natural to exploit location information in such an environment [24, 80]. Furthermore, with the help of GPS (Global Positioning Systems), every station can get absolute timing and location information; thus synchronization becomes easy [24, 37, 54, 59, 83]. The advantages of the ALAB protocol are as follows. (i) ALAB supports reliable unicast, multicast, and broadcast transmission services in an integrated manner. That is, unicast and multicast packets are considered as special cases of broadcast packets. (ii) ALAB is scalable and topology-transparent since it does not require any link state information. Moreover, the number of channels required for the MANET is independent of the network topology. (iii) All the starvation, deadlock, hidden terminal, and exposed terminal problems are completely eliminated in ALAB. Accordingly, ALAB is more reliable than other existing link-level broadcast protocols. (iv) ALAB is a merger of *condensed TDMA* and the *tree-splitting algorithm*, thus combining the advantages of the allocation- and contention-based protocols. Naturally, ALAB provides deterministic access delay bounds from its base TDMA allocation protocol. At low traffic or density, ALAB outperforms the pure CSMA/CA because of its embedded stable tree-splitting algorithm; at high traffic or

Table 3.1: Comparison of MAC protocols with link-level reliable broadcast support.

protocol	deadlock possibility	real-time support	topology transparent	location awareness	channel mode
CATA [76]	yes	yes	no	no	single
FPRP [83]	yes	no	no	no	single
TPMA [37]	yes	no	yes	no	single
RBRP [54]	yes	no	yes	no	single
ABROAD [13]	yes	yes	yes	no	single
ALAB	no	yes	yes	yes	multiple

density, ALAB outperforms the pure TDMA because of spatial reuse and dynamic slot management. In a nutshell, ALAB is well adaptable to local changes in traffic load and network topology. (v) Because of fully exploiting the frequency reuse and spatial reuse, ALAB delivers superior performance than ABROAD, which outperforms IEEE 802.11 and ADAPT [11, 13], even under the fixed-total-bandwidth model. In Table 3.1, we summarize and compare existing MAC protocols for link-level broadcast support with our yet-to-be-presented ALAB protocol.

The remainder of this chapter is organized as follows. In Section 2, we describe the ALAB protocol in detail. The approximate throughput analysis is evaluated in Section 3. In Section 4, extensive simulations are conducted to evaluate the proposed protocol in varying ad-hoc network conditions. Section 5 concludes this chapter.

3.2 The ALAB Protocol

3.2.1 Model and Assumptions

A multi-hop mobile radio network used to pass data or control packets can be modelled as an undirected graph $G = (\mathcal{V}, \mathcal{E})$ in which $\mathcal{V}$ ($|\mathcal{V}| = N$) is the set of mobile stations and there is an edge $(u, v) \in \mathcal{E}$ if and only if u and v are in the transmission range of each other. In this

case, we say that u and v are neighbors. The edge set may *vary* over time because of nodal mobility. The set of the neighbors of a station v is $\mathcal{N}(v) = \{u \,|\, (u, v) \in \mathcal{E}\}$ and $|\mathcal{N}(v)|$ is the degree of v. Each station v in the network is assigned a unique identifer (ID) by a number in $\aleph = \{0, 1, \ldots, N-1\}$, where $|\aleph| = N$. In this chapter, all logarithms are assumed to be base 2. Given an integer $v \in \aleph$, let $Binary(v) = (v_1 v_2 \ldots v_{k-1} v_k)$ denote its binary string, where $k = \lceil \log N \rceil$. Thus, every integer in $\aleph$ can be represented by a unique binary k-tuples $(v_1 v_2 \ldots v_{k-1} v_k)$, where $v_i \in \{0, 1\}$.

Within a TDMA network, the time axis is divided into units called (transmission) *frames*, and each frame is composed of time slots. Each slot in turn comprises mini-slots. Nodes in the network are assumed to be synchronized and that the frame length is the same for each node. Each mobile radio host in a multi-channel network is equipped with the transceivers (a single transmitter and multiple receivers). Depending on the ability of the transceivers, each node can communicate with others either in the full-duplex mode or in the half-duplex mode. In the half-duplex mode, each host cannot transmit and receive at the same time. In the full-duplex mode, each host can transmit only one packet on one channel but receive multiple packets on all channels simultaneously [41]. Throughout this chapter, we assume every node works in the full-duplex mode. On the same channel, two types of communication collisions will arise [41, 70]. The primary collision occurs when a node transmitting in a given mini-slot is receiving in the same mini-slot on the same channel. This also implies the converse: a receiving node cannot be transmitting on the same channel at the same time. The secondary collision occurs when node receives more than one packet in a mini-slot on the same channel. In both cases, all packets are rendered useless. To this end, we assume that if more than one node is transmitting on the same channel such that the packets overlap in time, then collision occurs on that channel. On the other hand, simultaneous reception of packets on other channels is not affected [41]. In this chapter, we also assume that a node is capable of determining the current status of a single radio channel [59]. That is, at the end of a mini-slot, each node can obtain feedback from the receiver specifying whether the status of a radio channel is:

- NULL: no transmission on the channel
- SINGLE: exactly one transmission on the channel

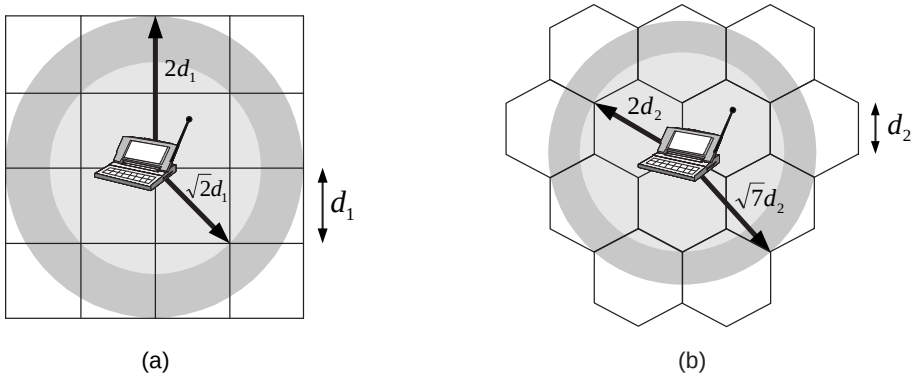

Figure 3.1: Parts (a) and (b) show the relations among transmission range r_i, the side length d_1 of grids, and the side length d_2 of hexagons. That is, $\sqrt{2}d_1 \leq r_i \leq 2d_1$ and $2d_2 \leq r_i \leq \sqrt{7}d_2$.

- COLLISION: two or more transmissions on the channel.

As indicated in [59], a number of radio and cellular networks including AMPS, GSM, ALOHA-net, as well as then well-known Ethernet are known to rely on their sophisticated collision detection capacities.

The basic idea behind the ALAB protocol is not sophisticated; in brief, we develop the GPS-based channel assignment scheme to imitate the organization of cellular networks. This approach has been widely adopted for ad hoc routing and broadcasting [17, 40]. Each station is assumed to know its own position by virtue of its GPS receiver but not the position of any other stations in the network. The pre-defined geographic region is partitioned into two-dimensional logical grids or hexagons as depicted in Figure 3.2. Each grid is a square of size $d_1 \times d_1$. The side length of the hexagons is d_2. Let r_i be the transmission range of station i. Determining the optimal values of r_i, d_1, and d_2 may not be an easy task. In our design, we restrict $\sqrt{2}d_1 \leq r_i \leq 2d_1$ for the grid configuration and $2d_2 \leq r_i \leq \sqrt{7}d_2$ for the hexagonal configuration as illustrated in Figure 3.1(a) and Figure 3.1(b), respectively.

Let $\aleph_\infty = \{0, 1, 2, \ldots\}$. Grids in the two-dimensional plane are numbered $\langle x, y\rangle$ following the traditional xy-coordinate (see Figure 3.2(a)). A MANET with hexagonal configuration in a coordinate system has the x and y axes with their positive portions crossing at a 60° angle (see Figure 3.2(b)). Every station must know how to map its physical location $(x', y') \in (\Re, \Re)$ to the corresponding grid/hexagon coordinate $\langle x, y\rangle \in \langle \aleph_\infty, \aleph_\infty\rangle$. Given

two grids $g_1 = \langle x_1, y_1 \rangle$ and $g_2 = \langle x_2, y_2 \rangle$, the distance between them is defined by

$$dist_{\mathcal{G}}(g_1, g_2) = \sqrt{(x_1 - x_2)^2 + (y_1 - y_2)^2}.$$

Given two hexagons $h_1 = \langle x_1, y_1 \rangle$ and $h_2 = \langle x_2, y_2 \rangle$, the distance between them is defined by

$$dist_{\mathcal{H}}(h_1, h_2) = \sqrt{(x_1 - x_2)^2 + (x_1 - x_2)(y_1 - y_2) + (y_1 - y_2)^2}.$$

Like most cellular networks [39], each grid/hexagonal cell is assigned a unique channel. When a station is located at a cell $\langle x, y \rangle$, it must use the channel assigned to the cell $\langle x, y \rangle$ for transmission. To exploit the frequency reuse, the minimum reuse distance D_{min} should be specified. A channel can be used simultaneously by a number of different cells only if the distance between each pair of cells using the channel is greater than or equal to D_{min}. The *interference neighborhood* IN_c associated with a specific cell $c = \langle x, y \rangle$ is defined as the set of cells whose distance is smaller than D_{min}. In other words, if a channel is assigned to the cell c, then it cannot be assigned to any cell in IN_c. Take the relation between allowable transmission ranges and the side length of cells into consideration, the interference neighborhood for grid and hexagonal configurations can be defined respectively as follows.

$$IN_c^{\mathcal{G}} = \{\, g' \mid dist_{\mathcal{G}}(c, g') < 5 \,\} \quad \text{and} \quad IN_c^{\mathcal{H}} = \{\, h' \mid dist_{\mathcal{H}}(c, h') < \sqrt{19} \,\}.$$

To attain this goal, we can simply apply the distance-D_{min} coloring algorithms [70, 80] for cellular or packet radio networks to assign a channel for each cell. Figures 3.2(c) and 3.2(d) depict possible channel assignments for grid and hexagonal configurations respectively. Let $|\mathcal{G}|$ ($|\mathcal{H}|$) be the total number of grids (hexagons) over the geographic region. By a simple counting, the lower bound of ρ for the hexagonal configuration is 19 when $|\mathcal{H}| \geq 19$. For the grid configuration, the lower bound of ρ is 25 when $|\mathcal{G}| \geq 25$.

The main purposes of these restrictions are as follows. Stations in the same cell form a *single-hop* cluster. In other words, all stations within the same cell can hear the transmission of others. By means of synchronization, all stations within the same cell are able to maintain a consistent channel view. Due to the channel consistency in every cell, no deadlock or hidden terminal problems will exist.

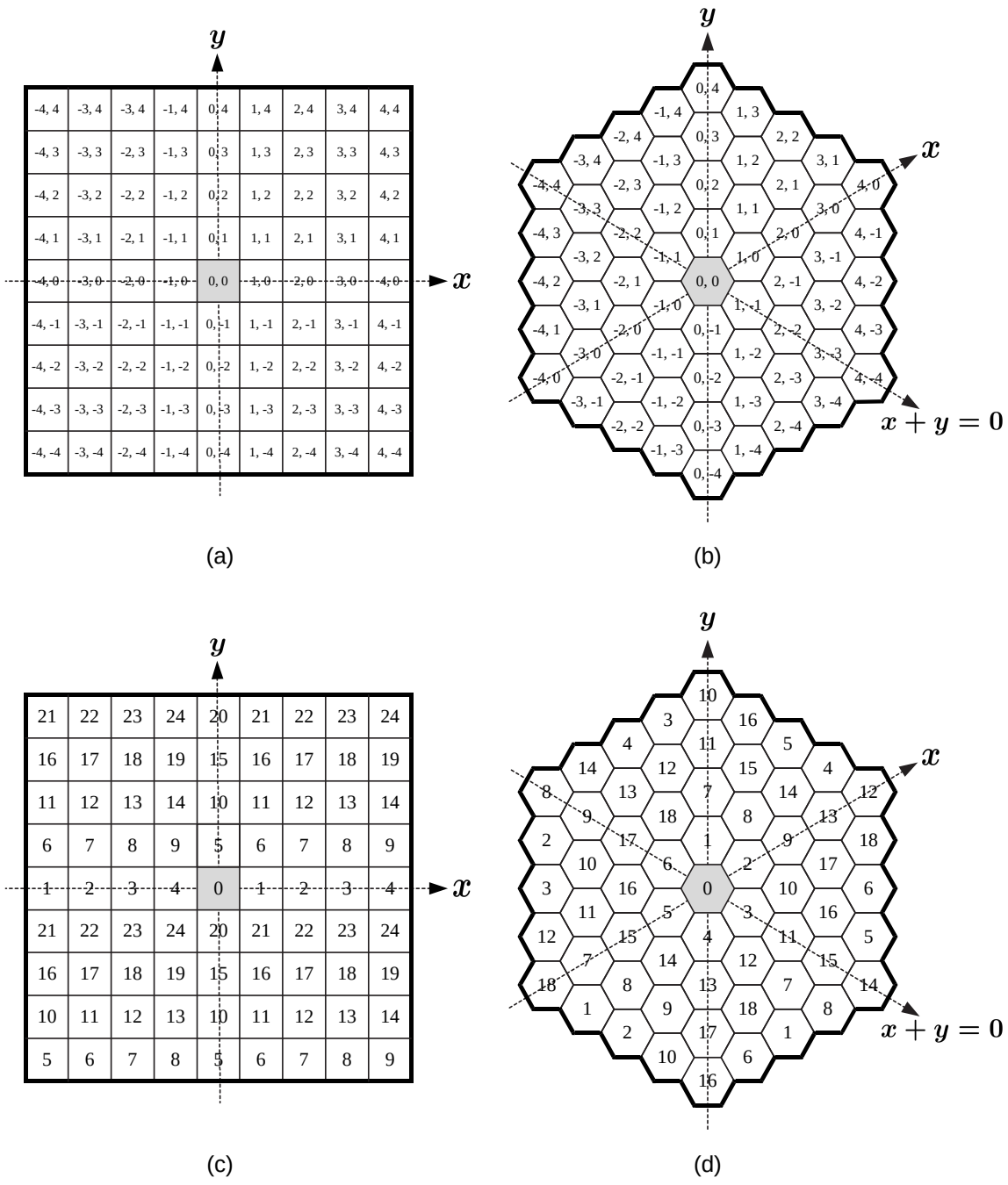

Figure 3.2: The geographical area is divided into logical grids or hexagons. The integer pairs in parts (a) and (b) are the grid/hexagon coordinates. Parts (c) and (d) represent the possible channel assignments for grid and hexagonal configurations respectively. The integer within in the cell is the channel number.

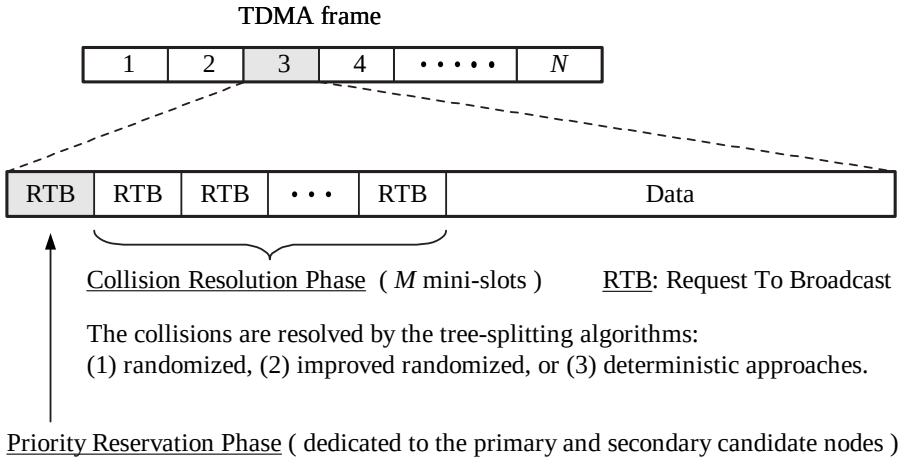

Figure 3.3: The ALAB slot and frame structure.

3.2.2 Protocol Description

The ALAB protocol integrates a tree-splitting collision resolution protocol within each slot of a TDMA allocation protocol. Each station is assigned a transmission schedule (frame) consisting of N slots. The slot and frame structure of the ALAB protocol is shown in Figure 3.3. The frame is divided into fixed-sized slots. Each slot is composed of three parts: a *priority reservation* phase and a *collision resolution* phase followed by a *data transmission* phase. The first two phases are called the *leader election* phase. The first mini-slot is meant for the priority reservation phase and the collision resolution phase consists of the next M mini-slots. The final mini-slot is the data transmission phase.

In the priority reservation phase, only the predetermined primary and secondary candidate stations have the chance to reserve the slot. However, when the first mini-slot remains unused, all active stations contend to use it by randomized or deterministic collision resolution algorithms. A station is said an *active* station if it has packets to send. Through the leader election phase, we guarantee that at most one active station will survive in a cell in a slot. The survival(s) gets the right of broadcast in the data transmission phase. The ALAB permits multiple reservations to be made *simultaneously* at various cells. Recall that the transmission range is limited and simultaneous reception of packets on other channels is not affected. As a result, inter-cell communications via data packets are collision-free. We will focus the protocol description on *a single cell*, say $\langle x, y \rangle$, in the sequel. Before describing

the ALAB protocol in detail, we also make the following assumptions.

- A station located in a cell $\langle x, y \rangle$ is assumed to continuously monitor the status of the channel assigned to $\langle x, y \rangle$.
- The stations can transmit packets only at the beginning of slots. New packets that arrive to the system are inhibited from being transmitted while the resolution of collisions is in progress.
- The channel introduces no errors, so control-packet collisions are the only source of errors. Stations can perfectly detect such collisions immediately at the end of each mini-slot.
- Each slot is designed to accommodate the packet transmission time and the guard time, which corresponds to the transmit/receive turn-around time plus the maximum propagation delay. For ease of presentation and analysis, the guard time is assumed to be negligible as compared with the packet transmission time.

Since the network are assumed to be synchronized, all active stations enter the priority reservation phase synchronously.

1) *Priority Reservation Phase*: In slot i of a frame, we let the station with the $ID = i - 1 \mod N$ be the *primary candidate* (PC for short) station and the station with the $ID = i - 1 + \lfloor \frac{N}{2} \rfloor \mod N$ be the *secondary candidate* (SC for short) station. Figure 3.4 shows the arrangement of the PC and SC stations in a frame, where $N = 8$. In our design, the PC station takes priority over the SC station. At the beginning of the first mini-slot, only the PC and SC stations are allowed to send RTB (request-to-broadcast) control packets with probability 1. At the end of the first mini-slot, if the status of the channel is COLLISION, then the PC station unconditionally wins the slot to broadcast a packet. If the status of the channel is SINGLE, all active stations except the winner quit the contention at the remaining mini-slots, abandon the corresponding packet transmission mini-slot and wait for the next slot. Otherwise, all active stations enter the collision resolution phase.

slots	1	2	3	4	5	6	7	8
primary candidate stations	0	1	2	3	4	5	6	7
secondary candidate stations	4	5	6	7	0	1	2	3

Figure 3.4: The schedule of the primary and secondary candidate stations in a frame. We assume that there are 8 stations in the network.

Though a packet may collide with another packet, the correct semantic is always inferred in the context of the protocol. ALAB needs merely a notification of NULL, SINGLE, or COLLISION (0/1/e) in each mini-slot in leader election phase, each mini-slot thus requires only a single logical *bit* (or *burst*) that is long enough for a transceiver to be able to distinguish. In collision resolution phase, our protocol proceeds in successive collision resolution periods to elect a winner that has a packet to send. The collisions can be resolved either by the randomized tree-splitting algorithm or by the deterministic ID-splitting algorithm. Network system designers can decide which is preferred according to the implementation considerations or the performance considerations such as throughput, delay, and fairness.

2.a) *Randomized Collision Resolution Phase*: At the beginning of the ith mini-slot, where $2 \leq i \leq M + 1$, all active stations send RTBs with probability 1. At the end of the ith mini-slot, if the status of the channel is NULL, then the collision resolution period is over. If a COLLISION is alarmed, every active station flips a coin. Those who obtain heads (with probability p) remain active in the next mini-slot; while those who obtain tails (with probability $1 - p$) withdraw from the remaining contention attempts and wait for the next slot. This process keeps running until a SINGLE is reported or i equals $M + 1$, whichever comes first. Figure 3.5 shows two possibilities of the entire process of the randomized tree-splitting algorithm. This approach is similar to TPMA [37] in principle. Observing Figure 3.5, we can find that the collision resolution process stops immediately once a NULL occurs. One can make a further improvement, however. On condition that a NULL is sensed, all previous contenders are allowed to flip a coin again and those who obtain heads can send RTBs in the next mini-slot. Thus the collision resolution phase will never terminate in the NULL state before

	stations								
mini-slot	0	1	2	3	4	5	6	7	channel status
2	1	1	1	1	1	1	1	1	COLLISION
3	1	0	1	0	0	1	0	1	COLLISION
4	0		1			1		0	COLLISION
5			0			0			NULL

	stations								
mini-slot	0	1	2	3	4	5	6	7	channel status
2	1	1	1	1	1	1	1	1	COLLISION
3	0	1	1	0	1	0	0	1	COLLISION
4		0	1		1			0	COLLISION
5			0		1				SINGLE

Figure 3.5: The randomized collision resolution process. We assume that active stations $0 \sim 7$ are located in the same cell. The contending stations involved in the COLLISION split randomly into two subsets by each flipping a coin. Those who obtain heads send a 1 (RTB) in the next mini-slot; while those who obtain tails become inactive (0) and wait for the next slot. The upper case shows the bad ending, i.e., no winner is elected. The lower case shows the lucky ending, i.e., station 4 wins the slot.

mini-slot $M + 1$. Figure 3.6 shows an example of the improved randomized collision resolution process. It is worth noticing that stations with bad luck in the randomized collision resolution phase will not starve because of the underlying TDMA protocol. The advantages of this approach are that it achieves fairness naturally and a winner may arise quickly. A reasonable value of M could be $1 + \lceil \log \frac{N}{|\mathcal{G}|} \rceil$, where $|\mathcal{G}|$ is the total number of cells over the geographic region.

2.b) *Deterministic Collision Resolution Phase*: We assume that every station keeps an integer variable $temporary\_ID$ used in this phase. Initially, $temporary\_ID := ID$. Let

	stations								
mini-slot	0	1	2	3	4	5	6	7	channel status
2	1	0	1	1	0	0	1	0	COLLISION
3	0		1	1			0		COLLISION
4			0	0					NULL
5			1	0					SINGLE

Figure 3.6: The improved randomized collision resolution process. We assume that active stations 0, 2, 3, and 6 are located in the same cell. The status of the channel is NULL at the end of mini-slot 4. All colliding stations (2 and 3) in mini-slot 3 are permitted to flip a coin again. Finally, station 2 luckily wins the slot.

$M = 1 + \lceil \log N \rceil$ and $(b_1 b_2, \cdots, b_k)$ be the binary representation of any given station $temporary\_ID$, where $k = \lceil \log N \rceil$. At the beginning of the second mini-slot, all active stations send RTB packets. If the status of the channel is NULL, then the collision resolution period is over. If a COLLISION occurs, all active stations with $b_1 = 0$ send RTB packets in the next mini-slot. The general rule on the $(i + 2)$th mini-slot, $1 \leq i \leq M - 1$, is that all active stations with $b_i = 0$ send RTBs; at the end of the mini-slot, if a COLLISION is alarmed, all active stations with $b_i = 1$ are backlogged and wait for the next slot; while a NULL is detected, all active stations with $b_i = 1$ remain active in the next mini-slot. This process continues running until a SINGLE is recognized. Clearly, at the end of the collision resolution process, only the active station with the lowest-numbered $temporary\_ID$ will be the winner. This approach is similar to [5] in principle. Figure 3.7 shows an example of the entire process in the deterministic collision resolution phase. To ensure fairness, each station subtracts one (mod N) from its current $temporary\_ID$ at the end of every slot. The advantage of the deterministic approach is that a winner is guaranteed to be elected if at least one active station exists. However, this scheme only achieves the partial fairness since it highly depends on the ID distribution within a cell. Besides, the value of M by the deterministic approach may be larger than that by the randomized approach.

	stations ($temporary\_IDs$)								
mini-slot	000	001	010	011	100	101	110	111	channel status
2	0	0	1	1	0	1	0	1	COLLISION
3	0	0	1	1					COLLISION
4	0	0							NULL
5			1						SINGLE

Figure 3.7: Deterministic logarithmic search for the active station with the lowest-numbered $temporary\_ID$. We assume that $N = 8$ and $temporary\_ID = ID$ for the current slot. Initially, active stations 010, 011, 101, and 111 fall in the same cell. At the beginning of mini-slot 3, all active stations with $b_1 = 0$ contend for the access right. At the end of mini-slot 3, the status of the channel is COLLISION. stations 101 and 111 therefore become inactive. In this figure, 1 stands for an RTB and 0 stands for nothing. At the end of mini-slot 5, station 010 wins the slot.

In the data transmission phase, every winner in every cell starts to transmit. Since simultaneous reception of packets on other channels is not affected, all stations can gain the data concurrently. ALAB has deterministic access guarantees by its base TDMA allocation protocol while providing flexible and efficient bandwidth management by reclaiming unused slots through the stable contention/collision resolution protocol. Consequently, each station can dynamically adapt its behavior according to local changes in the network load or node density. ALAB is thus not only topology transparent, but also density and load transparent. Since the control packet length is typically smaller than the data packet length, it is worthwhile taking multiple mini-slots to compete for the access right. To sum up, our hybrid MAC protocol is similar to the leader election among the active stations within each gird in every slot.

Since ALAB adopts the frequency reuse technique, each cell can “operate” independently. Thus the global clock synchronization is not necessary. As long as the timing is tight enough to allow local synchronization in a cell, drift at different cells of the network is allowable. With regard to signal interference, authors in [83] indicates that a combination of diversity receiver and Hadamard coding can effectively reduce the interference and

noise influence in CDMA systems in the presence of multipath dispersion. In our design, no acknowledgement mini-slot exists since we assume that transmission is error-free. If the wireless channel is lossy, packets are received in error and retransmissions are required. In this case, the *negative*-ACK (NACK) retransmission strategies [5, 46] are applicable hereinto. In other words, we can slightly modify the slot and frame structure such that NACKs can be sent immediately after data transmission phase is over. On erroneous receipt of the packet at receivers, the sender will receive the (possibly collided) NACK packets in the next mini-slot, prompting a retransmission.

3.3 Throughput Analysis

We assume that stations are randomly distributed over the geographic region. In our design, the geographic region is partitioned into logical grids or hexagons. Each grid is a square of size $d_1 \times d_1$ and the side length of the hexagons is d_2. The area of a hexagon is $\frac{3\sqrt{3}}{2}{d_2}^2$. Let r_i be the transmission range of station i. We restrict $\sqrt{2}d_1 \leq r_i \leq 2d_1$ for the grid configuration and $2d_2 \leq r_i \leq \sqrt{7}d_2$ for the hexagonal configuration. Let $\mathcal{A}$ denote the area of the pre-defined bounded geographic region. The total number of grids (hexagons) over the geographic region is $|\mathcal{G}| = \frac{\mathcal{A}}{{d_1}^2}$ ($|\mathcal{H}| = \frac{2\mathcal{A}}{3\sqrt{3}{d_2}^2}$). Given fixed $\mathcal{A}$ and r, we have $\frac{2\mathcal{A}}{r^2} \leq |\mathcal{G}| \leq \frac{4\mathcal{A}}{r^2}$ and $\frac{8\mathcal{A}}{3\sqrt{3}r^2} \leq |\mathcal{H}| \leq \frac{14\mathcal{A}}{3\sqrt{3}r^2}$.

Two bandwidth models have been proposed in [80, 82] to evaluate the network throughput performance for multi-channel ad-hoc networks.

- *fixed-channel-bandwidth*: Each channel has a fixed bandwidth. Clearly, the more the channels, the more bandwidth the network can potentially use. This model is especially suitable for CDMA environments, where each code has the same bandwidth, and we may utilize multiple codes to increase the actual bandwidth of the network.

- *fixed-total-bandwidth*: The total bandwidth offered to the network is fixed. Evidently, with more channels, each channel will have less bandwidth. This model is especially suitable for FDMA environments, where the total bandwidth is fixed, and our job is to use the appropriate number of channels to optimize the performance.

We follow the analytic model proposed in [13] to evaluate the approximate throughput in a multi-channel TDMA network using the ALAB protocol. Note that we will only consider the grid configuration based on the fixed-total-bandwidth model since other cases can be derived in the similar way. Let $f_{\mathcal{G}} = \min\{25, |\mathcal{G}|\}$ and $f_{\mathcal{H}} = \min\{19, |\mathcal{H}|\}$. The total number of channels required in our protocol is $f_{\mathcal{G}}$ for the grid configuration, and $f_{\mathcal{H}}$ for the hexagonal configuration. Since the total bandwidth B is fixed, the bandwidth in which each grid (hexagon) can offer is $B_{\mathcal{G}} = B/f_{\mathcal{G}}$ ($B_{\mathcal{H}} = B/f_{\mathcal{H}}$).

We consider a network of N identical stations with a uniformly homogeneous load distribution. Each station issues a request (at most one) at the beginning of each slot with probability α. Given a grid $\langle x, y\rangle$, we assume that ℓ radio stations are located in it. Hence, the probability of the event X that there are β requests at $\langle x, y\rangle$ in a given slot, where $0 \le \beta \le \ell$, is $\binom{\ell}{\beta}\alpha^{\beta}(1-\alpha)^{\ell-\beta}$. Let $\widetilde{P}(Y) = P(Y|X)$ be the conditional probability of an event Y, given that the event X has occurred and $2 \le \beta \le \ell$. We have

$$\begin{aligned}
& \widetilde{P}(\text{all contenders enter the collision resolution phase}) \\
= \;& \widetilde{P}(\text{all contenders are in an unassigned slot}) \\
= \;& \widetilde{P}(\text{neither the PC station nor the SC station is an active station}) \\
= \;& 1 - \frac{\beta}{N} - \left(1 - \frac{\beta}{N}\right)\frac{\beta}{N-1} \\
= \;& 1 - \Upsilon_{\beta}.
\end{aligned}$$

Let the coin land heads up with probability p on every toss and $q = 1-p$. If the collisions are resolved by the randomized approach, then we have

$$\begin{aligned}
D_k &= \widetilde{P}(\text{a winner arises in mini-slot } k \mid \text{all contenders are in an unassigned slot}) \\
&= \beta p^{k-2}(1-p)^{\beta-1}\left[\left(\sum_{i=0}^{k-3} p^i\right)^{\beta-1} - \left(\sum_{i=0}^{k-4} p^i\right)^{\beta-1}\right], \text{ for } 3 \le k \le M+1.
\end{aligned}$$

This formula can be proved by induction on k [37]. Thus, the conditional probability that a winner arises in the collision resolution phase is

$$w_{\beta} = \sum_{k=3}^{M+1} D_k,$$

since the conditional probability that a winner arises in the second mini-slot is 0, given $2 \le \beta \le \ell$. Altogether, the probability S_{ℓ} that exact one active station successfully transmit

a packet among ℓ mobile stations within the grid $\langle x, y\rangle$ in a slot is

$$S_\ell = \binom{\ell}{1}\alpha(1-\alpha)^{\ell-1} + \sum_{\beta=2}^{\ell}\binom{\ell}{\beta}\alpha^\beta(1-\alpha)^{\ell-\beta}\left[\Upsilon_\beta + (1-\Upsilon_\beta)\times w_\beta\right], \text{ for } 1 \le \ell \le N.$$

In fact, S_ℓ corresponds to an approximation of a grid's average throughput in terms of packets/slot. Like other existing collision resolution protocols [5, 37], optimal p depends on the average number of stations per grid and packet arrival rate; while optimal M depends on the ratio of control packet length to data packet length.

We label $|\mathcal{G}|$ grids over the geographic region $G_1, G_2, \ldots, G_{|\mathcal{G}|}$ respectively. In addition, we assume that the grid G_i contains ℓ_i stations, where $\sum_{i=1}^{|\mathcal{G}|}\ell_i = N$. Therefore, the average number of successful broadcasts over the entire network in a slot is

$$\mathcal{S} = \sum_{i=1}^{|\mathcal{G}|}\delta(\ell_i)\times S_{\ell_i}, \quad \text{where} \quad \delta(\ell_i) = \begin{cases} 1, & \text{if } \ell_i > 0 \\ 0, & \text{if } \ell_i = 0. \end{cases}$$

The *throughput* T is defined as the average number of bits successfully transmitted by all stations per second. We assume that a mini-slot in the leader election phase has L_c bits and the packet transmission mini-slot is L_d-bit long. The throughput $T_\mathcal{G}$ for the grid configuration is

$$T_\mathcal{G} = \mathcal{S}\times\left(\frac{B_\mathcal{G}\times L_d}{L_c(M+1)+L_d}\right).$$

This throughput can be further promoted if the improved randomized approach is used in the collision resolution phase. Figure 3.8 shows the state diagram of a grid. Let

$$\boldsymbol{x} = \begin{bmatrix} \binom{\beta}{1}pq^{\beta-1} & \binom{\beta-1}{1}pq^{\beta-2} & \cdots & \binom{2}{1}pq \end{bmatrix},$$

$$\boldsymbol{A} = \begin{bmatrix} \binom{\beta}{0}p^0q^\beta + \binom{\beta}{\beta}p^\beta q^0 & 0 & \cdots & 0 & 0 \\ \binom{\beta}{\beta-1}p^{\beta-1}q^1 & \binom{\beta-1}{0}p^0q^{\beta-1} + \binom{\beta-1}{\beta-1}p^{\beta-1}q^0 & \cdots & 0 & 0 \\ \vdots & \vdots & \vdots & \vdots & \vdots \\ \binom{\beta}{3}p^3q^{\beta-3} & \binom{\beta-1}{3}p^3q^{\beta-4} & \cdots & \binom{3}{0}p^0q^3 + \binom{3}{3}p^3q^0 & 0 \\ \binom{\beta}{2}p^2q^{\beta-2} & \binom{\beta-1}{2}p^2q^{\beta-3} & \cdots & \binom{3}{2}p^2q^1 & \binom{2}{0}p^0q^2 + \binom{2}{2}p^2q^0 \end{bmatrix},$$

and

$$\boldsymbol{y} = \begin{bmatrix} 1 & 0 & 0 & \cdots & 0 \end{bmatrix}^T,$$

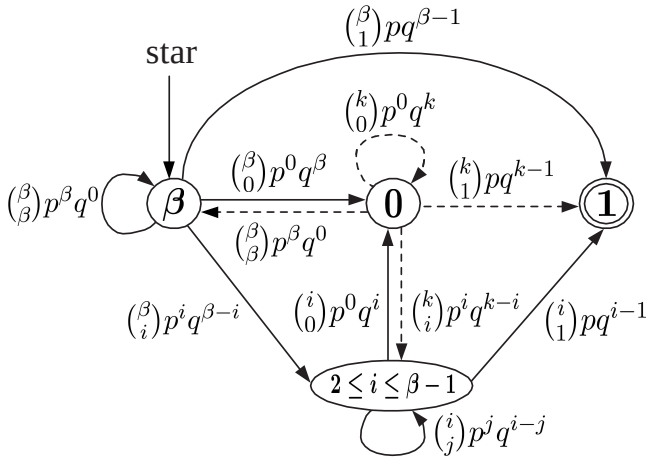

Figure 3.8: State transition diagram of a grid for the improved randomized collision resolution phase. It has four states, labelled $Q_1 = \beta$, $Q_2 = 0$, $Q_3 = i$, and $Q_4 = 1$. The solid arrow pointing at Q_j from Q_i indicates that Q_i contenders flip a coin at the beginning of the mini-slot and Q_j is the number of heads at the end of the mini-slot. The probability of state transition is also given. The dashed arrow starting from 0 shows that there are k contenders in the previous mini-slot. Initially, there are β active stations in a grid. The accept state is the one with a double circle. Once the accept state is reached, a winner is successfully elected.

where $\boldsymbol{x}$ is a row vector with $\beta - 1$ components, $\boldsymbol{y}$ is a column vector, and $\boldsymbol{A}$ is a $(\beta - 1) \times (\beta - 1)$ lower triangular matrix. The entry $a_{ij} = \binom{\beta-j+1}{\beta-i+1}p^{\beta-i+1}q^{i-j}$ of $\boldsymbol{A}$ below the main diagonal denotes the probability that $\beta - j + 1$ contenders flip a coin and $\beta - i + 1$ heads are obtained in the end. The diagonal element $a_{ii} = \binom{\beta-i+1}{0}p^0q^{\beta-i+1} + \binom{\beta-i+1}{\beta-i+1}p^{\beta-i+1}q^0$ signifies the probability that all $\beta - i + 1$ contenders send RTB packets or remain silent. The element $x_i = \binom{\beta-i+1}{1}pq^{\beta-i}$ of vector $\boldsymbol{x}$ expresses the probability that a winner successfully acquires the slot among $\beta - i + 1$ competitors. Given $\beta \geq 2$, from the step by step state transition, we can obtain

$$\begin{aligned}\mathcal{D}_k &= \widetilde{P}(\text{a winner arises in mini-slot } k \mid \text{all contenders are in an unassigned slot}) \\ &= \boldsymbol{x}\boldsymbol{A}^{k-3}\boldsymbol{y}, \text{ for } 3 \leq k \leq M+1.\end{aligned}$$

This formula can be proved by induction on k. Consequently, the conditional probability that a winner arises in the improved randomized collision resolution phase is

$$\omega_\beta = \sum_{k=3}^{M+1} \mathcal{D}_k,$$

Note that the conditional probability that a winner arises in the second mini-slot is 0, given $2 \leq \beta \leq \ell$. Finally, if the deterministic approach is used in the collision resolution phase, then $M = 1 + \lceil \log N \rceil$ and a winner will arise with probability 1 for $1 \leq \beta \leq N$.

3.4 Simulations

We use the *fixed-increment time advance* approach [50] for our discrete-event simulation model to evaluate the performance of ALAB. We have developed a simulator by C++. To simplify the analysis and simulation scenarios, the guard time is ignored in our experiments. The ad-hoc network is simulated by placing N stations randomly and uniformly within a bounded geographic region. For the grid configuration, each grid is a square of size $d_1 \times d_1$. The *geographic region size* ($|\mathcal{G}| = \frac{\mathcal{A}}{{d_1}^2}$) is measured by the number of grids. The transmission range of all simulated stations is r meters. The control packet length L_c is 20 bytes and the data packet length L_d is a multiple of L_c. Network traffic was generated according to a Poisson arrival process with a mean of λ packets per second, and uniformly distributed among the stations. If the fixed-channel-bandwidth model is assumed, each channel's bandwidth is 1 Mbps. If the fixed-total-bandwidth is assumed, the total bandwidth is 1 Mbps. We will focus our minds on the grid configuration (except for part B) since the trend for the hexagonal configuration will be similar. In addition, we will consider the effect of node density on the performance instead of the average degree, where the *node density of the grid plane* ($\eta = \frac{N}{|\mathcal{G}|}$) is defined as the average number of stations per grid.

A) Effect of Geographic Region Size: In this experiment, we vary the geographic region size from 1×1 (one grid) to 13×13 (169 grids) to observe its effect on the throughput performance under the fixed-total-bandwidth model. Figure 3.9 shows the simulation result with $\lambda = 2$, $\eta = 8$, and $L_d/L_c = 100$. We see that when $4 \leq |\mathcal{G}| \leq 25$, the throughput drops slightly with an increasing number of grids. This is because as the total number of grids increases, each grid provides less bandwidth. However, when $|\mathcal{G}| > 25$, a larger geographic region size yields higher throughput. This is because as the geographic region size increases, the bandwidth where each grid can offer remains the same; besides, the total number of grids is increased and every grid may make a contribution to the throughput in every slot. Above all, this scenario reveals that ALAB indeed gains the advantage from exploiting frequency

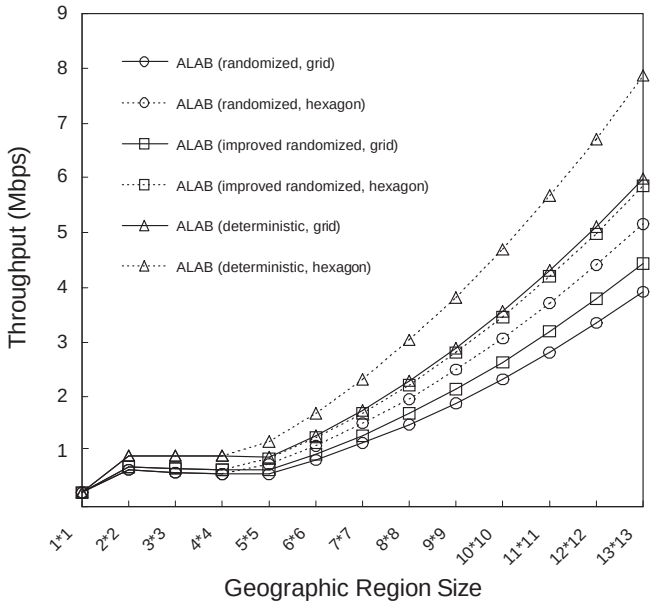

Figure 3.9: Geographic region size versus throughput under the fixed-total-bandwidth model with different cell configurations. ($\lambda = 2$, $\eta = 8$, and $L_d/L_c = 100$.)

reuse and spatial reuse.

B) Effect of Cell Configurations: Figure 3.9 also shows the effect of the cell configurations on the throughput performance under the fixed-total-bandwidth model. Given fixed N, $\mathcal{A}$, and r, if we let $d_1 = \frac{r}{\sqrt{2}}$ and $d_2 = \frac{r}{\sqrt{3\sqrt{3}}}$, then $|\mathcal{G}| = |\mathcal{H}|$ and the node density of the grid plane will be equal to that of the hexagonal plane. In Figure 3.9, we can see that, when $|\mathcal{G}| \geq 25$, ALAB for the hexagonal configuration achieves a throughput that is about $\frac{25}{19} \approx 1.3158$ times that for the grid configuration. This is expected since in this case, the number of channels required for the hexagonal configuration ($f_{\mathcal{H}} = 19$) is less than that for the grid configuration.

C) Effect of Data Packet Length: In Figure 3.10, we show the effect of the ratio L_d/L_c on the throughput performance under the fixed-total-bandwidth model. In this experiment, we fix η and $|\mathcal{G}|$ as 8 and 10×10, respectively. We can see that when $L_d/L_c \leq 125$, the throughput is highly promoted with the increasing length of data packet. This is because each successful leader election process can schedule more data bits to be sent. However, if we further increase the ratio L_d/L_c, the throughput of ALAB will be saturated at a certain point. As shown in Figure 3.10, as both offered load and L_d/L_c increase, the throughput of

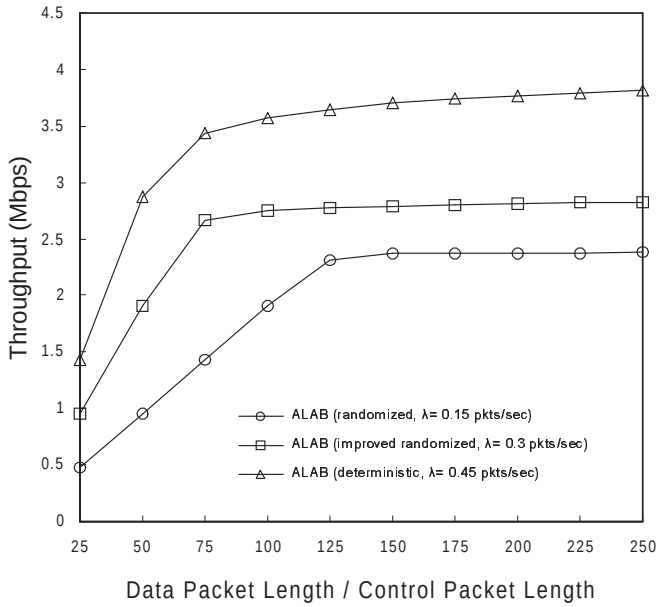

Figure 3.10: L_d/L_c versus throughput under the fixed-total-bandwidth model. ($\eta = 8$ and $|\mathcal{G}| = 10 \times 10$.)

ALAB (deterministic collision resolution approach) approaches the network capacity.

D) Effect of Arrival Rate and Bandwidth Models: In this experiment, we assume that $N = 512$, $r = 2d_1$, $|\mathcal{G}| = 8 \times 8$, $\eta = 8$, and $L_d/L_c = 50$. Figures 3.11 and 3.12 show the throughput versus the offered load under the fixed-total-bandwidth model and under the fixed-channel-bandwidth model respectively. Especially, even under the fixed-total-bandwidth model, we find a 70% increase in the peak performance for ALAB over ABROAD, which delivers superior performance than TDMA, IEEE 802.11, and ADAPT [11, 13]. The reasons are three-fold. (i) In ALAB, via the location-aware channel assignment scheme, the number of potential interfering terminals is significantly reduced from the size of *two-hop neighborhood* to the size of *intra-grid neighborhood*. (ii) Through the leader election process in ALAB, the probability for a station to reserve a slot is highly boosted. (iii) In such a crowed environment, the *erasure effect* [37] or deadlocks also cause the performance of ABROAD degradation. However, it is not very fair to compare ABROAD and ALAB because of their different hardware assumptions. In Figure 3.12, we see that the ALAB protocol with the deterministic collision resolution approach performs best since one active winner is guaranteed to be elected (if it exists) in each grid in every slot.

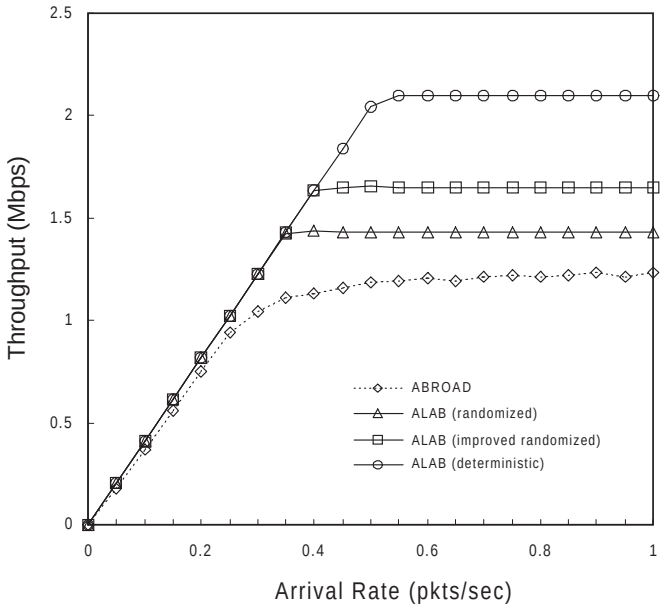

Figure 3.11: Arrival rate versus throughput under the fixed-total-bandwidth model. ($N = 512$, $r = 2d_1$, $\eta = 8$, $|\mathcal{G}| = 8 \times 8$, and $L_d/L_c = 50$.)

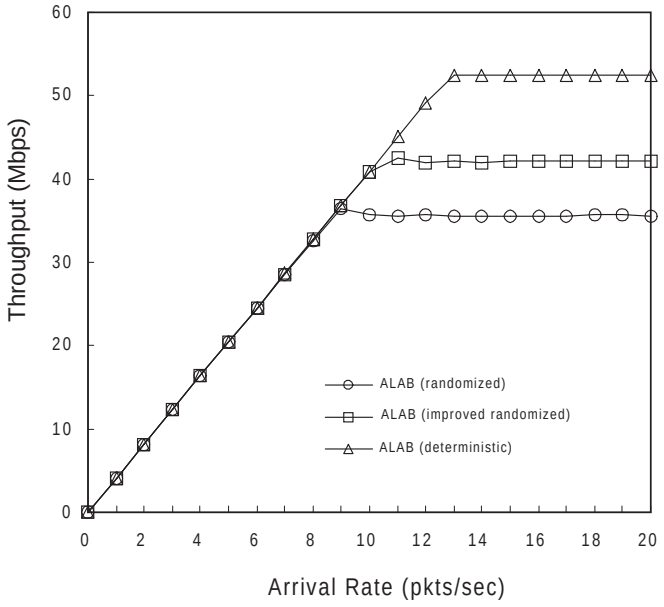

Figure 3.12: Arrival rate versus throughput under the fixed-channel-bandwidth model. ($N = 512$, $\eta = 8$, $|\mathcal{G}| = 8 \times 8$, and $L_d/L_c = 50$.)

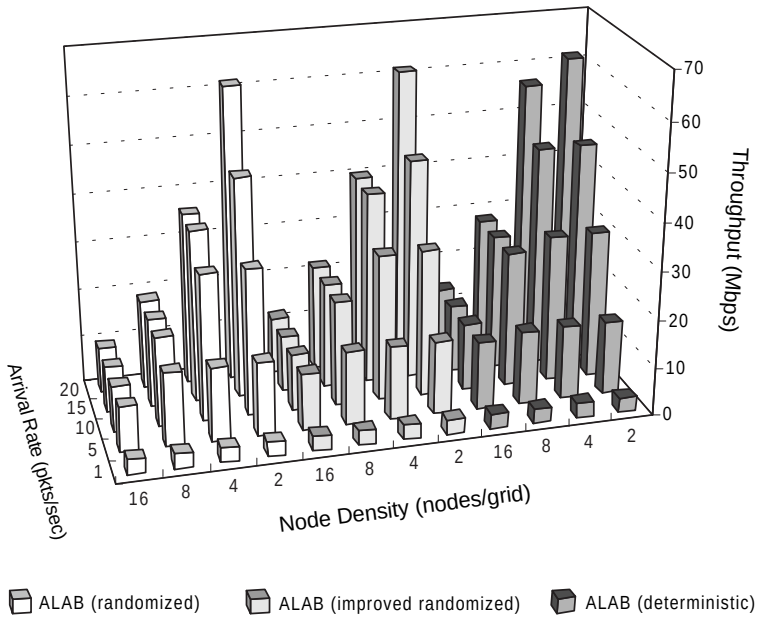

Figure 3.13: Throughput versus node density and arrival rate under the fixed-channel-bandwidth model. ($N = 256$ and $L_d/L_c = 75$.)

E) Effect of node density: Figure 3.13 shows the throughput versus node density and arrival rate under the fixed-channel-bandwidth model. We use $N = 256$ and $L_d/L_c = 75$. We see that as the node density decreases and/or the traffic load increases, the throughput increases monotonically and is finally saturated at a certain point. Especially, we find that when $\lambda = 15 \sim 20$ and $\eta = 4 \sim 16$, the deterministic collision resolution approach yields about $27.67\% \sim 56.67\%$ improvement in the throughput, as compared with the randomized one. This is reasonable due to the uncertainty in the leader election phase by the randomized approach.

Given fixed $\mathcal{A}$ and N, decreasing the node density will promote the throughput; meanwhile, it will cause the number of grids increase. Since we restrict $\sqrt{2}d_1 \leq r \leq 2d_1$ in our design, a larger number of grids implies a shorter transmission range. From a routing performance standpoint, this will result in more hops from sources to destinations. We will further investigate the effects of our MAC protocol on location-aware routing performance in future work. In a nutshell, determining the optimal values of r and d_1 is not an easy task.

F) Effect of station ID Distribution: All above experimental results show that the ALAB protocol with the deterministic collision resolution approach performs best. However, this

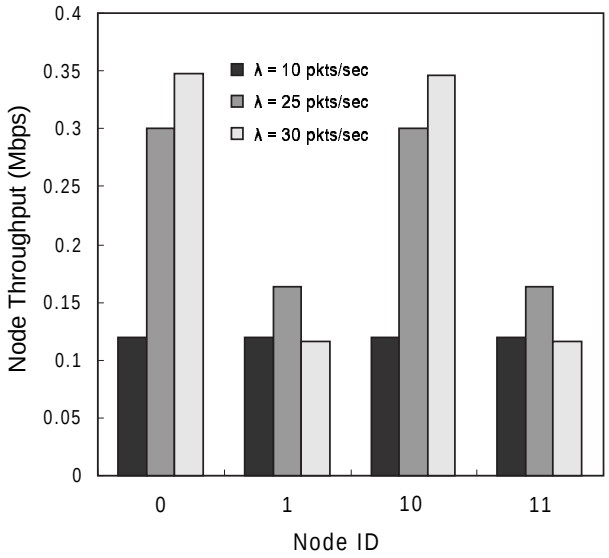

Figure 3.14: station ID versus station throughput under the fixed-channel-bandwidth model. ($N = 16$, $\eta = 4$, $|\mathcal{G}| = 4$, and $L_d/L_c = 75$.)

deterministic approach highly depends on the distribution of the station IDs. In spite of the multihop characteristic in ad-hoc networks, each contending station should receive an equal share of the transmission bandwidth. We conduct an experiment to understand this fairness issue. Let $N = 16$, $\eta = 4$, $|\mathcal{G}| = 4$, and $L_d/L_c = 75$. Four sample stations intended for our observation are 0000, 0001, 1010, and 1011. We further assume that they are located in a same grid. Figure 3.14 shows the simulation result under the fixed-channel-bandwidth model. We can see that as the offered load increases, the performance range of the sample stations increases significantly. That is, the unfairness problem becomes serious when traffic load is heavy. Therefore, if fairness is critical, the ALAB protocol with the improved randomized collision resolution approach may be a compromise solution.

3.5 Summary

In many literatures [13, 37, 46, 54], we know that reliable broadcast support at the MAC layer for multihop ad-hoc networks will be of great benefit to the routing function, multicasting applications, cluster management, and real-time systems. In this chapter, we have proposed new novel location-aware hybrid MAC protocols, called ALAB, for link-level broadcast

support in multi-channel networks. ALAB works efficiently even in the highly mobility environment or when the network becomes partitioned since it does not maintain any link state information. Our GPS-based channel assignment scheme has the following advantages. (i) The total number of channels required is independent of the nodal degree. (ii) All stations within the same cell are able to maintain a consistent channel view. Because of the channel consistency in every grid, both deadlock and hidden terminal problems are completely eliminated. (iii) The number of potential interfering terminals is significantly reduced from the size of two-hop neighborhood to the size of intra-grid neighborhood, thus increasing the spatial reuse.

Especially, ALAB combines both of the advantages of the allocation- and contention-based protocols and overcomes their individual drawbacks. Compared with the pure TDMA, ALAB inherits its deterministic access delay property while providing more flexible bandwidth management by reclaiming unused slots through contention resolution protocols. Compared with the pure CSMA/CA, ALAB uses the more stable tree-splitting algorithms to resolve bursty collisions in an efficient manner and without chaotic events.

We have conducted extensive experiments, which take many factors, such as geographic region size, cell configurations, data packet length, channel bandwidth models, arrival rate, node density, and fairness, into consideration. Approximate throughput analyses for different collision resolution methods are also provided. Simulation results do confirm the advantage of our scheme over other MAC protocols, such as IEEE 802.11, ADAPT [11], and ABROAD [13], even under the fixed-total-bandwidth model. All of these results make ALAB a promising protocol to enhance the performance of the MANET.

Chapter 4

Quality-of-Service Point Coordination Function for Wireless LANs

4.1 Introduction

Wireless local area networks (WLANs) are emerging as an attractive alternative or complementary to wired networks because of cost effectiveness, ease of installation, and tether-free access to the Internet. A WLAN typically consists of an *access point* (AP), playing the polling master, and a finite set of associated mobile stations. Recent advances in wireless technologies have been trying to push WLAN even further towards providing real-time multimedia services to mobile users. Polling schemes are a well-suited class of medium access control (MAC) protocols for a cell-based WLAN to handle parameterized quality-of-service (QoS) traffic because of contention-free transmissions during the polling period and centralized traffic scheduling via the polling master [16, 21, 27, 29, 66]. The simplest polling scheme is *roll-call polling* [44]; in other words, the AP polls every station in sequence and check whether it has data to send. However, this approach has three major drawbacks. First, if the AP fails, then the entire MAC system will become inoperative. Second, since the AP polls every station, it may happen that many stations are polled only to learn that they have nothing to transmit, thus unnecessarily wasting bandwidth and delaying the stations with packets. Last, roll-call polling does not provide any priority mechanism to support differentiated services. Definitely, it is a challenge to design a polling scheme that takes the

overall QoS into consideration. In this chapter, we will propose a new polling MAC protocol with priority reservation and flexible bandwidth allocation schemes to support multimedia applications with QoS requirements.

4.1.1 Related Work

The international MAC standard for WLAN, IEEE 802.11 [48], defines two modes of operation: the *distributed coordination function* (DCF) and the *point coordination function* (PCF). The DCF used in the contention period (CP) employs *carrier sense multiple access with collision avoidance* (CSMA/CA) strategy to provide asynchronous data service. The PCF used in the contention-free period (CFP) employs the polling strategy to provide time-bounded service. PCF uses a *point coordinator* (PC), which shall operate at the AP, to determine which station on a *polling list* currently has the right to transmit. When a PC is operating in a WLAN, the two coordination functions alternate, with a CFP followed by a CP, which are together referred to as a *CFP repetition interval* or a *superframe*. For a more complete and detailed presentation, please refer to the IEEE 802.11 standard [35, 48]. One of the advantages of the alternating period approach is that even if the AP/PC fails, the entire MAC system is still operative since it is only reduced to the DCF mode. However, there are several problems with PCF that make it less attractive for QoS utilization. (i) Any station intending to receive contention-free service shall first send the (re)association frame to the AP during the CP. Since DCF is governed by a contention-based protocol, the (re)association frames need to compete with all other stations in the same cell, resulting in an unbounded (re)association delay. Thus a real-time station with bad luck may never get on the polling list. (ii) IEEE 802.11 does not support the concept of differentiating frames with different user priorities [15]. The DCF is basically supposed to provide a long-term fair channel access to all contending stations in a distributed way. This implies that low-priority stations may join the polling list earlier and faster than high-priority stations. (iii) In an infrastructure WLAN, IEEE 802.11 does not allow a station to send frames directly to any other stations within the same cell, and instead the AP shall relay the frames always [15, 48]. In this way, the channel bandwidth is indeed consumed twice than directional communication between stations. (iv) In IEEE 802.11 PCF, the medium occupancy time or the transmission time

of polled station is unpredictable and unrestrained. Any polled station is allowed to send a single frame that may be of an arbitrary length, up to the maximum of 2312 bytes. This may adversely degrade and ruin the performance of the other stations on the polling list. (v) If pollable stations desiring to leave the polling list, they shall reassociate with the AP via DCF. The station without additional buffered data but having no chance to get off the polling list will response a *Null* frame when polled by the AP/PC. These Null frames are simply the wastage of bandwidth, thus causing the PCF performance down.

To improve the PCF performance, the authors in [66] presented the STRP protocol for a WLAN. In STRP, the PC splits the associated stations into two logical rings, the active ring and the idle ring, according to whether they have pending data. The PC utilizes a single poll to enable a station in the active ring to transmit a data frame by a stronger power, while allowing a station in the idle ring to response a lasting jamming signal by a weaker power. Once the jamming signal is detected by the PC, that station in the idle ring will be placed on the active ring. This approach may shorten the time to probe which station has data to send. However, once the active ring becomes empty, the STRP protocol is reduced to roll-call polling. Furthermore, STRP suffers from the near-far problem and costly dual transceivers. The authors in [66] proposed the SuperPoll protocol to reduce the overhead of polling frames during the CFP. Instead of polling each station individually, in SuperPoll, the PC broadcasts a *superpoll* frame which contains the list of stations to be polled after sending the beacon. After receiving the superpoll, each station on the polling list transmits the data frame in turn according to the polling order. However, if a polled station does not overhear its predecessor's transmission, then that station shall wait for the time interval allocated to it. This approach implies that, in CFP, the data frame length must be fixed. On the other hand, the PC will broadcast the CF-End to reset the network allocation vector (NAV) either after it receives the transmission from the last station on the polling list or until the CFPMaxDuration expires. Thus the SuperPoll protocol will face a disastrous risk: Once the PC has successfully sent the beacon frame to set the NAV to lock out DCF-based access, but the superpoll frame is lost due to channel errors, then the entire CFP will be nearly idle and completely wasted. This is because, after broadcasting the superpoll, the PC is *not* allowed to get involved in the PCF operation any more until the time to send the CF-End. The Multipoll protocol [27] proposed by the IEEE 802.11 task group E is similar to SuperPoll, except that it introduces

a TXOP (*transmission opportunity*) field in the superpoll frame to remove the restriction of fixed data frame length. However, how to determine the appropriate TXOP value for each admitted station is still an open issue [27, 49].

MAC protocols designed for QoS support shall provide priority schemes since we do not hope that high-priority stations must contend fairly with low-priority stations for joining the polling list. Although some priority MAC protocols [2, 22, 72, 73, 75] have been proposed for WLANs, they are mainly geared toward *ad hoc* network configurations. In IEEE 802.11 [48], prioritized access to the wireless medium is controlled through the use of different interframe spacings (IFSs), such as SIFS (Shortest InterFrame Space), PIFS (Priority InterFrame Space), and DIFS (Distributed InterFrame Space). However, the number of priority levels is limited to the number of different IFSs. The authors in [22] proposed a priority DCF scheme by modifying the backoff scheme so that higher-priority stations have a shorter backoff time. However, this approach may encounter a *priority reversal* phenomenon [72]: Since the contention window is exponentially proportional to the number of retransmission attempts, a high-priority *backlogged* station may experience a longer backoff time than a low-priority *unbacklogged* station. In [2, 72, 75], various *black-burst* (BB) contention schemes are proposed to provide multi-priority access in single-hop ad hoc networks. However, reference [73] pointed out that the BB contention is not a regular scheme defined in the IEEE 802.11 standard, thus it is difficult to be overlaid on the current CSMA implementations.

MAC protocols designed for QoS support shall provide time-bounded reservation schemes since we hope that real-time stations can promptly reserve the contention-free periodic access right. The authors in [73] proposed the DBASE protocol to support multimedia traffic in an ad hoc WLAN by mimicking the PCF operation in a distributed manner. During the CP, real-time stations in DBASE employ the p-persistent backoff scheme to compete for joining the reservation list during the time interval between PIFS and DIFS. The DBASE protocol assumes a small constant real-time contention window (3 slots) and a long period of $\mathrm{DIFS} = \mathrm{SIFS} + 5 \times \mathrm{SlotTime}$, which may severely degrade the channel utilization. On the other hand, collision resolution multiaccess strategies may be more suitable than collision avoidance ones to serve as contention-based reservation schemes since the former can exploit feedback information to resolve collisions algorithmically and aggressively, thus achieving a better channel utilization both at low and high loads [5, 31, 72]. The authors in [72] mod-

ified the randomized initialization protocol [59] to resolve real-time traffic contention based on coin flipping. However, the collision resolution process [72] may never terminate due to the nature of randomness. The CARMA protocol presented in [31] employs the deterministic first-success tree-splitting algorithm to resolve collisions in bounded time. However, in CARMA, a station can be added to the transmission queue (and thus reserve the floor) only if that station successfully receives the CTS (clear-to-send) frame in the collision resolution period. Hence the CARMA protocol is unsuitable for MAC-level broadcast traffic.

4.1.2 Our Contributions

IEEE 802.11 compliant products are currently popular on the market. However, all the above mentioned QoS challenges pose a strong demand of redesigning IEEE 802.11 PCF method. Accordingly, we will tailor the PCF operation so that our new protocol can coexist with the DCF, while providing QoS guarantees to real-time multimedia applications. We name the resulting protocol *Q-PCF* (Quality-of-service Point Coordination Function). The characteristics of Q-PCF are as follows. (i) Q-PCF employs the *handshaking* technique, instead of using BB mechanism, to provide multiple priority levels and guarantee that high-priority stations are always admitted to the polling list earlier than low-priority stations. (ii) Q-PCF adopts the deterministic tree-splitting algorithm as the reservation mechanism so that real-time stations can register with the PC in bounded time without relying on the (re)association. In addition, Q-PCF employs the *piggyback* technique so that admitted stations can get off the polling list easily and quickly without performing a reassociation. (iii) Q-PCF permits the PC to poll all stations on the polling list at a time using a single *multipoll* frame. Each polled station can transmit a unicast, multicast, or broadcast data frame of variable length to any other station(s) in the same cell without relying on the relay of the AP. During the polling period, the PC are still able to retain control of the medium, when a polled station does not respond, without leaving the medium idle for a *PIFS* period. By this way, we ensure that the *idling-CFP* disaster will never occur. (iv) With centralized bandwidth management scheme, Q-PCF provides *isolation* among admitted flows while utilizing bandwidth resources as efficiently as possible. More specifically, during the registration period, each real-time station can declare its desired amount of guaranteed bandwidth in each CFP. The PC will collect

the bandwidth requirement information and then dynamically allocates bandwidth such that, during each polling period, the bandwidth demand of each admitted station can be satisfied with high probability. Our bandwidth allocation scheme can be regarded as an enhancement of DBASE [73] in that Q-PCF is capable of offering *per-flow* probabilistic performance assurances. (v) Since the length of the maximum CFP duration is limited, we integrate the run-time *admission control* mechanism into the registration process such that the PC can admit as many newly arriving flows as possible, while not violating already-admitted flows' guarantees.

The remainder of this chapter is organized as follows. In Section 2, we describe the Q-PCF protocol in detail. The approximate throughput of Q-PCF is analyzed in Section 3. In Section 4, simulation results are demonstrated. The final conclusions are drawn in Section 5.

4.2 The Q-PCF Protocol

4.2.1 Network Model and Assumptions

Figure 4.1 illustrates the principal components of the infrastructure WLAN configuration. The basic building block of the IEEE 802.11 network is the *cell*, also known as the *basic service set* (*BSS*). A BSS is typically composed of a central base station, known as an AP, and a finite set of mobile stations. In IEEE 802.11 WLAN, the diameter of the basic service area (BSA) of a BSS is considered only on the order of 100 feet [73]. Therefore, all stations within the same BSS are able to communicate to each other directly. In real-world deployments, different BSSs may partially overlap to arrange contiguous coverage within the extended service area. When multiple point-coordinated BSSs are operating on the same channel in overlapping area, the potential exists for collisions between Q-PCF transfer activities by the independent PCs. We suggest that adjacent BSSs use different channels to avoid the potential inter-cell co-channel interferences. Hence in this chapter, we can safely focus on the Q-PCF operation only in a single cell WLAN configuration without worrying about the overlapping BSSs problem.

In IEEE 802.11 [48], a station shall associate with *an* AP (or reassociate with a new AP) to become a member of an infrastructure BSS. When the association request is granted, the

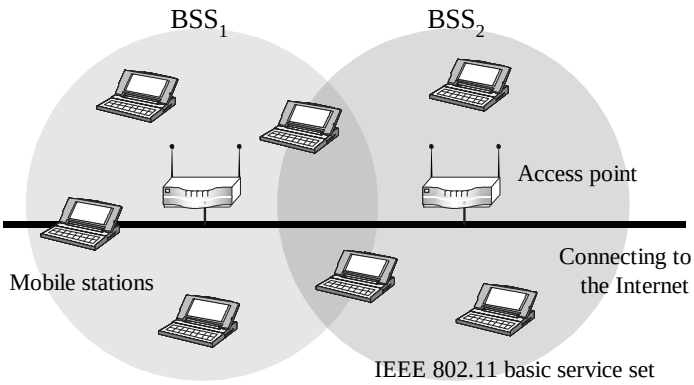

Figure 4.1: Reference model for IEEE 802.11 infrastructure wireless networks. BSS_1 and BSS_2 use different channels to prevent inter-cell interferences in overlapping space.

AP responds with a status code of 0 (successful) and the *associate ID* (*AID*). The AID is an integer identifer used to logically identify the mobile station. The AP/PC can thus maintain a list of finite stations associated within its BSS and updates it whenever a new station joins or a station leaves the BSS. However, Q-PCF disables the *CF-Pollable* and *CF-Poll Request* subfields of the *capacity information* field in (re)association request frames. Instead, Q-PCF provides a new tree-based reservation scheme so that real-time stations are able to get on/off the polling list quickly and efficiently without relaying on the (re)association.

4.2.2 CFP Structure and Timing

The Q-PCF mechanism in our MAC layer architecture, as shown in Figure 4.2, is built on the top of the CSMA/CA-based DCF to support real-time isochronous traffic. The DCF and Q-PCF can coexist in a manner that permits both to operate concurrently within the same BSS. In a BSS, the PC takes charge of bandwidth allocation and makes these two coordination functions alternative, with a CFP (during which Q-PCF is active) followed by a CP (during which DCF is active), which are together referred as a *superframe*.

At the nominal start of the CFP, known as the TBTT (*target beacon transmission time*), the PC continuously monitors the channel and then seizes its control by transmitting a beacon frame after the PIFS medium idle time. One component of the beacon announcement is the maximum duration of the CFP, *CFPMaxDuration*. Each mobile station receiving the beacon shall update its NAV to the CFPMaxDuration. This NAV is used for preventing a

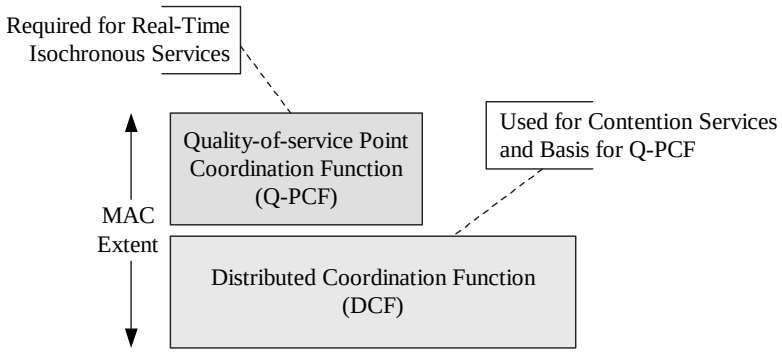

Figure 4.2: The MAC layer architecture.

DCF-based station from taking control of the medium during the CFP. In Q-PCF, as depicted in Figure 4.3, the CFP is further divided into three periods: the *prioritization* period, the *collision resolution* period, and the *polling* period. The first two periods are together called the *registration* period. During the prioritization period, the PC performs a series of handshakes to guarantee that high-priority stations are always admitted to the polling list earlier than low-priority stations. During the collision resolution period, the PC performs a deterministic tree-splitting algorithm to probe which stations undergo the prioritization period desire to join the polling list. During the polling period, the PC uses a single multipoll frame to enable each station on the polling list to send a data frame in turn according to the polling order. After the end of the polling period, the PC broadcasts a CF-End to let all stations reset their NAV and enter the CP.

Consistent with the IEEE 802.11 [48], the minimum length of the CP, CP_{min}, is the time required to transmit and acknowledge one maximum-sized MPDU (*MAC protocol data unit*); namely, $\mathrm{CP}_{min} = \mathrm{DIFS} + T_{max\mathrm{MPDU}} + \mathrm{SIFS} + T_{\mathrm{ACK}}$, where T_{ACK} is the time needed for sending the ACK frame. The value of CFPMaxDuration shall be limited to allow coexistence between DCF and Q-PCF traffic. So we have $\mathrm{CFPMaxDuration} = \mathrm{SF} - \mathrm{CP}_{min}$, where SF is the length of the superframe. On the other hand, it is possible for contention-based service runs past the nominal start of the CFP (TBTT). In the case of a busy medium due to DCF traffic, the CFP is *foreshortened* and the beacon should be delayed for the time required to complete the existing DCF frame exchange. Such a phenomenon is called *stretching* and we depict the stretching event in Figure 4.3. The length of the stretching time T_s may be up to $\widehat{T}_s = T_{\mathrm{RTS}} + T_{\mathrm{CTS}} + T_{max\mathrm{MPDU}} + T_{\mathrm{ACK}} + 3 \times \mathrm{SIFS}$.

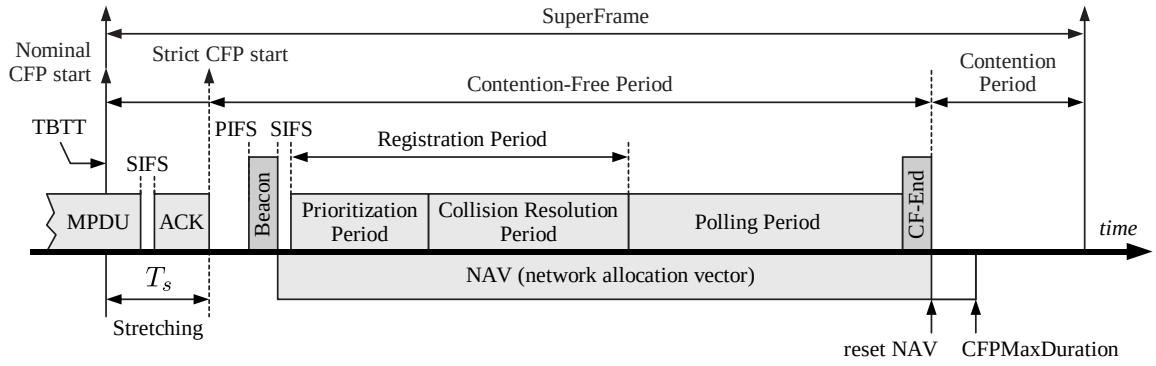

Figure 4.3: Superframe structure and an example of foreshortened CFP.

Since the length of CFPMaxDuration is limited, the overrun of the registration process may shorten the polling period, thus violating the quality of already-admitted connections. Hence a run-time admission control is established to assist the PC in determining when the registration period shall be terminated. Especially, when the polling list size reaches saturation point (see subsection 4.2.7), the PC may directly dive into polling period at the start of the CFP without first performing the registration procedure. An interesting phenomenon in Q-PCF is that collisions may occur during the CFP. However, during the entire CFP, associated stations can transmit frames only when they are allowed to do so by the PC. Consequently, the PC can control these collisions effectively and without chaotic events.

4.2.3 Prioritization Procedure

In Q-PCF, priority levels are numbered from 0 to H, with H denoting the highest priority level. A frame with priority zero shall be sent via the DCF. An active station that has a *flow* with priority level ranging from 1 to H has a chance to join the polling list. Note that a station is said an *active* station if it has traffic waiting to send. Besides, a flow is a continuous stream of frames that have the same source, destination(s), priority level, and quality of service.

After broadcasting a beacon and waiting for a SIFS period, the PC sends the control frame PE_H (*priority enquiry*) to invite active stations whose priority equals to H to reply the PR (*priority response*) frame. On receiving the PE_H frame, an active station with priority level H shall acknowledge a PR frame after a SIFS period. At the end of the handshake, the PC can obtain the ternary feedback information according to stations' responses: (i) NULL:

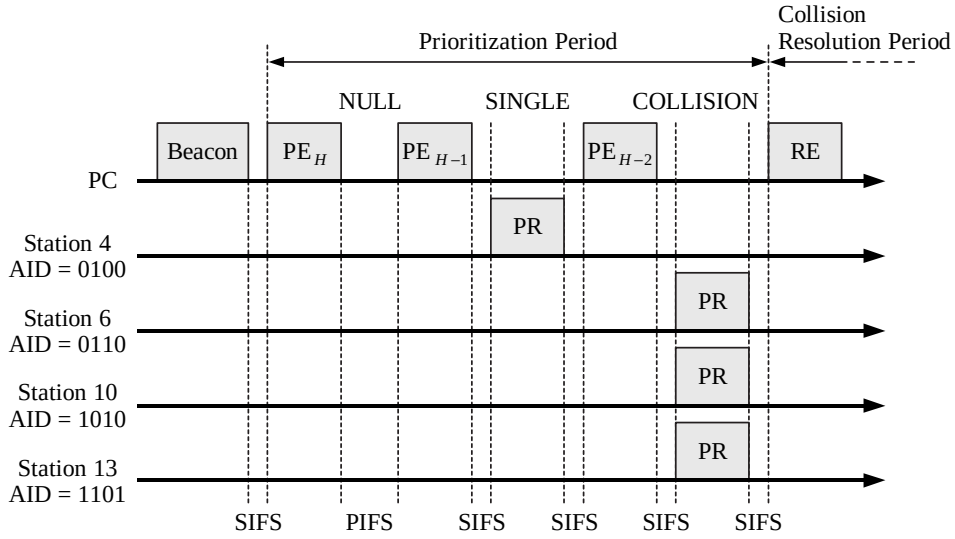

Figure 4.4: An example of the prioritization procedure. We assume that there are 16 associated stations in a BSS. Stations 4, 6, 10, and 13 intend to join the polling list. In the first round, the PC sends the PE_H frame and no one responses. In the second round, only station 4 replies the PR frame and joins the polling list successfully. At the end of the third round (handshake), the PC perceives a COLLISION event and then performs a collision resolution procedure.

The PC does not receive any PR frames. (ii) SINGLE: The PC successfully receives a single PR frame which contains the AID of the sender. That AID will be placed on the polling list. (iii) COLLISION: This event occurs if the outcome of the handshake is neither NULL nor SINGLE.

If the conclusion of the current handshake is NULL (SINGLE), the PC may proceed to the next handshake by issuing the PE_{H-1} frame after an elapsed PIFS (SIFS). The priority probing process keeps running until the occurrence of a COLLISION, the delivery of the PE_1 frame, or a failure in the run-time admission test (see subsection 4.2.7), whichever comes first. Especially, once the PC recognizes a COLLISION event, it will send an RE (*registration enquiry*) frame to announce the start of the collision resolution period. During the collision resolution period, the PC executes the deterministic collision resolution procedure to discover which active stations bring the COLLISION event. The prioritization operation is essentially that of polling, with the PC polling each of the priority groups in a descending order. The average overhead of the prioritization operation is expected to be low since the

value of H is usually small. (Generally, $H \leq 8$. In our simulations, we set $H = 2$.). It is noteworthy that a lower priority station will be blocked if it has no chance to send out a PR frame during the entire prioritization period. We could adopt the *aging* policy [74] (As time progresses, so does the priority of the flow.) to conquer the problem of indefinite blockage or starvation.

The illustration in Figure 4.4 shows how the prioritization procedure works. From Figure 4, we can observe that, in Q-PCF, the synchronization among the PC and associated stations is well controlled by using different interframe spaces. Actually, all Q-PCF transmissions during the CFP are separated only by the SIFS or the PIFS. Thus the PC can safeguard its control of the medium against DCF-based interference. Consistent with the IEEE 802.11 [48], we let $\mathrm{PIFS} = \mathrm{SIFS} + \mathrm{SlotTime}$ and $\mathrm{DIFS} = \mathrm{SIFS} + 2 \times \mathrm{SlotTime}$. As per IEEE 802.11, the SIFS interval is equal to the sum of receiver radio frequency delay, receiver PLCP (physical layer convergence procedure) delay, the MAC processing delay, and the transceiver turnaround time. The SlotTime accounts for the carrier sensing time, the transceiver turnaround time, the MAC processing delay, and the air propagation delay.

4.2.4 Collision Resolution Procedure

Once the prioritization period ends up with a COLLISION event, the PC will execute a collision resolution algorithm to probe which contending stations intend to get on the polling list. Theoretically, any collision resolution multiaccess strategy can be applied here as the collision resolution process. The reasons for choosing the address-based tree-splitting algorithm [5] are due to its simplicity, stability, and bounded collision resolution period. However, our protocol uses different interframe spaces to realize synchronous operations and hence has no need for time slotting as prior MAC protocols based on collision resolution do [5, 16, 42, 44, 59].

We assume that there are N mobile stations associated with the PC and each station is assigned a unique associated ID (AID) $a \in \aleph = \{0, 1, \cdots, N-1\}$. Every integer $a \in \aleph$ can be represented by a binary k-tuples $(a_k a_{k-1} \cdots a_2 a_1)$, where $a_i \in \{0, 1\}$ and $k = \lceil \lg N \rceil$. We write $\lg N \equiv \log_2 N$ (binary logarithm) and $\ln N \equiv \log_e N$ (natural logarithm). Note that the ith bit corresponds to the ith *dimension*. For example, let $\aleph = \{0, 1, 2, 3\} = \{00, 01, 10, 11\}$.

```
01  Let {d_1, d_2, ··· , d_k} be the random permutation of {1, 2, ··· , k};
    /* k = ⌈lg N⌉. Line 01 is used to ensure fairness with the tree-splitting
    algorithm. For example, in Figure 4.6, we set (d_1, d_2, d_3, d_4) = (1, 2, 3, 4). */
02  P := {0, 1, ··· , N − 1};    // Initially, P contains all associated stations.
03  STACK := ∅;    // The PC maintains a local stack.
04  PUSH(1, 0);    // The PC pushes the vector (1, 0) onto the stack.
05  while (STACK ≠ ∅) {
06    do {  (dim, value) := POP();    // The PC popes a vector from its stack.
07          P := P ⋄ (d_dim, vlaue);    // The PC updates the AddressPattern P.
08    } while (value == ∗)
      // This do-while loop helps the PC to avoid a pointless poll.
09    for (i := dim + 1; i ≤ k; i++)
10        P := P ⋄ (d_i, ∗);    // This for loop controls the level of the splitting tree.
11    send RE(h, P);
      /* The PC sends an RE frame which contains the value of priority level h
      and the AddressPattern P. */
12    status := receive(RR(AID));
      /* Upon reception of the RE(h, P) frame, the active station with priority h
      and AID ∈ P shall acknowledge an RR frame including its AID. Then the PC
      updates the channel state variable status according to received RR frames. */
13    switch (status) {
14      case SINGLE:
15        The PC places that AID on the polling list;
16        if (value == 0)  PUSH(dim, 1);  break;
17      case NULL:
18        if (value == 0) {
19          PUSH(dim + 1, 0);  PUSH(dim, ∗);  }  break;
          // The PC pushes an alarm "∗" onto the stack to avoid a pointless poll.
```

```
20          case COLLISION:
21              if (value == 0)
22                  PUSH(dim, 1);
23              PUSH(dim + 1, 0);   break;   // To explore the next level subtree.
24      }
25  }
```

Figure 4.5: The deterministic tree-splitting algorithm executed by the PC.

We can partition the set $\aleph$ along the first dimension into two subsets $\{*0\} = \{00, 10\}$ and $\{*1\} = \{01, 11\}$, where "$*$" means "*don't care*". Given a set $\mathcal{P} \subseteq \aleph$ of binary strings, the set $\mathcal{P} \diamond (dim, value)$ is defined by letting all the dim-th bit values of the strings in $\mathcal{P}$ equal to $value$, where $1 \leq dim \leq k$ and $value \in \{0, 1\}$. For example, let $\mathcal{P} = \{10*0\}$ and we have $\mathcal{P} \diamond (3, 1) = \{11*0\} = \{1100, 1110\}$. Besides, $\mathcal{P} \diamond (3, *) = \{1**0\} = \{1000, 1010, 1100, 1110\}$. Namely, we can regard "$\diamond$" as the overwrite operator.

The basic idea of the tree-splitting algorithm is to use the stack to implement a *preorder* traversal of the *dimension splitting tree*. Specifically, when a COLLISION occurs, the PC splits the set $\mathcal{P}$ of stations involved in the collision into two subsets, $\mathcal{P}_1$ and $\mathcal{P}_2$, along a dimension dim. The PC first recursively resolves the collision of $\mathcal{P}_1$, and then resolves the collision of $\mathcal{P}_2$ independently. Figure 4.5 specifies the tree-splitting algorithm written in C-like language. We assume that the close of the prioritization period results from the transmission of multiple PR_h frames, where $1 \leq h \leq H$. During the collision resolution period, the PC first popes a vector $(dim, value)$ from its local stack and updates the set of binary strings, *AddressPattern* $\mathcal{P}$, according to this popped vector. (See Figure 4.5, lines 05 to 10.) Then the PC sends the RE (*registration enquiry*) frame which contains the value of h and the AddressPattern $\mathcal{P}$ to invite active stations to reply the RR (*registration response*) frame. Upon reception of the $\mathrm{RE}(h, \mathcal{P})$ frame, the active station with priority level h and $\mathrm{AID} \in \mathcal{P}$ shall acknowledge an RR frame after a SIFS period. At the end of the handshake, the PC pushes the proper vector(s) onto its local stack according to stations' responses (SINGLE/NULL/COLLISION). Especially, if the PC successfully receives a single RR frame which contains the AID of the sender, then the PC will add that AID to the polling list. This

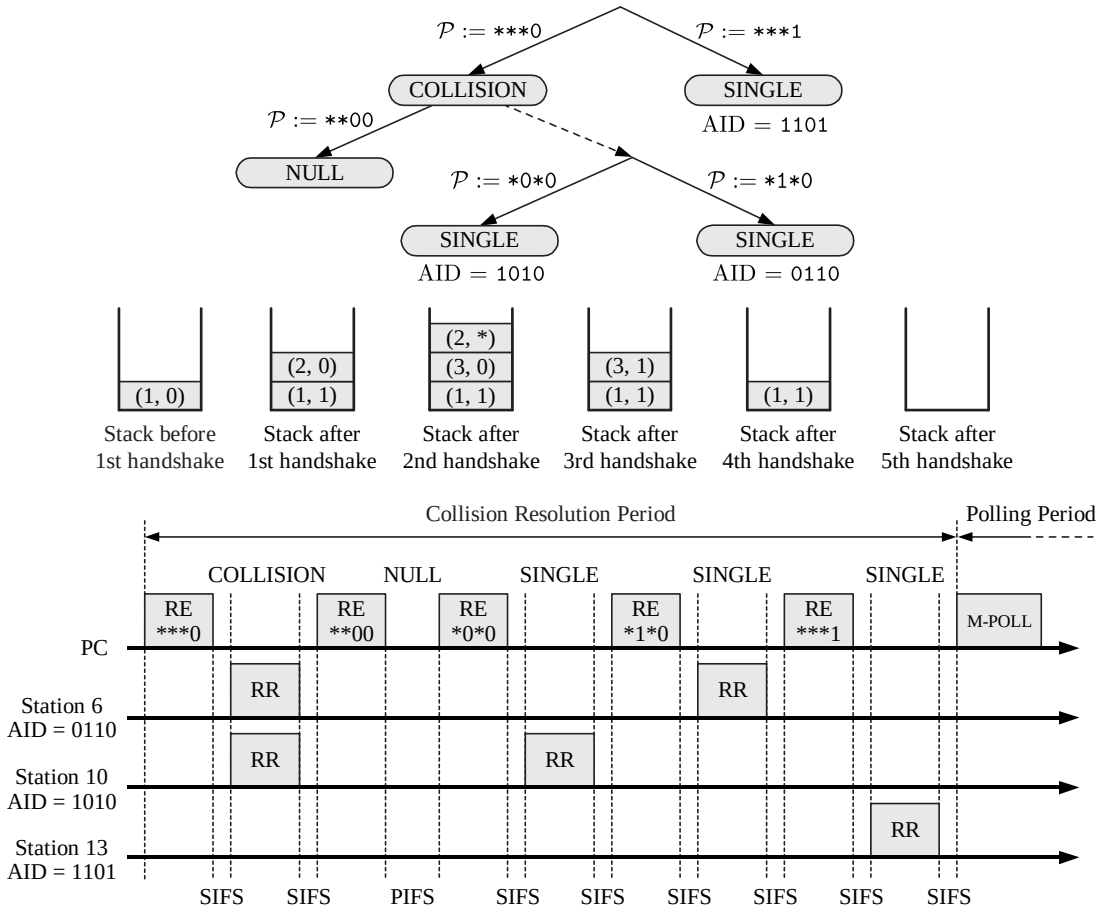

Figure 4.6: This tree structure represents a particular pattern of NULLs, SINGLEs, COLLISIONs resulting from a sequence of splitting. This figure also depicts the operations of the collision resolution procedure and the contents of the stack before/after each RE/RR handshake.

AID probing process keeps running until the emptiness of the stack or a failure in run-time admission test (see subsection 4.2.7), whichever comes first.

Continuing the example in Figure 4.4, Figure 4.6 shows how the deterministic tree-splitting procedure works. In the first round, the PC sends out the RE frame with $\mathcal{P} = \{***0\}$, asking for responses. Since both the AIDs of stations 6 and 10 belong to the set $\mathcal{P}$, then they reply, and their replies collide. On recognizing the COLLISION event, the PC halves the range of $\mathcal{P}$ ($\mathcal{P} = \{**00\}$) and enquires again. This time, the PC will discover a NULL event. However, it is pointless for the PC to further probe the range $\mathcal{P} = \{**10\}$ since it is predictable to have a COLLISION. At the end of the third round (handshake), the

PC correctly receives a single RR frame which contains the $\mathrm{AID} = 10$ of the sender. The PC then places that $\mathrm{AID} = 10$ on the polling list. Continuing in this manner, the PC can skip over large chunks of the address space that have no active stations. In the worst case, when all stations are active and have the same priority level, this will result in doubling the number of RE frames, as compared with roll-call polling. However, once real-time stations get on the polling list, they will reserve the periodic access right and will not participate in the contention resolution process again. When contending real-time traffic is not heavy, tree-splitting algorithm is quite efficient [5, 31, 42, 44]. After five handshakes, stations 6, 10, 13 join the polling list; meanwhile, the stack becomes empty and then the PC broadcasts an M-POLL (*multi-poll*) frame to announce the start of the polling period. The M-POLL frame contains the polling list that consists of AIDs of the stations which are going to be polled in sequential order. Upon receipt of the M-POLL frame, each active station clearly knows whether it has been successfully placed on the polling list. To ensure fairness with the splitting algorithm, the sequence of dimensions the PC explores shall be randomized in each collision resolution period. (See Figure 4.5, line 01.) In a nutshell, the tree-splitting operation is essentially that of polling, with the PC systemically and adaptively controlling the number of allowably contending stations to finally identify each active station.

4.2.5 Polling Procedure

At the beginning of the polling period, the PC issues an M-POLL frame to specify the access order and the medium occupancy time (TXOP) for each polled station. Figure 4.8(b) presents the format of the M-POLL frame suggested by the IEEE 802.11e task group [27]. The TXOP (transmission opportunity) subfield specifies the time duration during which the polled station has the right to transmit. The *record count* field equals to the number of polled stations. (We will describe how the PC dynamically assigns the value of TXOP for each admitted station in the next subsection.) On receiving the M-POLL frame, each polled station needs to monitor the channel activity and automatically initiates its transmission a SIFS period after the end of the transmission of its predecessor in the polling order. Figure 4.7(a) depicts how the polling procedure works. Clearly, if the PC has data to send, it can also add its BSSID to the polling list. During the polling period, the time gap between two successive

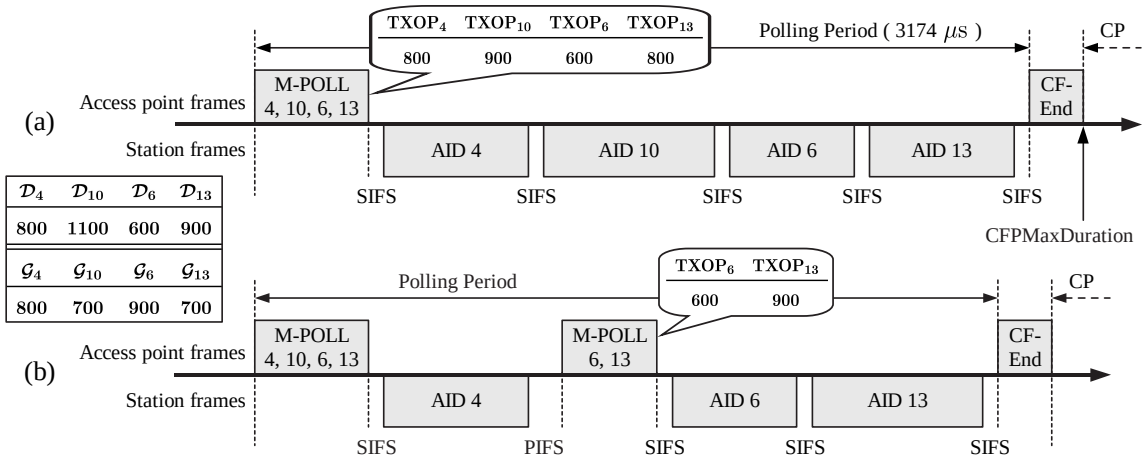

Figure 4.7: The left small table indicates that, during the registration period, station 4 declares $(\mathcal{D}_4, \mathcal{G}_4) = (800, 800)$ and station 10 declares $(\mathcal{D}_{10}, \mathcal{G}_{10}) = (1100, 700)$, etc. Part (a) shows that, at the start of the polling period, the PC broadcasts the M-POLL frame to specify the station transmission order and time, namely, $((4, 800), (10, 900), (6, 600), (13, 800))$. Part (b) shows that, since station 10 does not react, the PC seizes the medium by sending the M-POLL frame after an elapsed PIFS. Note that, in this case, the bandwidth demand of station 13 is luckily satisfied.

transmissions is generally a SIFS period. However, as depicted in Figure 4.7(b), if a polled station, say $\mathrm{AID} = j$, makes no response (due to station failure or the loss of its predecessor's frame), then the PC resumes sending the M-POLL frame which contains the remaining members on polling list after an elapsed *PIFS*. This permits the PC to retain control of the medium, thus ensuring that the idling-CFP disaster will never happen. It is worth pointing out that, in Q-PCF, the PC will not remove that station j from the polling list until its no-response event has occurred for $\mathcal{K}$, say $\mathcal{K} = 3$, consecutive superframes. During the polling period, each polled station can send a unicast, multicast, or broadcast data frame of variable length. Moreover, Q-PCF supports the direct station-to-station traffic transfer; namely, each polled station can directly send an MPDU to neighboring station(s) without relying on the relay of the AP. Figure 4.8(c) shows the MPDU frame format used in the CFP. Notice that, in IEEE 802.11, the PC has an obligation to acknowledge the receipt of data received from each polled station when performing the polling procedure. However, it is well known that real-time services, such as voice and video, can tolerate a small amount ($1\% \sim 3\%$) of dropped frames without suffering a large quality degradation [73]. To strike the right balance

between reliability and channel utilization, we consider an *optional-ACK* design for Q-PCF; in other words, each polled station shall explicitly indicate whether it requires an ACK when sending out an MPDU. In case the positive ACK is required but the MPDU was not properly received at the destination, the source station will be able to retransmit that MPDU when it is polled the next time. Figure 4.7 shows an example that all real-time stations require no acknowledgements.

Once an admitted station finishes sending its real-time flow at the present polling period and desires to tear down the connection, it shall set the *more data* bit to 0 in the *frame control* filed. When the PC receives this information, it will remove that station from the polling list. By this way, each admitted station can easily and quickly get off the polling list without performing a reassociation. (Note that IEEE 802.11 PCF [48] uses the more data bit in a different way. Specifically, in PCF, if a station polled by the PC without sufficient time to send its queued MPDU before the end of the CFP, it will respond with a Null frame and set the more data bit to 1 to allow the PC to distinguish between an empty queue and a response due to insufficient time to transfer an MPDU. However, such an unhappy event (insufficient medium occupancy time) will never occur in Q-PCF. See subsections 4.2.6 and 4.2.7.)

4.2.6 Bandwidth Allocation Procedure

To receive performance assurance and make a reservation, an application (station) shall first characterize the traffic flow that it will inject into the WLAN and specify its desired amount of bandwidth $\mathcal{G}$ that the PC must guarantee in each polling period. During the delivery of a continuous media stream, a real-time station may demand different amount of bandwidth $\mathcal{D}$ in each polling period. Obviously, in case that $\mathcal{D} > \mathcal{G}$ happens, the PC may not be able to satisfy station's bandwidth demand. Thus given $0 \leq \varepsilon < 1$, each active real-time station shall estimate the value of $\mathcal{G}$ that satisfies the inequality $\Pr[\mathcal{D} \leq \mathcal{G}] \geq 1 - \varepsilon$, where the value of ε reflects individual user's QoS requirement.

For variable bit rate (VBR) traffic (e.g., video stream) with mean μ and variance σ^2 of the bit rate, we can obtain

$$\mathcal{G} = \left(\mu + \sigma \sqrt{\frac{1-\varepsilon}{\varepsilon}} \right) \times \frac{\mathrm{SF}}{\mathrm{CDR}} \tag{4.1}$$

using the one-sided Chebyshev inequality [63], where SF is the length of the superframe and CDR is the channel data rate. In [1, 72, 73], the authors assume that VBR video traffic follows the truncated exponential distribution with the minimum bit rate α, the peak bit rate β, and the mean bit rate μ. In this case, the value of $\mathcal{G}$ can be expressed as

$$\mathcal{G} = \left[\alpha - \gamma \ln\left(\varepsilon + (1-\varepsilon)e^{\frac{\alpha-\beta}{\gamma}}\right)\right] \times \frac{\mathrm{SF}}{\mathrm{CDR}}, \tag{4.2}$$

where γ is the solution of the following nonlinear equation

$$\mu = \gamma + \frac{\alpha - \beta \times e^{\frac{\alpha-\beta}{\gamma}}}{1 - e^{\frac{\alpha-\beta}{\gamma}}}. \tag{4.3}$$

Derivations of equations (4.2) and (4.3) are shown in Appendix C. Note that the value of γ can be solved using numerical techniques. For example, the authors in [1, 72, 73] set $\alpha = 120$ K, $\beta = 420$ K, and $\mu = 240$ K; so we can get $\gamma \approx 244$ K. For constant bit rate (CBR) traffic (e.g., audio stream) with bit rate μ, we can assign

$$\mathcal{G} = \mu(1-\varepsilon) \times \frac{\mathrm{SF}}{\mathrm{CDR}}. \tag{4.4}$$

In sum, each active real-time station shall declare its determined value of $\mathcal{G}$ using the PR or RR frame during the registration period. Expectably, the higher level of performance warrant the mobile user desires, the larger value of $\mathcal{G}$ the mobile station should request, the more access fee the mobile user may be charged by the wireless service provider. The PR/RR frame format is shown in Figure 4.8(a). Each real-time station uses the *guaranteed bandwidth* field and the *demanded bandwidth* field, respectively, to inform the PC the value of $\mathcal{G}$ and its bandwidth demand in the current CFP. Besides, as shown in Figure 4.8(c), each polled station piggybacks the *demanded bandwidth* field with the MPDU to declare its required bandwidth in the next polling period. In what follows, we will present how the PC dynamically allocates bandwidth to provide isolation among admitted flows while utilizing bandwidth resources as efficiently as possible. The primary principle underlying the bandwidth allocation procedure is that all flows with demands less than their declared amounts of guaranteed bandwidth will be satisfied, while the unused CFP bandwidth will be allocated according to the weighted fair sharing scheme for the remaining flows with demands larger than their declared amounts of guaranteed bandwidth. The bandwidth allocation procedure is formally presented below.

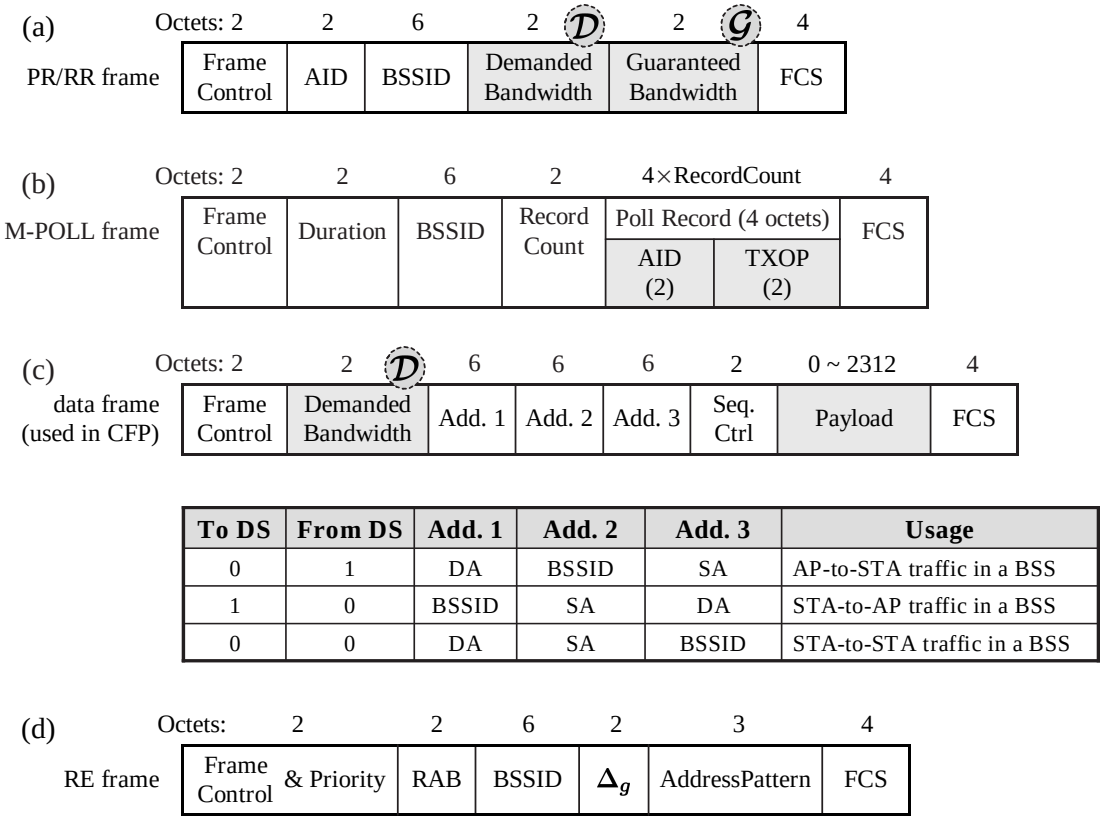

To DS	From DS	Add. 1	Add. 2	Add. 3	Usage
0	1	DA	BSSID	SA	AP-to-STA traffic in a BSS
1	0	BSSID	SA	DA	STA-to-AP traffic in a BSS
0	0	DA	SA	BSSID	STA-to-STA traffic in a BSS

Figure 4.8: The formats of Q-PCF frames.

Let $\mathcal{L} = \{A_1, A_2, \cdots, A_\ell\}$ be the polling list, where A_i denotes the station with $\mathrm{AID} = A_i$ and $\ell = |\mathcal{L}|$ equals to the cardinality of the polling list. Let $\mathcal{G}_{A_i}$ and $\mathcal{D}_{A_i}$, respectively, be the guaranteed bandwidth and demanded bandwidth declared by station A_i. Before broadcasting the M-POLL frame, the PC calculates the value

$$\begin{aligned}\Upsilon \;=\; & \mathrm{CFPMaxDuration} - (T_s + \mathrm{PIFS} + T_{\mathrm{beacon}} \\ & + \mathrm{SIFS} + T_{\mathrm{reg}} + T_{\mathrm{M-POLL}} + \mathrm{SIFS} + T_{\mathrm{CF-End}}),\end{aligned} \tag{4.5}$$

where T_{reg} is the length of the registration period. Note that the run-time admission control scheme described in subsection 4.2.7 will ensure that each admitted station A_i can acquire the medium occupancy time at least $\min\{\mathcal{D}_{A_i}, \mathcal{G}_{A_i}\}$. Hence the residual bandwidth RSB in the current CFP that can be fairly shared by those admitted stations whose demanded

bandwidth exceeds its declared guaranteed bandwidth can be expressed as

$$RSB = \Upsilon - \sum_{i=1}^{\ell} \Big(\min\{\mathcal{D}_{A_i}, \mathcal{G}_{A_i}\} + \mathrm{SIFS} \Big). \tag{4.6}$$

The PC then allocates bandwidth TXOP_{A_i} to station A_i according to the following formula.

$$\mathrm{TXOP}_{A_i} = \begin{cases} \mathcal{D}_{A_i} & \text{if } \mathcal{D}_{A_i} \le \mathcal{G}_{A_i}, \\ \min\left\{ \mathcal{D}_{A_i},\ \mathcal{G}_{A_i} + \left\lfloor RSB \times \dfrac{\mathcal{D}_{A_i} - \mathcal{G}_{A_i}}{\sum_{\mathcal{D}_{A_k} > \mathcal{G}_{A_k}} (\mathcal{D}_{A_k} - \mathcal{G}_{A_k})} \right\rfloor \right\} & \text{if } \mathcal{D}_{A_i} > \mathcal{G}_{A_i}. \end{cases} \tag{4.7}$$

Take Figure 4.7(a) for example, $\mathcal{L} = \{A_1 = 4, A_2 = 10, A_3 = 6, A_4 = 13\}$, $\mathrm{CDR} = 11$ Mbps, $T_{\mathrm{M-POLL}} = 24\ \mu s$, $T_{\mathrm{CF-End}} = 15\ \mu s$, $\mathrm{SIFS} = 10\ \mu s$, and $\mathrm{PIFS} = 30\ \mu s$; according to equations (4.5), (4.6), and (4.7), we have $\Upsilon = 3100\ \mu s$, $RSB = 300\ \mu s$, $\mathrm{TXOP}_4 = 800\ \mu s$, $\mathrm{TXOP}_6 = 600\ \mu s$, $\mathrm{TXOP}_{10} = 700 + \lfloor 300 \times \frac{400}{400+200} \rfloor = 900\ \mu s$, and $\mathrm{TXOP}_{13} = 700 + \lfloor 300 \times \frac{200}{400+200} \rfloor = 800\ \mu s$.

It is noteworthy that once a polled station A_j does not respond during the polling period, the PC will recompute the residually sharable bandwidth RSB and retransmit the M-POLL frame to announce the newly calculated TXOP values to the remaining members on polling list. Besides, in the next polling period, the PC will reserve $\mathrm{TXOP}_{A_j} = \mathcal{G}_{A_j}$ for that station A_j since its demanded bandwidth is unknown while its QoS requirement still needs to be guaranteed. Consider the example shown in Figure 4.7(b), since no response is heard from station 10, the PC rebroadcasts the M-POLL frame after an elapsed PIFS and reports that $\mathrm{TXOP}_6 = 600\ \mu s$ and $\mathrm{TXOP}_{13} = 900\ \mu s$. Further, the PC will allocate $\mathrm{TXOP}_{10} = 700\ \mu s$ for station 10 in the next polling period.

4.2.7 Run-Time Admission Control

We now present how the run-time admission control operates in Q-PCF. Since the length of CFPMaxDuration is limited, the PC shall persist in monitoring the bandwidth usage and determine when to terminate the registration process in order not to violate bandwidth guarantees made to already admitted stations. Conventional admission control approaches [16, 21, 44] require that the mobile user proposes its QoS requirement when making a reservation, and then the PC executes the admission test to decide whether to accept/reject that

connection request according to available bandwidth resources. However, such a traditional approach is not suitable for Q-PCF in that the reservation request/response frame exchange failing the admission test simply wastes the scarce wireless bandwidth. Instead, Q-PCF adopts the *mobile-assisted* admission control scheme. During the registration period, the PC evaluates the bandwidth capacity based on the bandwidth quota reserved for admitted stations and piggybacks the available bandwidth information with the PE/RE frame. Upon receipt of the PE/RE frame, active real-time stations take the admission test and check whether remaining available bandwidth is sufficient to meet their QoS needs. Those who pass the admission test can reply the PR/RR frames and report their QoS requirements; while those who fail the admission test shall abort the contention in the remaining registration period and wait for the next CFP. The benefit of this approach is that contending traffic may be further reduced. The PC then decides whether to proceed to the next PE/PR or RE/RR handshake according to received PR/RR frames. The following two principles guide the design of Q-PCF admission control algorithm.

P1. The PC must make sure that the progress of the registration process will not affect the default medium occupancy time, $\min\{\mathcal{D}_{A_i}, \mathcal{G}_{A_i}\}$, of each admitted station $A_i \in \mathcal{L}$ on the polling list. Recall that, after the end of the registration period, the PC will recalculate TXOP values for all admitted stations via equations (4.5), (4.6), and (4.7).

P2. The PC must make sure that QoS requirements of all stations on the polling list will be guaranteed even in the worst case scenario, that is, $T_s = \widehat{T}_s$ and $\mathcal{D}_{A_i} \geq \mathcal{G}_{A_i}$ for all $A_i \in \mathcal{L}$.

We now introduce some notations used to facilitate the presentation of run-time admission control algorithm.

- Let O_{CFP} denote the fixed overhead in a CFP. If $\mathcal{L} \neq \emptyset$, then we have

$$O_{\mathrm{CFP}} = \mathrm{PIFS} + T_{\mathrm{beacon}} + T_{\mathrm{M-POLL}} + T_{\mathrm{CF-End}} + 2 \times \mathrm{SIFS}. \tag{4.8}$$

- During the registration period, we let

$$\delta_1 = \begin{cases} T_{\mathrm{PE}} & \text{if the PC sends out the PE frame,} \\ T_{\mathrm{RE}} & \text{if the PC sends out the RE frame.} \end{cases}$$

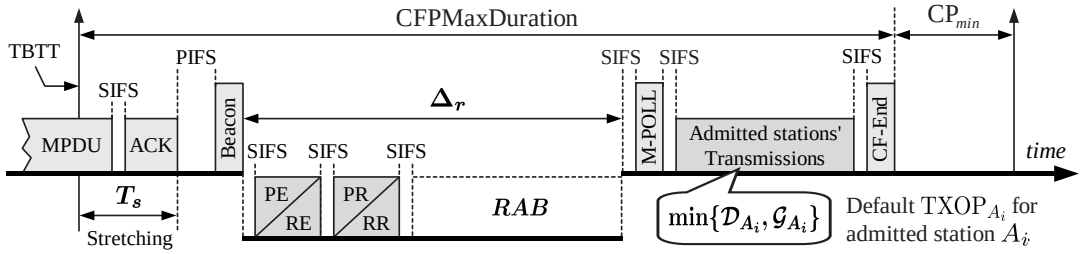

Figure 4.9: Run-time admission control process and timing relationships between RAB and Δ_r.

$$\delta_2 = \begin{cases} T_{\mathrm{PR}} & \text{if the mobile replies the PR frame,} \\ T_{\mathrm{RR}} & \text{if the mobile replies the RR frame.} \end{cases}$$

- We define two auxiliary variables Δ_r and Δ_g, respectively, to assist the PC in verifying whether **P1** and **P2** are always satisfied, where

$$\Delta_r = \mathrm{CFPMaxDuration} - \left[T_s + O_{\mathrm{CFP}} + \sum_{A_i \in \mathcal{L}} (\mathrm{SIFS} + \min\{\mathcal{D}_{A_i}, \mathcal{G}_{A_i}\}) \right] \quad (4.9)$$

and

$$\Delta_g = \mathrm{CFPMaxDuration} - \left[\widehat{T}_s + O_{\mathrm{CFP}} + \sum_{A_i \in \mathcal{L}} (\mathrm{SIFS} + \mathcal{G}_{A_i}) \right]. \quad (4.10)$$

Refer to Figure 4.9, Figure 4.10 specifies the admission control operations performed cooperatively by the PC and all active real-time stations during the registration period. Note that the RE frame format is shown in Figure 4.8(d).

4.3 Throughput Analysis

We follow the analytic model proposed in [30, 31] to evaluate the approximate throughput of the Q-PCF protocol in a single-hop WLAN, which consists of an AP and N associated stations. We consider that there are merely real-time and non-real-time stations in a WLAN; however, only the formers can get on the polling list. Let N_{rt} and N_{nrt} be the number of real-time and non-real-time stations respectively, where $N_{rt} = 2^m$ and $N_{rt} + N_{nrt} = N$. For ease of analysis, we assume that, at the start of each CFP, each non-admitted real-time

01 After broadcasting the beacon, the PC computes Δ_g, Δ_r, and the variable $RAB := \Delta_r - (\delta_1 + \delta_2 + 3 \times \mathrm{SIFS})$;
/* The variable RAB denotes the remaining available bandwidth if the PC proceeds to the next PE/PR or RE/RR handshake. */
02 **while** ($\Delta_g > 0$ **and** $RAB > 0$ **and** (registration process is not finished)) {
03 The PC sends the PE/RE frame and announces (Δ_g, RAB);
/* On receiving the PE/RE frame, each active real-time station, say A_k, takes the following admission test. */
04 **if** ($\mathcal{G}_{A_k} \leq \Delta_g$ **and** $\min\{\mathcal{G}_{A_k}, \mathcal{D}_{A_k}\} \leq RAB$)
05 Station A_k replies the PR/RR frame and declares $(\mathcal{D}_{A_k}, \mathcal{G}_{A_k})$;
06 $status$:= **receive**$(\mathrm{PR\ or\ RR})$;
/* The PC updates the channel state variable $status$ according to received PR/RR frames. */
07 **switch** ($status$) {
08 **case** SINGLE:
09 The PC places the real-time station A_k on the polling list;
10 $\Delta_g := \Delta_g - (\mathrm{SIFS} + \mathcal{G}_{A_k} + \frac{4\times 8}{\mathrm{CDR}})$;
11 $\Delta_r := \Delta_r - (\delta_1 + \delta_2 + \min\{\mathcal{G}_{A_k}, \mathcal{D}_{A_k}\} + 3 \times \mathrm{SIFS} + \frac{4\times 8}{\mathrm{CDR}})$; **break**;
/* Note that the length of the M-POLL frame will increase by 4 bytes (32 bits) if a new real-time station is admitted. */
12 **case** NULL:
13 $\Delta_r := \Delta_r - (\delta_1 + \mathrm{SlotTime})$; **break**; // $\mathrm{PIFS} = \mathrm{SIFS} + \mathrm{SlotTime}$.
14 **case** COLLISION:
15 $\Delta_r := \Delta_r - (\delta_1 + \delta_2 + 2 \times \mathrm{SIFS})$; **break**;
16 }
17 $RAB := \Delta_r - (\delta_1 + \delta_2 + 3 \times \mathrm{SIFS})$;
18 }

Figure 4.10: The Q-PCF admission control algorithm.

station has a probability p of intending to join the polling list. Thus given $|\mathcal{L}| = \ell$, we have

$$\begin{aligned} &\Pr[\text{ There are } i \text{ active real-time stations at the beginning of CFP }] \\ = \quad & R[i, N_{rt} - \ell] \;=\; \binom{N_{rt} - \ell}{i} p^i (1-p)^{N_{rt}-\ell}. \end{aligned} \tag{4.11}$$

In what follows, we will derive the average length of the polling period, which starts from the M-POLL frame and finishes before the CF-End frame (Refer to Figure 4.7). Since N_{rt} is finite, given i active real-time stations, the deterministic tree-splitting algorithm ensures that the maximum length of the registration period is finite and its value only depends on N_{rt} and i. For simplicity, we consider a homogeneous CBR traffic scenario where $\mathcal{D} = \mathcal{D}_{A_i} = \mathcal{D}_{A_j}$, $\mathcal{G} = \mathcal{G}_{A_i} = \mathcal{G}_{A_j}$, and $\mathcal{D} = \mathcal{G} \leq T_{max\text{MPDU}}$ for all real-time stations $A_i, A_j \in \mathcal{L}$ and $A_i \neq A_j$. As a result, the PC can allocate the same TXOP value, $\mathcal{D}$, to each polled station. By exploiting equation (4.10), the maximum number of admitted stations $\widehat{\ell}$ in Q-PCF is bounded by

$$\widehat{\ell} \leq \left\lfloor \frac{1}{\mathcal{G} + \text{SIFS}} (\text{CFPMaxDuration} - \widehat{T}_s - O_{\text{CFP}}) \right\rfloor. \tag{4.12}$$

Hence we tune the values of $\widehat{\ell}$ and SF such that the following inequality always holds.

$$\text{PIFS} + T_{\text{beacon}} + \text{SIFS} + \max\{T_{\text{reg}} + T_{\text{polling}}\} + T_{\text{CF-End}} \leq \text{SF} - (\text{CP}_{min} + \widehat{T}_s). \tag{4.13}$$

Note that $\max\{T_{\text{reg}} + T_{\text{polling}}\}$ is finite and its value only relies on the number of active real-time stations, $\widehat{\ell}$, and N_{rt}. In this way, the PC performs the run-time admission control during the registration period to merely maintain the polling list size. In other words, if there are already $\widehat{\ell}$ stations on the polling list, the registration process will be skipped until at least one admitted station get off the polling list. On the other hand, if there are only $\ell < \widehat{\ell}$ admitted stations, given i active real-time stations, the PC shall keep executing the collision resolution procedure during the registration period until the $\min\{\widehat{\ell} - \ell, i\}$-th SINGLE event occurs.

For each admitted real-time station, we assume that it will sojourn S superframes to complete its entire flow transmission, where S is a geometric random variable with parameter q, that is, $\Pr[S = s] = (1-q)^{s-1} q$ for $s = 1, 2, \cdots$. Because of the memoryless property of the geometric distribution, this assumption implies that each polled station will set more data bit to 0 with probability q when transmitting an MPDU. Given N_{rt} and ℓ, we define

$$W[i, N_{rt} - \ell] = \begin{cases} R[i, N_{rt} - \ell] & \text{if } 0 \leq i \leq \widehat{\ell} - \ell - 1, \\ \sum_{j=\widehat{\ell}-\ell}^{n} R[j, N_{rt} - \ell] & \text{if } \widehat{\ell} - \ell \leq i \leq N_{rt} - \ell. \end{cases} \tag{4.14}$$

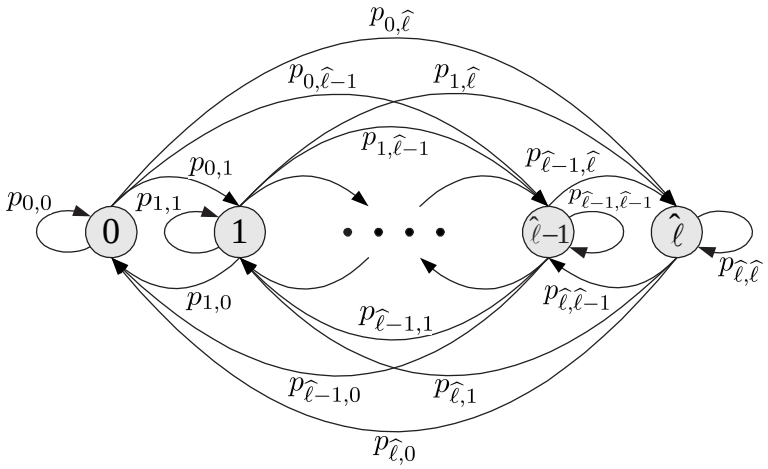

Figure 4.11: Markov chain for the Q-PCF protocol.

The state transition diagram of the Markov chain is shown in Figure 4.11, where the state π_ℓ represents the stationary probability that there are ℓ stations on the polling list. Notice that the number of admitted stations can increase up to $\widehat{\ell}$ after the end of the registration period, but can decrease by up to ℓ after the end of the polling period. Let $p_{i,j}$ be the transition probability from state i to state j and X_t be the state index in the t-th polling period. The transition probabilities can be specified as

$$\begin{aligned} p_{i,j} &= \Pr[\, X_{t+1} = j \mid X_t = i \,] \\ &= \begin{cases} \displaystyle\sum_{k=0}^{j} \binom{i}{i-j+k} q^{i-j+k}(1-q)^{j-k} W[k, N_{rt}-i] & \text{if } 0 \le j \le i \le \widehat{\ell}, \\ \displaystyle\sum_{k=0}^{i} \binom{i}{k} q^{k}(1-q)^{i-k} W[j-i+k, N_{rt}-i] & \text{if } 0 \le i < j \le \widehat{\ell}. \end{cases} \end{aligned} \tag{4.15}$$

Let $\boldsymbol{\pi} = [\, \pi_0, \pi_1, \cdots, \pi_{\widehat{\ell}}\,]$ be the stationary probability vector and $\boldsymbol{P} = [\, p_{i,j}\,]$ be the transition probability matrix. The balance equation for this Markov chain is $\boldsymbol{\pi} = \boldsymbol{\pi}\boldsymbol{P}$. From this, together with the normalization condition that $\sum_{\ell=0}^{\widehat{\ell}} \pi_\ell = 1$, we can obtain the vector $\boldsymbol{\pi}$. Accordingly, the average number of stations on the polling list is $\overline{\ell} = \sum_{\ell=0}^{\widehat{\ell}} \ell \times \pi_\ell$. Let $\overline{T}_{\text{polling}}$ denote the expected length of the polling period. We have the following result.

$$\overline{T}_{\text{polling}} = (1 - \pi_0 \times R[0, N_{rt}]) \times (T_{\text{M-POLL}} + \text{SIFS}) + \overline{\ell} \times (\mathcal{D} + \text{SIFS}). \tag{4.16}$$

In what follows, we will derive the average length of the registration period, which starts from the PE_1 frame and finishes before the M-POLL frame (Refer to Figures 4.4 and 4.6).

During the registration period, the PC evenly splits the AddressPattern $\mathcal{P}$ involved in the collision along a predetermined dimension into two subsets, $\mathcal{P}_1$ and $\mathcal{P}_2$. Note that $|\mathcal{P}_1| = |\mathcal{P}_2| = |\mathcal{P}|/2$. The PC first recursively resolves the collision of $\mathcal{P}_1$, and then resolves the collision of $\mathcal{P}_2$ independently. Given i active real-time stations, the notations $\overline{C}(N_{rt}, i, k)$, $\overline{N}(N_{rt}, i, k)$, and $\overline{S}(N_{rt}, i, k)$ denote the average number of COLLISION steps (rounds), number of NULL steps, and number of SINGLE steps, respectively, required to resolve collisions until the k-th SINGLE event takes place, where $1 \le k \le i \le N_{rt}$. Clearly, $\overline{S}(N_{rt}, i, k) = k$ regardless of N_{rt}. With each further splitting, the set of remaining possible numbers in one of the new subsets is halved. The number of active stations in the left or right subsets is according to a hyper-geometrical distribution. Based on derivations in [30, 31], $\overline{C}(N_{rt}, i, k)$ and $\overline{N}(N_{rt}, i, k)$ can be expressed in the following recursive forms.

$$\overline{C}(N_{rt}, i, k) = \begin{cases} 1 + \sum_{j=\nu}^{\omega} \frac{\binom{2^{m-1}}{i-j}\binom{2^{m-1}}{j}}{\binom{2^m}{i}} \Big[\overline{C}(2^{m-1}, i-j, i-j) + \overline{C}(2^{m-1}, j, k-i+j)\Big] & \text{if } k > i-j, \\ 1 + \sum_{j=\nu}^{\omega} \frac{\binom{2^{m-1}}{i-j}\binom{2^{m-1}}{j}}{\binom{2^m}{i}} \times \overline{C}(2^{m-1}, i-j, i-j) & \text{otherwise,} \end{cases} \tag{4.17}$$

where $N_{rt} = 2^m$, $\nu = \max\{0, i - 2^{m-1}\}$, and $\omega = \min\{0, 2^{m-1}\}$. Besides,

$$\overline{N}(N_{rt}, i, k) = \begin{cases} \sum_{j=\nu}^{\omega} \frac{\binom{2^{m-1}}{i-j}\binom{2^{m-1}}{j}}{\binom{2^m}{i}} \Big[\overline{N}(2^{m-1}, i-j, i-j) + \overline{N}(2^{m-1}, j, k-i+j)\Big] & \text{if } k > i-j, \\ \sum_{j=\nu}^{\omega} \frac{\binom{2^{m-1}}{i-j}\binom{2^{m-1}}{j}}{\binom{2^m}{i}} \times \overline{N}(2^{m-1}, i-j, i-j) & \text{otherwise.} \end{cases} \tag{4.18}$$

Notice that the actual values of $\overline{C}(N_{rt}, i, k)$ and $\overline{N}(N_{rt}, i, k)$ may be smaller than those calculated by equations (4.17) and (4.18) in that our tree-splitting algorithm can intelligently avoid some pointless polls (See Figure 4.5).

Let $\overline{T}_{\text{reg}}$ denote the expected length of the registration period. Given ℓ already-admitted stations and i active real-time stations, $\overline{T}_{\text{reg}}$ equals the sum of the average number of SINGLE steps times their duration $\delta_1 + \delta_2 + 2 \times \text{SIFS}$, plus the average number of NULL steps times their duration $\delta_1 + \text{PIFS}$, plus the average number of COLLISION steps times their duration $\delta_1 + \delta_2 + 2 \times \text{SIFS}$ until $\min\{i, \widehat{\ell} - \ell\}$ SINGLE events are recognized by the PC. The sum of all three portions has to be multiplied by the fraction $\sum_{\ell=0}^{\widehat{\ell}-1} \pi_\ell$, which represents the fraction of non-skipped registration periods. Note that it is possible to have skipping registration

periods; however, there is no cost for skipping a registration period. Accordingly, we have the following result.

$$\begin{aligned}\overline{T}_{\rm reg} \;=\; & \sum_{\ell=0}^{\widehat{\ell}-1} \pi_\ell \times \Big\{ R[0, N_{rt}-\ell] \times (\delta_1 + \mathrm{PIFS}) + R[1, N_{rt}-\ell] \times (\delta_1 + \delta_2 + 2 \times \mathrm{SIFS}) \\ & + \sum_{i=2}^{N_{rt}-\ell} R[i, N_{rt}-\ell] \times \Big[(\delta_1 + \delta_2 + 2 \times \mathrm{SIFS}) \times (\overline{C}(N_{rt}, i, \widehat{\ell}-\ell) + \overline{S}(N_{rt}, i, \widehat{\ell}-\ell)) \\ & + (\delta_1 + \mathrm{PIFS}) \times \overline{N}(N_{rt}, i, \widehat{\ell}-\ell) \Big] \Big\}. \end{aligned} \tag{4.19}$$

Let $\overline{\mathrm{CP}}$ be the expected length of the contention (DCF) period. By exploiting equations (4.16) and (4.19), we obtain

$$\overline{\mathrm{CP}} = \mathrm{SF} - (\mathrm{PIFS} + T_{\rm beacon} + \mathrm{SIFS} + \overline{T}_{\rm reg} + \overline{T}_{\rm polling} + T_{\rm CF-End}). \tag{4.20}$$

We are finally in the condition to determine the normalized system throughput $\mathcal{S}$, defined as the fraction of time, during which the channel is being used to successfully transmit data frames. Let $\mathcal{S}_{\rm DCF}(N_{nrt})$ be the normalized throughput of DCF in the presence of N_{nrt} non-real-time stations and its value can be found in [6, 77]. When Q-PCF and DCF coexist in a WLAN, we can express $\mathcal{S}$ as the ratio

$$\begin{aligned}\mathcal{S} \;&=\; \frac{E[\,\text{time used for successful data transmission in a superframe}\,]}{E[\,\text{length of a superframe}\,]} \\ &=\; \frac{\overline{\ell} \times \mathcal{D} + \overline{\mathrm{CP}} \times \mathcal{S}_{\rm DCF}(N_{nrt})}{\mathrm{SF}}. \end{aligned} \tag{4.21}$$

4.4 Performance Evaluation

We have developed event-driven simulators to verify the performance of Q-PCF and compare our results to the PCF. Each simulation run was executed for a duration of 1.8×10^8 μs in a single-hop wireless LAN with one AP and 256 associated mobile stations. Table 4.1 summaries the system parameter values, which follow the IEEE 802.11 MAC specifications for the direct sequence spread spectrum (DSSS) physical layer [48].

4.4.1 Traffic Models and Performance Metrics

The following three types of traffic are considered in our simulations.

Table 4.1: System parameters used in the simulation.

Parameter	Value
Channel bit rate	11 Mbps
Superframe length	25 ms
SIFS	10 μs
PIFS	30 μs
DIFS	50 μs
SlotTime	20 μs
RTS frame length	20 bytes
CTS frame length	14 bytes
ACK frame length	14 bytes
CWmin	31 slots
CWmax	1023 slots
MAC header	24 bytes
PHY header	16 bytes
Reassociation Request frame length	38 bytes
Reassociation Response frame length	34 bytes
Beacon frame length	57 bytes
Null frame length	44 bytes
PE frame length	18 bytes
PR frame length	16 bytes
RE frame length	20 bytes
RR frame length	19 bytes
M-POLL frame length	$16 + 4\times$ polling list size
CF-End frame length	20 bytes

Table 4.2: Traffic parameter values for the CBR and VBR models.

CBR Traffic Parameter	Value
Conversation length	180 sec
Principle talkspurt	1.00 sec
Principle silent gap	1.35 sec
Data bit rate (CBR)	64 Kbps
Maximum voice frame tolerable delay	25 ms
VBR Traffic Parameter	**Value**
Peak bit rate	420 Kbps
Minimum bit rate	120 Kbps
Mean bit rate	240 Kbps
Mean state holding time	160 ms
Mean video call length	180 sec
Maximum video frame tolerable delay	50 ms

1) *Data Traffic*: The arrival of data frames at each mobile station follows the Poisson distribution with the mean value λ. The data payload size is fixed at 2312 bytes. Since the data frame is quite large, each DCF-station shall employe the RTS/CTS exchange procedure to transmit data frames.

2) *CBR Voice Traffic*: The voice traffic is generally modelled as a two-state (ON/OFF) Markov process with talkspurt and silent states. In the talkspurt state, the CBR station generates a continuous bit-stream; in the silent state, no voice frame will be generated. The mean values for talkspurt duration and silent duration are 1.00 second and 1.35 second respectively. Notice that, when measuring the Q-PCF capacity (maximum polling list size), we will consider the always-ON model; that is, the silent duration is 0. Voice frames that can not be transmitted within the maximum tolerable time will be dropped.

3) *VBR Video Traffic*: The video traffic is modelled as a multi-state model where a state generates a continuous bit stream for a certain holding duration [1, 73]. The bit rate values of

different states are obtained from a truncated exponential distribution with a minimum and a maximum bit rate values. The state holding time follows an exponential distribution with the mean 160 ms. Video frames that can not be transmitted within the maximum tolerable time will be dropped.

Table 4.2 summaries the traffic parameter values. We assume that voice traffic has the highest priority since its maximum tolerable delay is minimum among all kinds of traffic. The video traffic has the second highest priority, and the data traffic has the lowest priority. For ease of exposition, we assume that each CBR (VBR) station selects the same value of $\varepsilon_{\mathrm{CBR}}$ ($\varepsilon_{\mathrm{VBR}}$) and declares the same value of $\mathcal{G}_{\mathrm{CBR}}$ ($\mathcal{G}_{\mathrm{VBR}}$) during the registration period. Moreover, in Q-PCF (PCF), real-time stations on the polling list are polled in a FCFS (round-robin) fashion. Two performance metrics considered in the simulation study are defined as follows.

1) *Goodput*: The fraction of time devoted by real-time (CBR/VBR) stations and non-real-time (DCF) stations to successfully transmit their pure payload. Note that goodput excludes time lost to protocol overhead, collisions, and retransmissions [44].

2) *Frame Delay Dropped Rate* (*FDDR*): The FDDR is defined as the fraction of dropped voice/video frames caused by violating the delay constraints.

4.4.2 Simulation Results

To verify the correctness of the run-time admission control scheme, we measure the Q-PCF capacity (the maximum number of real-time stations that the PC can admit) under the pure CBR/VBR traffic models through the simulation program and equation (4.12). For the pure CBR (VBR) traffic scenario, we let the number of CBR (VBR) stations 150 (0) and the the number of VBR (CBR) station 0 (150). Besides, $\varepsilon_{\mathrm{CBR}} = 0$ and $\varepsilon_{\mathrm{VBR}} = 0.5$. In Figure 4.12(a), we can find that the maximum number of real-time stations admitted by Q-PCF exactly reaches the theoretical upper bound derived by equation (4.12). When the value of $\varepsilon_{\mathrm{CBR}}$ or $\varepsilon_{\mathrm{VBR}}$ varies, Figures 4.14(b) and 4.15(b) indicate that, in Q-PCF, the maximum polling list size also matches the theoretical upper bound exactly. These results justify the superiority of the mobile-assisted admission control scheme. Recall that, in IEEE 802.11, all communications in an infrastructure WLAN shall be relayed through the AP. This implies

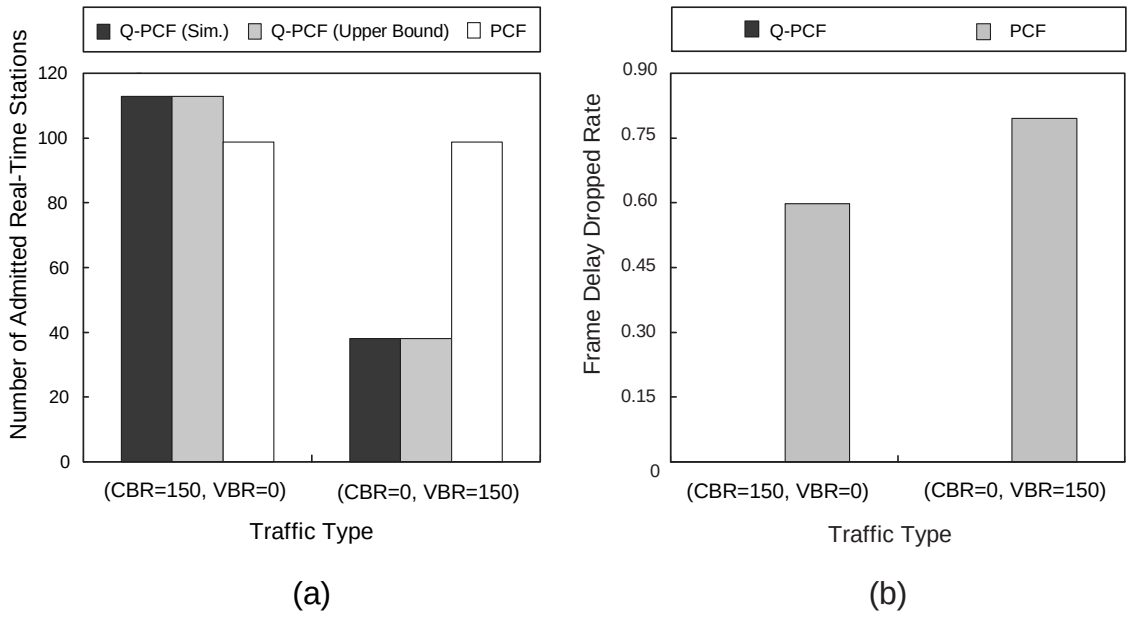

Figure 4.12: (a) The number of real-time stations admitted by the Q-PCF/PCF during the entire simulation time. (b) Comparisons of the derived FDDR by Q-PCF and Q-PCF under the pure CBR and VBR traffic environments. ($\varepsilon_{\rm CBR} = 0$, $\varepsilon_{\rm VBR} = 0.5$, and $\lambda = 0.1$ frames/sec/DCF-station.)

that, in saturated condition, the optimal polling list size in PCF should be about half that of the Q-PCF. Since PCF does not perform any admission control, the PC admits a large number of real-time stations, which may be far beyond its capacity. In this case, several real-time stations will not be polled during the entire CFP. As a result, the FDDR of PCF is remarkably large. On the other hand, Figure 4.12(b) shows an interesting result that the FDDR of Q-PCF is very close to 0 even $\varepsilon_{\rm VBR} = 0.5$. The reasons are as follows. Let $\mathcal{D}_{\rm VBR}$ be a random variable that equals to the demanded bandwidth of each VBR station. By definition, when $\varepsilon_{\rm VBR} = 0.5$, $\mathcal{G}_{\rm VBR}$ is the *median* of $\mathcal{D}_{\rm VBR}$ [63]; that is, $\Pr[\mathcal{D}_{\rm VBR} \geq \mathcal{G}_{\rm VBR}] = \Pr[\mathcal{D}_{\rm VBR} \leq \mathcal{G}_{\rm VBR}]$. Recall that Q-PCF bandwidth allocation scheme tries to allocate unused bandwidth from those VBR stations whose bandwidth needs are less than $\mathcal{G}_{\rm VBR}$ to those stations whose bandwidth needs are greater than $\mathcal{G}_{\rm VBR}$. Since the cardinalities of these two sets are statistically equal, we can expect that, in this case, the FDDR is 0.

To acquire contention-free services, we hope that real-time stations can promptly register with the PC and the registration process should not be adversely affected by the low-priority

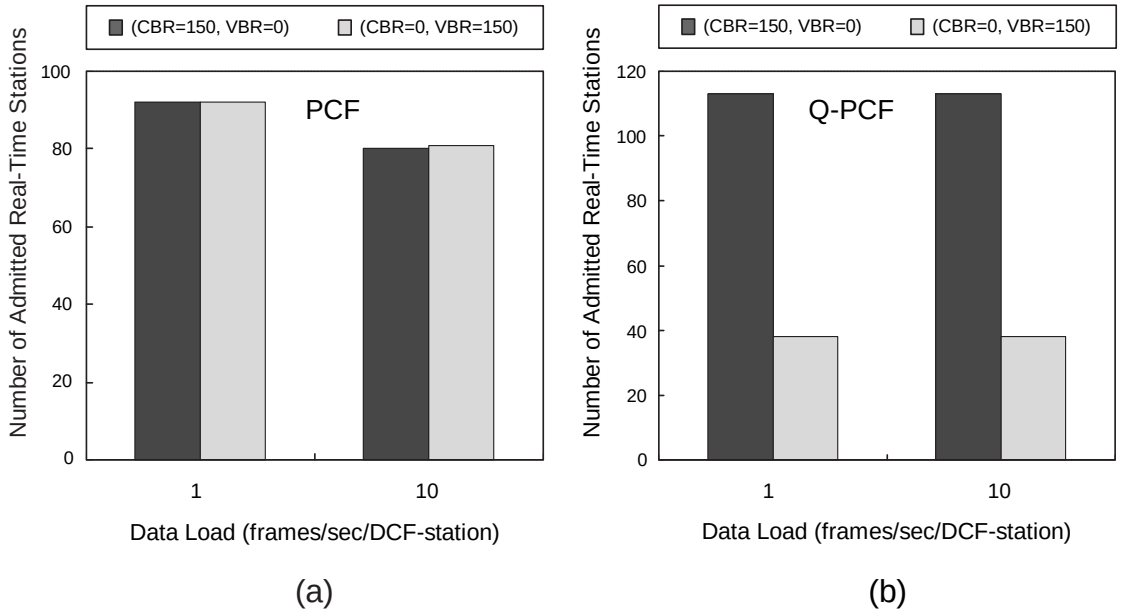

Figure 4.13: The number of CBR/VBR stations admitted by the Q-PCF/PCF during the entire simulation time under the different asynchronous data load. ($\varepsilon_{\mathrm{CBR}} = 0$ and $\varepsilon_{\mathrm{VBR}} = 0.5$.)

(DCF) stations. Since, in IEEE 802.11, the registration (reassociation) process relies on DCF, we can find that, in Figure 4.13(a), the number of admitted real-time stations decreases as the data load becomes heavier. However, in Figure 4.13(b), we observe that the number of admitted real-time stations in Q-PCF is not affected by the behaviors of non-real-time stations at all. This result justifies the creation of the registration period dedicated to real-time stations.

Next, we explore the relationships among ε, goodput, and FDDR for the Q-PCF protocol under the pure CBR traffic condition. For CBR sources, we consider the always-ON model. Figure 4.14(b) indicates that the number of admitted CBR stations is linearly proportional to the value of $\varepsilon_{\mathrm{CBR}}$. This is expected since, according to equation (4.4), a larger $\varepsilon_{\mathrm{CBR}}$ will lead to a smaller $\mathcal{G}_{\mathrm{CBR}}$. As the value of $\mathcal{G}_{\mathrm{CBR}}$ decreases, more CBR stations can be accommodated. Figure 4.14(a) shows that, when $\varepsilon_{\mathrm{CBR}} < 0.1$, the goodput and FDDR increase gradually as the value of $\varepsilon_{\mathrm{CBR}}$ increases. However, when $\varepsilon_{\mathrm{CBR}} \geq 0.1$, the FDDR rises steeply and the goodput declines suddenly. This is because, even $T_s = 0$, the protocol overhead plus the total bandwidth demanded by all CBR stations in a CFP exceeds the system

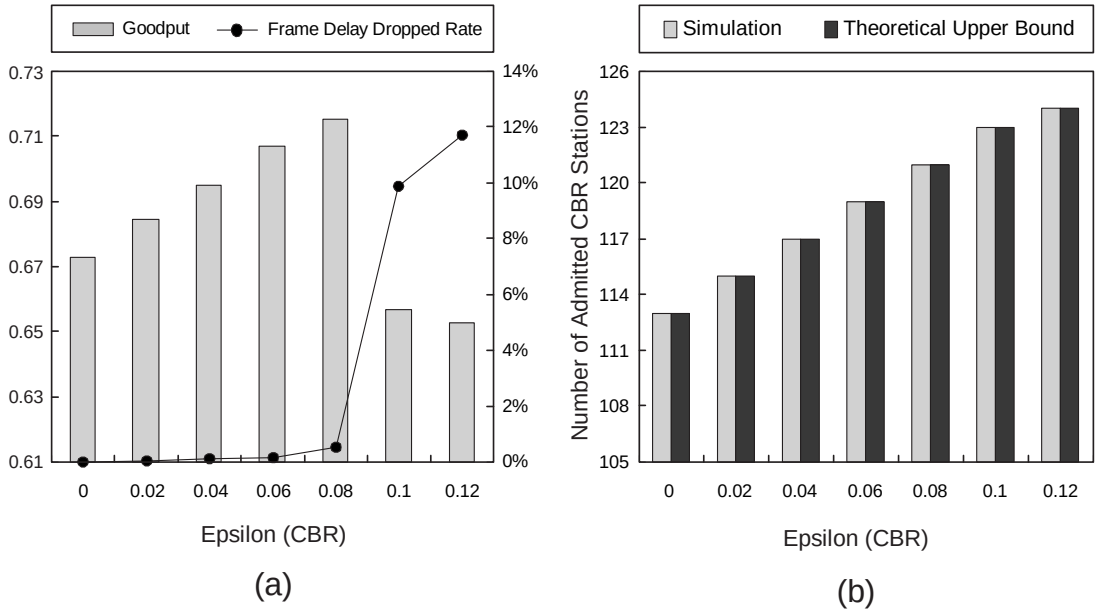

Figure 4.14: (a) The relationships among $\varepsilon_{\mathrm{CBR}}$, goodput, and FDDR for Q-PCF under the pure CBR traffic environment. (b) As the value of $\varepsilon_{\mathrm{CBR}}$ increases, so does the number of admitted CBR stations. ($\mathrm{CBR} = 150$, $\mathrm{VBR} = 0$, and $\lambda = 0.1$ frames/sec/DCF-station.)

capacity (CFPMaxDuration). In this case, the value of FDDR naturally rises to $\varepsilon_{\mathrm{CBR}}$; meanwhile, the goodput plunges due to a rapid amount of dropped frames. Figure 4.15 depicts the relationships among $\varepsilon_{\mathrm{VBR}}$, goodput, and FDDR under the pure VBR traffic condition. We see that, as the value of $\varepsilon_{\mathrm{VBR}}$ increases, so does the number of admitted VBR stations. On the other hand, the FDDR increases and the goodput decreases when $\varepsilon_{\mathrm{VBR}} \geq 0.6$. The reasons are similar to those described above.

Finally, we examine the performance of Q-PCF and PCF under the heterogeneous traffic scenarios. We let the number of CBR stations 100 and the number of VBR stations 30. In addition, $\varepsilon_{\mathrm{CBR}} = 0.02$ and $\varepsilon_{\mathrm{VBR}} = 0.5$. For CBR sources, we consider the ON-OFF model. Figure 4.16(a) reveals that, when $\lambda \geq 1.9$, the goodput of Q-PCF achieves nearly 90%, while the goodput of PCF is only around 47%. Figure 4.16(b) reveals that the FDDR of Q-PCF is very close to 0 regardless of DCF traffic load; by contrast, the FDDR of PCF is over 50% in most situations. The results conclude that Q-PCF delivers high goodput and indeed provides QoS guarantees for real-time multimedia applications.

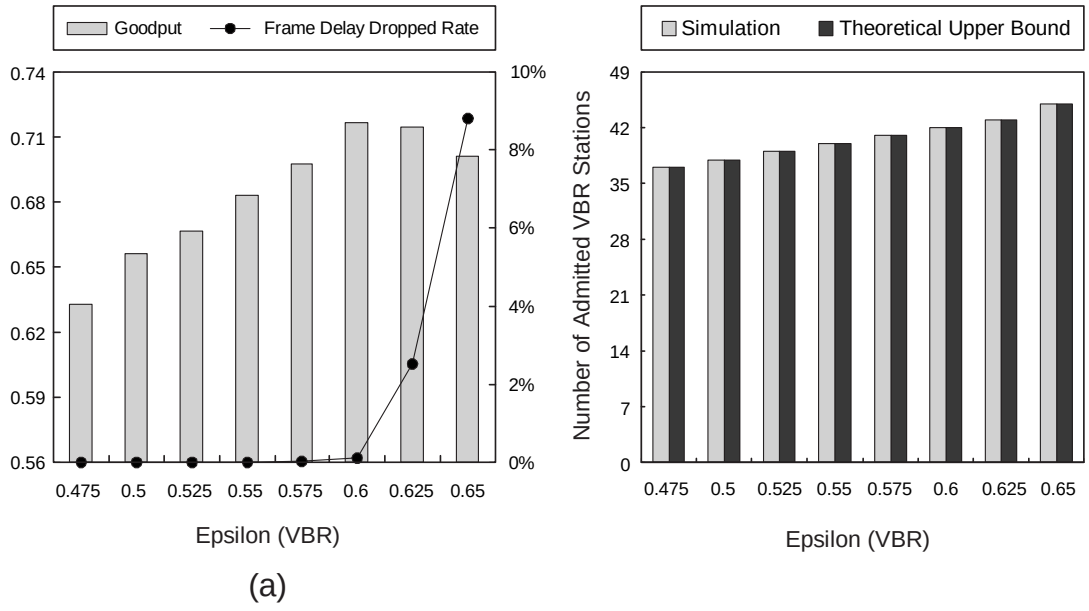

Figure 4.15: (a) The relationships among $\varepsilon_{\mathrm{VBR}}$, goodput, and FDDR for Q-PCF under the pure VBR traffic environment. (b) As the value of $\varepsilon_{\mathrm{VBR}}$ increases, so does the number of admitted VBR stations. ($\mathrm{CBR} = 0$, $\mathrm{VBR} = 150$, and $\lambda = 0.1$ frames/sec/DCF-station.)

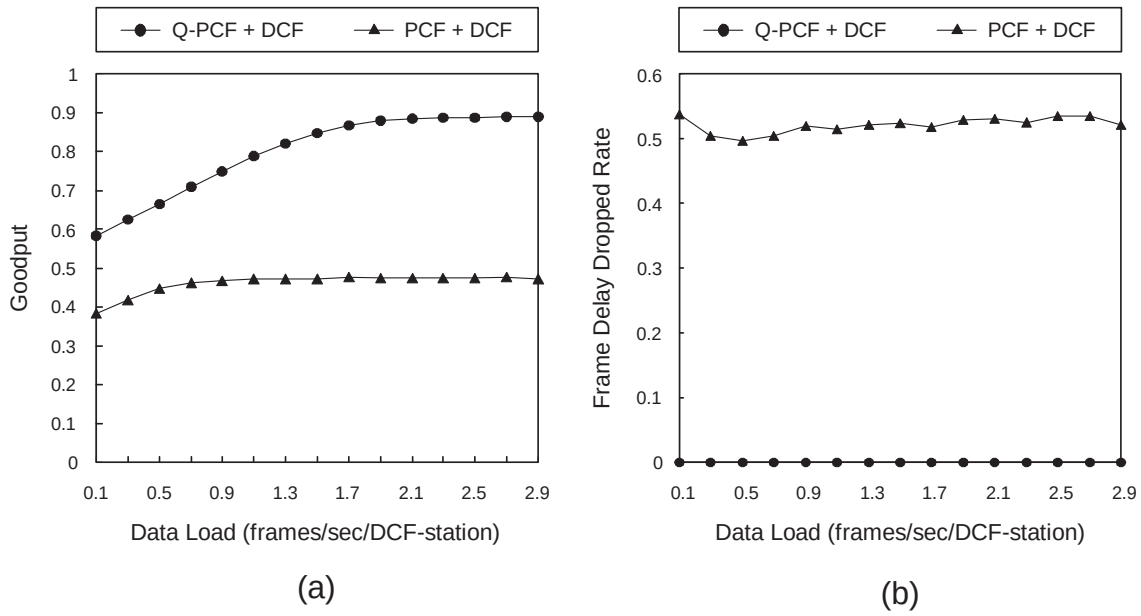

Figure 4.16: Performance comparison for (Q-PCF+DCF) versus (PCF+DCF) under the heterogeneous traffic scenarios. (a) Goodput. (b) FDDR. ($\mathrm{CBR} = 100$, $\mathrm{VBR} = 30$, $\varepsilon_{\mathrm{CBR}} = 0.02$, and $\varepsilon_{\mathrm{VBR}} = 0.5$.)

4.5 Summary

In this chapter, we have proposed a new novel polling-based MAC protocol, called Q-PCF, which can coexist with the IEEE 802.11 DCF, while supporting real-time multimedia applications in an infrastructure WLAN. The Q-PCF protocol not only overcomes the entire drawbacks of the IEEE 802.11 PCF but also possesses several distinctive characteristics. First, Q-PCF adopts the handshaking technique to provide multiple priority levels and guarantees that high-priority stations always get on the polling list earlier than low-priority stations. Second, Q-PCF adopts the deterministic tree-splitting algorithm as the contention-based reservation scheme such that real-time stations can register with the PC in bounded time. Third, Q-PCF employs the multipoll technique to reduce the polling overheads and support directional data transfer. In addition, Q-PCF guarantees that the idling-CFP disaster will never occur. Forth, Q-PCF adopts dynamic bandwidth allocation scheme to support CBR/VBR transportation and offer per-flow probabilistic performance assurances. Fifth, Q-PCF integrates the unique mobile-assisted admission control process into the registration procedure so that the PC can admit as many newly arriving flows as possible, while not violating already-admitted flows' guarantees. Sixth, the performance of Q-PCF has been evaluated via both mathematical analysis and simulation experiments. Simulation results do confirm that Q-PCF much outperforms PCF both in terms of goodput and frame delay dropped rate even under the heterogeneous traffic scenarios. Last but not least, we believe that the Q-PCF protocol can be easily applied to the present IEEE 802.11 compliant products without major modifications.

Chapter 5

Asynchronous Power Management Protocols for Ad Hoc Networks

5.1 Introduction

With the evolutionary advancement of wireless technologies and the proliferation of portable computers, the applications of the MANET (*mobile ad hoc network*) are getting more and more important, especially in the emergency, military, entertainment, and outdoor business environments, in which instant fixed infrastructure or centralized administration is difficult or too expensive to install. However, the finite and nonrenewable battery power of mobile stations represents one of the greatest limitations to the utility of MANETs. It is well known that, due to technology limitations, the battery capacity will not be dramatically promoted in the not-so-distant future. Therefore, it is essential to investigate power saving strategies to prolong the lifetime of both individual nodes and the network. One way to reduce energy consumption is simply to use low-power hardware components. Another way is to adopt software-controllable power management protocols that allow transceivers to be used in energy conserving ways. One of the most common techniques to attain this goal is the *discontinuous reception* [64]; namely, battery power could be greatly saved by periodically turning the radio off when not in use since the network interface may often be idle [26]. However, in such environments, it may take longer time to activate the link between power-saving (PS, for short) neighbors. Definitely, a good power management protocol ought to minimize

the power consumption without significantly deteriorating the connectivity or capacity of the network.

5.1.1 Synchronous Power Management Protocols

In the literature, several power management protocols for wireless networks have been proposed [9, 43, 48, 57, 64, 67, 68, 78]. The authors in [57] presented TDMA-based birthday protocols for saving energy during the neighbor discovery phase in static wireless sensor networks. The IEEE 802.11 MAC (medium access control) protocol [48] specifies different power saving mechanisms for use within the infrastructure wireless LAN and the independent basic service set (IBSS) respectively. In an IBSS (also known as a single-hop MANET), all stations are within each other's transmission range and time is divided into fixed-sized *beacon intervals*. Clock synchronization by periodic broadcast of a *beacon* frame is required to ensure that all PS stations wake up prior to each *target beacon transmission time* (TBTT). If a sender intends to transmit buffered frames to a destination station that is in a PS mode, the sender should first announce a directed *ad hoc traffic indication message* (ATIM) frame during the *ATIM window*, in which all PS stations are awake. Upon receipt of a directed ATIM frame, the PS station shall acknowledge the ATIM frame and remain in the awake state for the entire beacon interval. The PS station that neither transmitted nor received a directed ATIM frame may return to the *doze* state at the end of the ATIM window. In the doze state, the transceivers are powered down and stations are unable to transmit or receive. Immediately following the ATIM window, the pending buffered frames should be sent using the conventional DCF (distributed coordination function) access procedure. Figure 5.1 illustrates an example of power management in an IEEE 802.11 ad hoc network. The more complete and detailed explanation can be found in [48]. The authors in [81] discussed different aspects of power saving addressed in IEEE 802.11 and HYPERLAN standards. They further showed that any fixed size of the ATIM window can not perform very well in all situations. Hence the authors in [43] proposed several energy conserving optimization techniques, called DPSM, for IEEE 802.11. In DPSM, each station in an IBSS can dynamically tune its ATIM window size according to observed network conditions. Unfortunately, all the above-mentioned protocols [43, 48, 57, 81] are only suitable for synchronous environments.

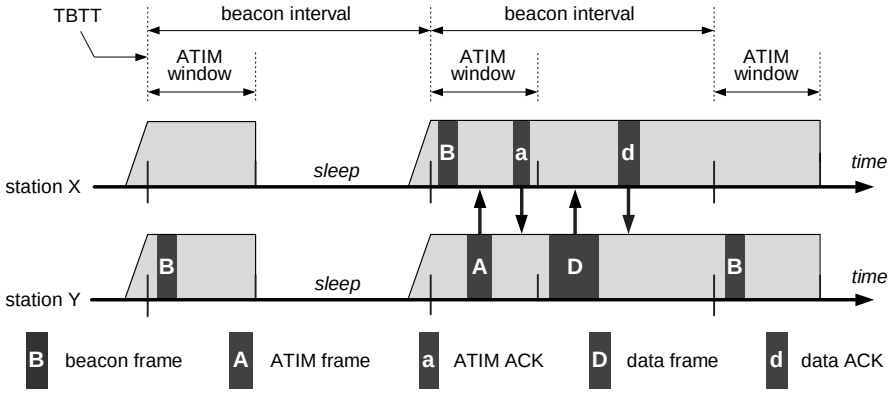

Figure 5.1: Power management operation in an IBSS. A beacon frame is broadcasted after each TBTT. All PS stations stay awake for the ATIM window as shown in the first beacon interval, and go to sleep again if no frame is buffered for them. In the second beacon interval, station Y announces a buffered data frame for station X using a directed ATIM frame. X replies by sending an ATIM-ACK, and both X and Y remain active during the entire beacon interval. After the ATIM window, Y sends the data frame, and X acknowledges its receipt.

5.1.2 Challenges

When designing power management protocols for a large-scale MANET, we will unavoidably encounter three major challenges:

- *Beacon contention*: In IEEE 802.11 [48], every station has to periodically compete with others to broadcast its beacon at around TBTT. Due to the absence of RTS/CTS dialogue, the deficiency of backoff mechanism, and the lack of acknowledgement, the beacon broadcast procedure defined by IEEE 802.11 is highly unreliable. Besides, the higher the node density, the more serious the beacon contention and collisions. As a result, the out of synchronization problem easily arises even in a small IBSS configuration [38].

- *Timing synchronization*: It is extremely difficult (if not impossible) for all nodes to keep synchronized at all times because of severe beacon contention, unpredictable node mobility, and heavy traffic of timing information exchange. Although the Global Positioning System (GPS) can simplify the synchronization problem, it is not necessarily true that all future mobile stations will be equipped with GPS receivers. Once stations get out of synchronization, then IEEE 802.11 power saving operation may

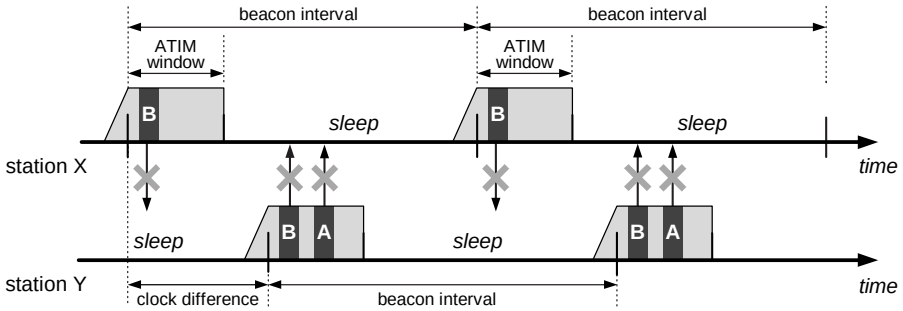

Figure 5.2: Because of out of synchronization, PS stations, X and Y, are unable to receive each other's beacons or ATIM frames.

completely fail since PS neighbors may forever lose each other's beacons or ATIM frames. See Figure 5.2.

- *Neighbor maintenance*: For an active station, it may be unaware of a PS station at its neighborhood since a PS station will reduce its transmitting activity. For a PS station, it may be unaware of a station at its neighborhood since its listening activity is confined to the ATIM window. Besides, without a consistent common reference clock, a PS station may wake up too late to hear neighbors' signals. Such incorrect neighbor information may be an obstacle to many existing protocols, such as zone routing protocol [36] and neighbor coverage-based broadcasting protocol [79], whose success relies on accurate neighbor table. To make matters worse, since PS stations do not stand much chance of being detected, if some of them constitute a *vertex cutset*, whose removal will disconnect the network, then the *virtual network partition* problem [78] may arise.

Power management protocols introduced in [9, 64, 67, 68, 78] are asynchronous. The authors in [64] proposed the PSPA protocol for reducing the power consumption of portable stations operating in a mobile network with a *base station* support. The base station will keep on sending page messages whenever there are buffered packets. Each mobile station may control its duty cycle relative to its current needs. The authors in [9] assume that a sleeping station can be remotely activated by a wake-up signal using a *remote activated switch* (RAS) receiver. With the aid of RAS, stations can select different sleep patterns to enter various sleep states depending on their battery status and quality of service. The authors in [67, 68]

Table 5.1: Comparison of power management protocols for ad hoc networks.

protocol	timing synchronization	special hardware support	beacon transmission
IEEE 802.11 [48]	yes	no	not scalable
Birthday [57]	yes	no	scalable
DPSM [43]	yes	no	not scalable
PSPA [64]	no	base station	not handled
Chiasserini *et al.* [9]	no	remote activated switch	not handled
STEM [67, 68]	no	dual transceivers	not handled
Tseng *et al.* [78]	no	no	not scalable
Ours	no	no	scalable

presented the STEM protocol that trades power savings for path setup latency in wireless sensor networks, in which all stations are equipped with *dual transceivers*. Unfortunately, these asynchronous protocols [9, 64, 67, 68] require special hardware support. In addition, they did not take neighbor maintenance into consideration.

5.1.3 Our Contributions

Currently, IEEE 802.11 compliant interface cards are greatly popular. However, three above-mentioned challenges pose a strong demand of redesigning IEEE 802.11 power saving mechanism for asynchronous MANETs, in which the clock difference between any pair of stations ranges from zero to any large bounded number. Accordingly, we will make minor modifications to IEEE 802.11 so that our new protocols have the following characteristics. (i) The delivery of a beacon frame is relatively reliable and insensitive to the nodal density, thus alleviating the beacon contention problem substantially. (ii) Our protocols achieve energy conservation and flexible neighbor maintenance in an integrated manner. Precisely, given a predefined number $0 \leq \varepsilon \ll 1$, our solutions carefully arrange the awake/sleep patterns such that any two PS neighbors, regardless of their clock difference, are able to discover each other in finite time $\mathcal{T}$ with high probability $1 - \varepsilon$. (iii) The mechanisms for delivering

data frames to PS stations have no need to rely on clock synchronization or any special hardware support. More specifically, in our protocols, each PS station piggybacks its timestamp and awake/sleep pattern with the beacon frame. Once station X received a beacon from PS station Y, X is capable of predicting the timing of the Y's ATIM windows via their clock difference and Y's awake/sleep pattern. By this way, buffered frames destined for PS station Y will be eventually delivered.

Recently, based on IEEE 802.11, three asynchronous power saving protocols for a multihop MANET have been proposed in [78], whose work is the most relevant to ours. Compared with their protocols, two major distinctive contributions are described as follows. (i) While the beacon contention problem is completely ignored in [78]; in this chapter, we borrow the idea from the design of HYPERLAN [2] to propose a new backoff mechanism such that the probability of successful *broadcast* of a beacon frame is drastically boosted. While some modified backoff algorithms have been designed for achieving maximum throughput [7] or real-time transmissions [22]; our backoff scheme is specifically geared towards scalable beacon broadcast. While some proposed MAC-level broadcast protocols are based on black burst signals [2] or handshaking [18], which are not regular schemes defined in IEEE 802.11; our scalable beacon broadcast protocol is completely compatible with IEEE 802.11. (ii) In this chapter, we design three randomized asynchronous power management protocols, called *randomized coterie-based*, *naive cyclic finite projective plane-based* (CFPP-based) and *interleaving CFPP-based* protocols. In contrast with deterministic approaches [78], our randomized schemes achieve additional energy saving gains in neighbor maintenance by also exploiting the *accuracy* dimension. Namely, our protocols may fail to discover a link which joins two PS stations; however, such a neighbor discovery loss can be bounded to any predefined small number ε. Intuitively, the higher the neighbor discovery probability, the more battery power the protocol may consume. In a nutshell, our protocols can offer the network designers full flexibility in trading energy, latency, and accuracy versus each other by appropriately setting ε and $\mathcal{T}$. Especially, the CFPP-based protocol always guarantees a 100% neighbor discovery probability even though it is a randomized algorithm. Above all, we obtain a nearly 75% reduction in *radio active ratio* (which will be defined in Section 5.3) for the CFPP-based protocol as compared with the most energy conserving protocol in [78].

The remainder of this chapter is organized as follows. In Section 2, the new backoff

mechanism for scalable beacon transmission is proposed and analyzed. In Section 3, we present and analyze three randomized asynchronous power management protocols, in which flexible neighbor maintenance is also realized. The directed frame transfer procedure based on our power saving mechanisms is presented in Section 4. In Section 5, simulation experiments are conducted to evaluate the proposed protocols. Section 5 demonstrates simulation results and Section 6 concludes this chapter.

5.2 Scalable Beacon Transmission

5.2.1 General Structure of the Beacon Interval

In mobile ad hoc networks, the beacon frame plays an important role in neighbor maintenance. Periodically, a station should advertise its presence to its neighbors by broadcasting a beacon frame. On the other hand, a station should maintain its up-to-date neighbor table according to its newly received beacons. In IEEE 802.11, every station prepares to transmit a beacon frame at each TBTT. To avoid collisions among beacons, each station calculates a random delay uniformly distributed in the range between 0 and CW (*contention window*) before sending out its beacon. If a beacon arrives before the random delay timer has expired, the pending beacon transmission should be cancelled [48]. Because of the cancellation of the beacon transmission, the chance for the PS station to announce its existence is significantly reduced. Hence the authors in [78] modified the IEEE 802.11 so each station shall persist in explicitly sending its beacon during the ATIM window even others' beacons have been heard. Following this principle, we design and show the new general structure of a beacon interval in Figure 5.3. As the Figure 5.3(a) indicates, time is divided into fixed-sized beacon intervals. Each beacon interval includes four windows, named *beacon window*, ATIM window, *data window*, and *active window*. During the beacon window, multiple beacon frames are allowed and every station should broadcast its beacon via our proposed beacon transfer procedure. During the active window, a PS station should turn its radio on and take proper actions as usual. The ATIM window is responsible for ATIM related traffic and the data window is responsible for data traffic. Excluding these windows, a PS station that does not have any traffic to send or receive may enter the doze state.

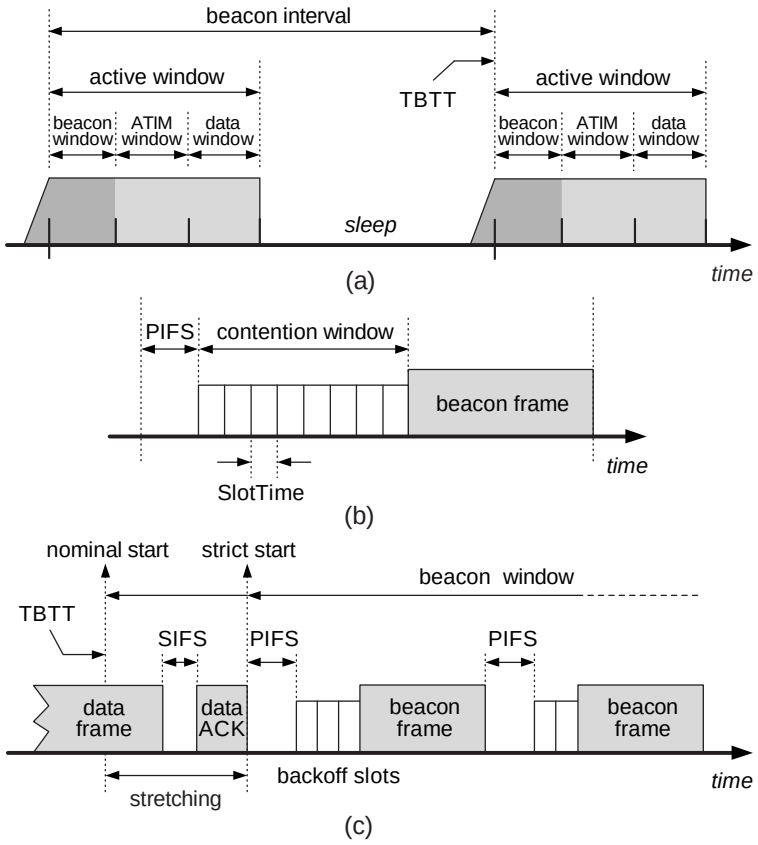

Figure 5.3: (a) The general structure of the beacon interval. (b) Beacon transfer procedure. (c) An example of beacon transmission and the stretching event.

5.2.2 Beacon Transfer Procedure

In IEEE 802.11 [48], after each TBTT, all stations contending for the beacon transmission *immediately* dive into the random backoff stage when the medium becomes idle. However, in our implementations, as shown in Figure 5.3(b), every station should first wait for the duration of $T_{\rm IFS} = {\rm PIFS}$ (Priority InterFrame Space) before performing the backoff procedure. The design considerations for setting $T_{\rm IFS}$ are described as follows. (i) Claim $T_{\rm IFS} < {\rm DIFS}$. Varying interframe spaces including SIFS (Short InterFrame Space), PIFS, and DIFS (Distributed InterFrame Space) are defined in IEEE 802.11 to provide different priority levels for different types of frames. Besides, SIFS $<$ PIFS $<$ DIFS. We argue that the beacon management frame should take priority over the data frame. (ii) Claim $T_{\rm IFS} > {\rm SIFS}$. Due to a busy medium, the strict start of the beacon window may begin later than the nominal start

of the beacon window. Such a phenomenon is called *stretching* and we show the stretching event in Figure 5.3(c). After TBTT, if a PS station unaware of the NAV (network allocation vector) set during the previous beacon interval selects the zero backoff time and transmits a beacon frame immediately after the medium becomes idle, then that beacon frame may destroy an on-going stretching directed data frame transmission, which includes the associated ACK and the intervening *SIFS*. Therefore, we set $T_{\mathrm{IFS}} = \mathrm{PIFS}$ to avoid such an undesired event.

After the PIFS medium idle time, the station shall then generate a random backoff period $\mathrm{SlotTime} \times B$, $0 \leq B \leq CW$, for an additional deferral time before transmitting a beacon. Definitely, the station choosing the smallest backoff time among the competitors will seize the medium. If conforming to the IEEE 802.11 conventional approach, B will be a random variable with *discrete uniform* distribution over the set $\{0, 1, 2, \ldots, CW\}$, and we have

$$\Pr[B = b] = \frac{1}{CW + 1} \qquad 0 \leq b \leq CW. \tag{5.1}$$

However, in our proposed scheme, $\mathcal{B}$ is a *reverse truncated geometric* random variable with parameter q, $0 < q < 1$. And we assign

$$\Pr[\mathcal{B} = b] = \begin{cases} q^{CW} & \text{if } b = 0, \\ (1 - q)q^{CW-b} & \text{if } 1 \leq b \leq CW. \end{cases} \tag{5.2}$$

5.2.3 Analysis of Beacon Contention

We follow the analytic model proposed in [2, 38] to compare our beacon transfer procedure with the IEEE 802.11 approach on the success probability of a beacon transmission. This metric is our chief concern since there is no MAC-level recovery on beacon frames [48]. For tractability and ease of analysis, we only consider the IBSS configuration with m stations. Moreover, we assume that the channel introduces no errors, so frame collisions are the only source of errors. A beacon transmission is considered successful if it encounters no collision.

After TBTT and an elapsed PIFS, each station i, $1 \leq i \leq m$, independently generates a random backoff timer $\mathcal{B}_i$ for beacon transmission, where $\mathcal{B}_i$ follows the reverse truncated geometric distribution. Let $P_{\mathcal{G}}[m]$ be the probability that at least one of the m stations succeeds in beacon transmission by using the scalable beacon transfer procedure. Let $m \geq 2$, then

the event that there is a successful beacon transmission in the contention window $[0,\ CW]$ if and only if (i) exactly *one* station transmits in slot j, for some $0 \leq j \leq CW-1$, and (ii) all other stations are scheduled to transmit *after* slot j. Thus, we have

$$\begin{aligned} P_{\mathcal{G}}[m] &= \sum_{j=0}^{CW-1} \binom{m}{1} \Pr[\mathcal{B}=j] \Big(\Pr[\mathcal{B}>j]\Big)^{m-1} \\ &= \binom{m}{1} \times \left\{ \Pr[\mathcal{B}=0] \Big(\Pr[\mathcal{B}>0]\Big)^{m-1} + \sum_{j=1}^{CW-1} (1-q) q^{CW-j} (1-q^{CW-j})^{m-1} \right\} \\ &= \binom{m}{1} \times \left\{ q^{CW} (1-q^{CW})^{m-1} + \sum_{j=1}^{CW-1} (1-q) q^{j} (1-q^{j})^{m-1} \right\}. \end{aligned} \tag{5.3}$$

To compare with the IEEE 802.11 approach, let us consider the case that the backoff timer of each station B_i is independently sampled from a discrete uniform distribution over the set $\{0, 1, \ldots, CW\}$. Under the circumstances, let and $P_{\mathcal{U}}[m]$ denote the probability that one of the m stations succeeds in beacon transmission. By the similar way, we have

$$\begin{aligned} P_{\mathcal{U}}[m] &= \sum_{j=0}^{CW-1} \binom{m}{1} \Pr[B=j] \Big(\Pr[B>j]\Big)^{m-1} \\ &= \frac{m}{CW+1} \sum_{j=0}^{CW-1} \left(\frac{CW-j}{CW+1}\right)^{m-1}. \end{aligned} \tag{5.4}$$

For the standard value of $CW = 31$, the functions $P_{\mathcal{G}}[m]$ and $P_{\mathcal{U}}[m]$ are plotted in Figure 5.4 for various values of m. The data points on the curves are generated by simulations. We can see that, when $q = 0.8$, $P_{\mathcal{G}}[m]$ is very close to 0.9 and decreases very slowly with an increasing number of contending stations. On the contrary, $P_{\mathcal{U}}[m]$ drops sharply and rapidly as the number of competing stations increases. The results do confirm that, in contrast with IEEE 802.11, our scheme delivers a more scalable and reliable performance, thus relieving the beacon contention problem remarkably.

5.3 Neighbor Maintenance in PS Mode

In this section, we present three randomized power management protocols, which allow stations operating in a PS mode to save a great deal of energy by periodically entering the doze state, while also allowing PS stations a high probability of discovering their neighbors in an

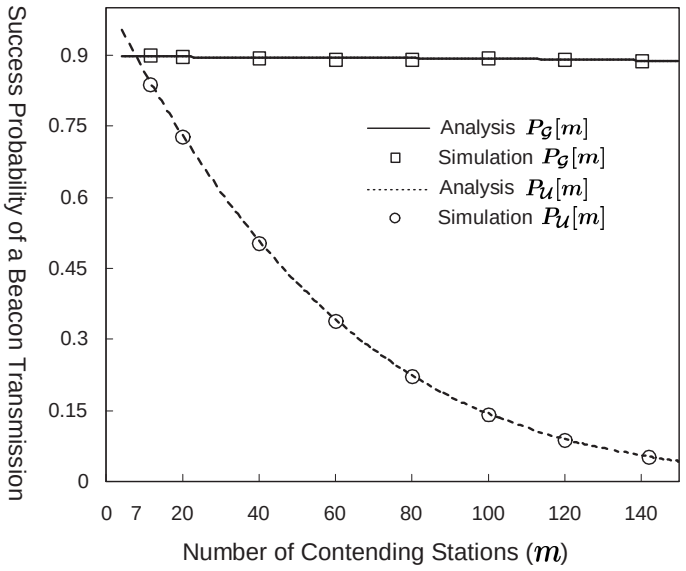

Figure 5.4: Success probability of a beacon transmission versus number of contending stations.

asynchronous MANET. Each of these protocols has a different awake/sleep pattern for PS stations. In other words, the structure of a beacon interval may vary for different protocols. Note that all stations are assumed to have the same clock rate. Besides, in all our settings, the lengths of the beacon window and ATIM window remain constant in every beacon interval. The notations used to facilitate the forthcoming presentation are listed below.

- BI: the length of a beacon interval
- BW: the length of a beacon window
- AW: the length of an ATIM window
- DW: the length of a data window
- $actW$: the length of an active window

5.3.1 Randomized Coterie-Based Protocol

We design two types of beacon intervals for this protocol; one is the *fully-awake* beacon interval, and the other is the *fully-sleep* beacon interval. The structures of these beacon intervals are defined as follow.

- Each fully-awake beacon interval starts with a beacon window followed by a data window such that $BW + DW = actW = BI$. During the fully-awake interval, a PS station always stays awake. The purposes of the fully-awake beacon interval are (i) for a PS station to discover all its neighbors by extending its listening duration to the maximum, and (ii) for a PS station to announce its presence by trying to send out its beacon during the beacon window. In IEEE 802.11, the purpose of the ATIM window is for a PS station to receive the notification that it should remain active after the end of the ATIM window because there is pending data. Since a PS station always keeps its transceiver on during the whole fully-awake beacon interval, the ATIM window thus can be removed.

- Each fully-sleep beacon interval starts with an ATIM window. After the ATIM window concludes, a PS station may enter the doze state. That is, we set $AW = actW$. The purpose of the fully-sleep beacon interval is for a PS station to reduce its energy consumption by condensing its listening activity to the minimum.

Take Figure 5.5 for example, for PS station X, 0th, 1st, 2nd, and 9th beacon intervals are fully-awake while the remaining beacon intervals are fully-sleep. We can find that, for a PS station, the fully-awake beacon intervals take on the burden of announcing its presence and detecting the existence of neighbors. As a result, the chance for two PS neighbors to discover each other relies on the overlaps of their fully-awake beacon intervals. With the intersection property, a *coterie* system [34] is expected to be a powerful tool in developing power management protocols. The definition of a coterie [34] is formally given below.

Definition 5.3.1. Let U be the universe set of finite objects. A collection of subsets (*quorums*) $\mathcal{L} = \{L_1, \ldots, L_m\}$, where $L_i \subseteq U$, is called a *coterie* if and only if (i) For any two quorums L_i and L_j in $\mathcal{L}$, $L_i \cap L_j \neq \emptyset$. (ii) There are no two quorums L_i and L_j in $\mathcal{L}$ such that $L_i \subseteq L_j$.

Example 5.3.1. A special kind of coteries, called the *finite projective plane* (FPP, for short), can be obtained by letting $U = \{0,\ 1, \cdots, 12\}$ and $\mathcal{L} = \{L_0 = \{0, 1, 2, 9\}, L_1 = \{0, 3, 6, 10\}, L_2 = \{0, 4, 8, 11\}, L_3 = \{0, 5, 7, 12\}, L_4 = \{3, 4, 5, 9\}, L_5 = \{1, 4, 7, 10\}, L_6 = \{1, 5, 6, 11\}, L_7 = \{1, 3, 8, 12\}, L_8 = \{6, 7, 8, 9\}, L_9 = \{2, 5, 8, 10\}, L_{10} = \{2, 3, 7, 11\}, L_{11} = \{2, 4, 6, 12\}, L_{12}$

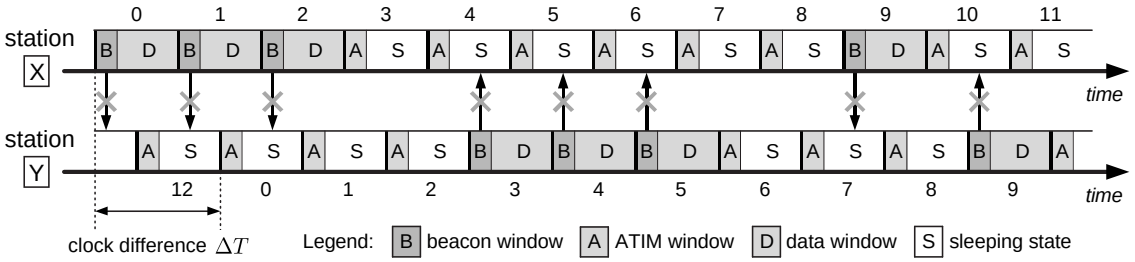

Figure 5.5: A snapshot of the worst case scenario for FPP-based protocol.

$= \{9, 10, 11, 12\}\}$. It is easy to verify that $L_i \cap L_j \neq \emptyset$ and $L_i \nsubseteq L_j$ for all $i \neq j$ and $0 \leq i, j \leq 12$. Although the coterie techniques have been widely used in distributed systems [34, 53], such as mutual exclusion and data replication, a coterie without any proper modifications may not be directly applicable to the power management protocols especially in asynchronous environments. For instance, let us consider an FPP-based power management protocol which formally works as follows. When a station decides to switch to the PS mode, it randomly selects a quorum L_i from $\mathcal{L}$ as the set of fully-awake beacon intervals within a pattern repetition interval $\mathcal{R}$, where $\mathcal{R}$ is a global parameter. The remaining beacon intervals are all fully-sleep beacon intervals. The *pattern repetition interval* is defined as the consecutive $\mathcal{R}$ beacon intervals that comprise some different awake/sleep patterns repeat at regular intervals. Figure 5.5 shows an example of the FPP-based protocol, in which station X chooses jth beacon intervals, for all $j \in L_0 = \{0, 1, 2, 9\}$, as its fully-awake beacon intervals from a pattern repetition interval $\mathcal{R}$ (13 consecutive beacon intervals); while station Y selects beacon intervals in $L_4 = \{3, 4, 5, 9\}$ as its fully-awake beacon intervals. Obviously, when two PS neighbors, X and Y, are perfectly synchronized, i.e., their clock difference $\Delta T = 0$, they may discover each other in the 9th beacon interval since $L_0 \cap L_4 = \{9\}$. However, as shown in Figure 5.5, if X's clock is ahead of Y's clock by $BI + \Delta t$, where $\max\{BW, AW\} < \Delta t < BI - \max\{BW, AW\}$, then they forever lose each other's beacon frames.

To mitigate the asynchronism problem, we relax the nonempty intersection property and introduce a randomized coterie, in which every two distinct quorums intersect with high probability. The randomized coterie is in essence a special case of the probabilistic quorum systems [53]. The randomized coterie-based power management protocol operates formally

as follows. When a station switches to the PS mode, it selects k beacon intervals randomly and uniformly from a pattern repetition interval $\mathcal{R}$ as the set of fully-awake beacon intervals, while the remaining beacon intervals are all fully-sleep beacon intervals. With appropriately setting parameters $\mathcal{R}$ and k, this simple yet novel approach guarantees that, even in an asynchronous environment, the fully-awake beacon intervals of two PS neighbors overlap with high probability. The more precise result is given in the following theorem. Moreover, via Corollary 5.3.1, we demonstrate the power of the randomized coterie-based protocol.

Theorem 5.3.1. In the randomized coterie-based protocol, if no collisions in beacon reception, then the probability $P[\mathcal{R}, k]$ that any two PS neighbors, regardless of their clock difference, are able to discover each other within a pattern repetition interval is given below.

$$\begin{cases} P[\mathcal{R}, k] = 1 & \text{if } \lfloor \frac{\mathcal{R}}{2} \rfloor + 1 \leq k \leq \mathcal{R}, \\ P[\mathcal{R}, k] \geq 1 - \frac{\binom{\mathcal{R}}{k}\binom{\mathcal{R}-k}{k} + \binom{\mathcal{R}}{1}\binom{\mathcal{R}-2}{k-1}\binom{\mathcal{R}-k-1}{k-1}}{\binom{\mathcal{R}}{k}\binom{\mathcal{R}}{k}} & \text{if } 1 \leq k \leq \lfloor \frac{\mathcal{R}}{2} \rfloor. \end{cases} \tag{5.5}$$

Proof. In the randomized coterie-based protocol, the chance for two PS neighbors, X and Y, to discover each other relies on the overlaps of their fully-awake beacon intervals. By using the well-known pigeonhole principle, it is easy to verify that $P[\mathcal{R}, k] = 1$ when $k \geq \lfloor \frac{\mathcal{R}}{2} \rfloor + 1$.

Now, let us consider the case that $k \leq \lfloor \frac{\mathcal{R}}{2} \rfloor$. Without loss of generality, we can assume that the worst case scenario (refer to Figure 5.5) occurs when X's clock is faster than Y's clock by $\Delta T = h \times BI + \Delta t$, where $\max\{BW, AW\} < \Delta t < BI - \max\{BW, AW\}$ and $h \geq 0$ is an integer. In the following derivation, we use X's clock as a reference clock to derive Y's clock. Note that other cases can be derived via the similar way. We define $i \ominus h \equiv i - h \mod \mathcal{R}$. Thus X can receive Y's beacons within a pattern repetition interval if and only if both $\langle i \rangle_{\mathrm{X}}$ and $\langle i \ominus h \rangle_{\mathrm{Y}}$ are fully-awake beacon intervals, for some $0 \leq i \leq \mathcal{R} - 1$, where $\langle i \rangle_{\mathrm{X}}$ denotes the ith beacon interval in X's pattern repetition interval. Let us denote by $\mathrm{X} \leftarrow \mathrm{Y}$ the event that X hears the beacons issued from Y within a pattern repetition interval. And we have

$$\Pr[\mathrm{X} \leftarrow \mathrm{Y}] = 1 - \frac{\binom{\mathcal{R}}{k}\binom{\mathcal{R}-k}{k}}{\binom{\mathcal{R}}{k}\binom{\mathcal{R}}{k}}. \tag{5.6}$$

On the other hand, X's beacons can be received by station Y during a pattern repetition interval if and only if both $\langle j \rangle_{\mathrm{X}}$ and $\langle j \ominus (h+1) \rangle_{\mathrm{Y}}$ are fully-awake beacon intervals for some $0 \leq j \leq \mathcal{R} - 1$. Let us denote by $\mathrm{X} \rightarrow \mathrm{Y}$ ($\mathrm{X} \not\rightarrow \mathrm{Y}$) the event that Y can (cannot) receive X's

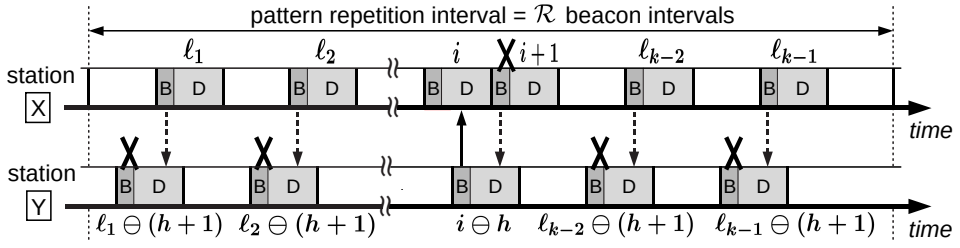

Figure 5.6: The event that, during a pattern repetition interval, X can receive Y's beacons, while Y cannot receive X's beacons.

beacons during a pattern repetition interval. By exploiting conditional probabilities, $P[\mathcal{R}, k]$ can be expressed as

$$\begin{aligned} P[\mathcal{R}, k] &= \Pr[(\mathrm{X} \rightarrow \mathrm{Y}) \cap (\mathrm{X} \leftarrow \mathrm{Y})] = \Pr[\mathrm{X} \rightarrow \mathrm{Y} | \mathrm{X} \leftarrow \mathrm{Y}] \times \Pr[\mathrm{X} \leftarrow \mathrm{Y}] \\ &= \Big(1 - \Pr[\mathrm{X} \not\rightarrow \mathrm{Y} | \mathrm{X} \leftarrow \mathrm{Y}]\Big) \times \Pr[\mathrm{X} \leftarrow \mathrm{Y}]. \end{aligned} \tag{5.7}$$

In what follows, we derive the probability $\Pr[\mathrm{X} \not\rightarrow \mathrm{Y} | \mathrm{X} \leftarrow \mathrm{Y}]$. The event $\mathrm{X} \leftarrow \mathrm{Y}$ can occur in any of $\binom{\mathcal{R}}{k}\binom{\mathcal{R}}{k} - \binom{\mathcal{R}}{k}\binom{\mathcal{R}-k}{k}$ possible ways. Given that the event $\mathrm{X} \leftarrow \mathrm{Y}$ has occurred, we want to determine the number of possible outcomes in which the event $\mathrm{X} \not\rightarrow \mathrm{Y}$ also happens. First, there are $\binom{\mathcal{R}}{1}$ ways for station X to arbitrarily select a fully-awake beacon interval, say $\langle i \rangle_{\mathrm{X}}$. In order to guarantee that X can hear Y's beacons, Y must choose $\langle i \ominus h \rangle_{\mathrm{Y}}$ as its fully-awake beacon interval. At this moment, X cannot select $\langle i+1 \rangle_{\mathrm{X}}$ as the fully-awake beacon interval, otherwise the event $\mathrm{X} \rightarrow \mathrm{Y}$ will take place. Then station X has $\binom{\mathcal{R}-2}{k-1}$ ways to choose its remaining $k-1$ fully-awake beacon intervals from a pattern repetition interval, excluding $\langle i \rangle_{\mathrm{X}}$ and $\langle i+1 \rangle_{\mathrm{X}}$. We label these $k-1$ beacon intervals $\langle \ell_1 \rangle_{\mathrm{X}}, \langle \ell_2 \rangle_{\mathrm{X}}, \ldots, \langle \ell_{k-1} \rangle_{\mathrm{X}}$ respectively, as illustrated in Figure 5.6. To avoid the event $\mathrm{X} \rightarrow \mathrm{Y}$, station Y is forbidden to choose $\langle \ell_1 \ominus (h+1) \rangle_{\mathrm{Y}}, \langle \ell_2 \ominus (h+1) \rangle_{\mathrm{Y}}, \ldots, \langle \ell_{k-1} \ominus (h+1) \rangle_{\mathrm{Y}}$. As a result, Y has only $\binom{\mathcal{R}-k-1}{k-1}$ ways to select its remaining $k-1$ fully-awake beacon intervals. However, we may not obviate the possibility of counting the redundant outcomes. Thus, we have

$$\Pr[\mathrm{X} \not\rightarrow \mathrm{Y} | \mathrm{X} \leftarrow \mathrm{Y}] \leq \frac{\binom{\mathcal{R}}{1}\binom{\mathcal{R}-2}{k-1}\binom{\mathcal{R}-k-1}{k-1}}{\binom{\mathcal{R}}{k}\binom{\mathcal{R}}{k} - \binom{\mathcal{R}}{k}\binom{\mathcal{R}-k}{k}}. \tag{5.8}$$

By substituting (5.6) and (5.8) in (5.7), we can derive the inequality (5.5). □

Corollary 5.3.1. In the randomized coterie-based protocol, if every PS station randomly selects $\beta\sqrt{\mathcal{R}}$ fully-awake beacon intervals from a pattern repetition interval $\mathcal{R}$, where $1 \leq$

$\beta \leq \frac{\sqrt{\mathcal{R}}}{2}$, then we have

$$P[\mathcal{R}, \beta\sqrt{\mathcal{R}}] \geq 1 - (1 + \beta^2)e^{-\beta^2}. \tag{5.9}$$

For example, $P[\mathcal{R}, \sqrt{3\mathcal{R}}] \geq 0.801$, $P[\mathcal{R}, 2\sqrt{\mathcal{R}}] \geq 0.908$, and $P[\mathcal{R}, 3\sqrt{\mathcal{R}}] \geq 0.999$.

Proof. See Appendix A. □

Remark 5.3.1. The choice of $\mathcal{R}$ and k demands the tradeoff among power consumption, neighbor discovery probability, and neighbor discovery time. For instance, by Corollary 5.3.1, we can obtain $P[10000, 300] \geq 0.999$. This means that each PS station can be awake only about 3% of the time, yet it can discover neighbors with probability at least 99.9%. However, if we require that neighbor discovery probability must be 100%, then, by Theorem 5.3.1, each PS station should stay awake at least 50% of the time. This implies that, in the randomized coterie-based protocol, if we can tolerate a little more neighbor discovery loss, then we can earn a significant energy saving. We defer the power consumption analysis until subsection 5.3.3. If the designer demands the probability that a PS neighbor can be discovered within the duration $\mathcal{T} \geq \mathcal{R}$ shall be at least $1 - \varepsilon$, then the value of $P[\mathcal{R}, k]$ must satisfy the following inequality.

$$1 - \Big(1 - P[\mathcal{R}, k]\Big)^{\lfloor \frac{\mathcal{T}}{\mathcal{R}} \rfloor} \geq 1 - \varepsilon.$$

Remark 5.3.2. To simplify our theoretical analysis and presentation, the assumption of collision-free beacon reception is made only in this section. Obviously, collision is inevitable in any random-access networks. However, when $0 \leq \Delta t \leq BW$, a high success probability of a beacon delivery is guaranteed via scalable beacon transfer procedure; when $BW < \Delta t < BI - BW$, the asynchronism is also of help in relieving the beacon contention. In our simulations, we will remove this assumption.

5.3.2 Cyclic Finite Projective Plane-Based Protocols

Though the randomized coterie-based protocol is simple, flexible, and easy implementable, it does not always guarantee a 100% neighbor discovery probability (especially when $k \approx \sqrt{\mathcal{R}}$). In this subsection, on the basis of the *cyclic finite projective plane*, we propose new randomized power saving protocols, in which a PS station is able to discover its neighbors

with probability 1, while it sends beacon frames only $\lceil\sqrt{\mathcal{R}}\rceil$ times a pattern repetition interval $\mathcal{R}$. The finite projective plane (FPP, for short) [56] is formally defined as follows.

Definition 5.3.2. Let U be a finite set, and let $\mathcal{L}$ be a system of subsets of U. The pair $(U, \mathcal{L})$ is called a *finite projective plane* if it satisfies the following properties. (i) There exists a 4-element set $F \subseteq U$ such that $|L_i \cap F| \leq 2$ holds for each set $L_i \in \mathcal{L}$. (ii) Any two distinct sets $L_i, L_j \in \mathcal{L}$ intersect in exactly one element; i.e., $|L_i \cap L_j| = 1$. (iii) For any two distinct elements $u_i, u_j \in U$, there exists exactly one set $L_k \in \mathcal{L}$ such that $u_i \in L_k$ and $u_j \in L_k$.

An example of an FPP can be found in Example 5.3.1. The FPP is a finite analogy of the so-called real projective plane (an extension of Euclidean plane and all elements are real numbers) studied in geometry. Therefore, if $(U, \mathcal{L})$ is an FPP, we call the elements of U *points* and the sets of $\mathcal{L}$ *lines*. The following two theorems [56] are useful in the presentation of our algorithms.

Theorem 5.3.2. Let $(U, \mathcal{L})$ be an FPP. Then all its lines have the same number of points; i.e., $|L_i| = |L_j|$ for any two lines $L_i, L_j \in \mathcal{L}$.

Accordingly, we can define the *order* of the FPP as the number *one less* than the number of points on each line; i.e., $|L_i| - 1$, where $L_i \in \mathcal{L}$.

Theorem 5.3.3. Let $(U, \mathcal{L})$ be an FPP of order $n \geq 2$. Then the following statements are equivalent. (i) Every line contains $n + 1$ points. (ii) Every point is on exactly $n + 1$ lines. (iii) There are exactly $n^2 + n + 1$ points in U. (iv) There are exactly $n^2 + n + 1$ lines in $\mathcal{L}$.

However, as illustrated in Example 5.3.1, the FPP-based power management protocol may fail when operating over asynchronous environments. Thus we call for the cyclic FPP (CFPP for short).

Definition 5.3.3. Let $\mathcal{R} = n^2 + n + 1$ and $U = \{0, 1, \ldots, \mathcal{R} - 1\}$. An FPP $(U, \mathcal{L})$ of order n is called a *cyclic FPP* of order n if and only if, for any line $L_i = \{\ell_0, \ell_1, \ldots, \ell_n\} \in \mathcal{L}$ and an integer h, the coset $h \oplus L_i = \{h + \ell_j \mod \mathcal{R} \,|\, \text{for all } \ell_j \in L_i\}$ is also a line in $\mathcal{L}$.

An example of the CFPP of order 2 can be obtained by letting $U = \{0, 1, \ldots, 6\}$ and $\mathcal{L} = \{L_0 = \{0, 1, 3\}, L_1 = \{1, 2, 4\}, L_2 = \{2, 3, 5\}, L_3 = \{3, 4, 6\}, L_4 = \{4, 5, 0\}, L_5 =$

$\{5, 6, 1\}$, $L_6 = \{6, 0, 2\}\}$. $3 \oplus L_0 = \{3, 4, 6\} = L_3 \in \mathcal{L}$ and $-3 \oplus L_0 = \{4, 5, 0\} = L_4 \in \mathcal{L}$. The CFPP is in essence a special case of Abelian difference sets [55]. By Singer's theorem [55], we can conclude that if $n \geq 2$ is a power of a prime, then there exists a CFPP of order n. By Theorem 5.3.3 and Definition 5.3.3, we can obtain the following important corollary.

Corollary 5.3.2. Let $(U, \mathcal{L})$ be a CFPP of order n and $\mathcal{R} = n^2 + n + 1$. Then for any two lines $L_i, L_j \in \mathcal{L}$, (i) $|L_i| \leq \lceil \sqrt{\mathcal{R}} \rceil$ and (ii) $(h_1 \oplus L_i) \cap (h_2 \oplus L_j) \neq \emptyset$, for any two integers h_1 and h_2.

The naive CFPP-based randomized power management protocol operates formally as follows. When a station switches to the PS mode, it selects a line L_i randomly from $\mathcal{L}$ as the set of fully-awake beacon intervals within a pattern repetition interval $\mathcal{R}$, where the parameter $(U, \mathcal{L})$ is globally maintained. The remaining beacon intervals are all fully-sleep beacon intervals. By enforcing $AW \geq BW$, we have the following theorem.

Theorem 5.3.4. The naive CFPP-based protocol guarantees that, given $AW \geq BW$ and no collisions in beacon reception, any two PS neighbors, regardless of their clock difference, are able to discover each other in every pattern repetition interval.

Proof. We prove this theorem by showing that, given any two PS neighbors X and Y, at least one X's entire beacon window is fully covered by Y's active windows during a pattern repetition interval, and vice versa. We assume that X and Y randomly select the lines L_x and L_y respectively from the same CFPP $(U, \mathcal{L})$ as the set of their fully-awake beacon intervals within a pattern repetition interval, and $\mathcal{R} = n^2 + n + 1$. Without loss of generality, we can assume that X's clock is faster than Y's clock by $\Delta T = h \times BI + \Delta t$, where $0 \leq \Delta t < BI$ and $h \geq 0$ is an integer. In the following derivation, we use X's clock as a reference clock to derive Y's clock. Note that other cases can be derived by the similar way.

As illustrated in Figure 5.7, X can receive Y's beacons within a pattern repetition interval if and only if both $\langle i \rangle_{\mathrm{X}}$ and $\langle i \ominus h \rangle_{\mathrm{Y}}$ are fully-awake beacon intervals, for some $0 \leq i \leq \mathcal{R} - 1$. Since $L_x \cap \{-h \oplus L_y\} \neq \emptyset$ (by Corollary 5.3.2), there must exist an element i such that $i \in L_x$ and $i \in \{-h \oplus L_y\}$. This implies that both $\langle i \rangle_{\mathrm{X}}$ and $\langle i \ominus h \rangle_{\mathrm{Y}}$ are fully-awake beacon intervals. On the other hand, X's beacons can be received by Y if and only if both $\langle j \rangle_{\mathrm{X}}$ and $\langle j \ominus (h+1) \rangle_{\mathrm{Y}}$ are fully-awake beacon intervals, for some $0 \leq j \leq \mathcal{R} - 1$. Since

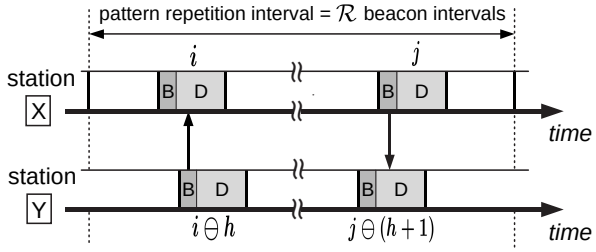

Figure 5.7: The event that stations X and Y are able to discover each other within a pattern repetition interval.

$L_x \cap \{-(h+1) \oplus L_y\} \neq \emptyset$ (by Corollary 5.3.2), there must exist an element j such that $j \in L_x$ and $j \in \{-(h+1) \oplus L_y\}$. This implies that both $\langle j \rangle_{\mathrm{X}}$ and $\langle j \ominus (h+1) \rangle_{\mathrm{Y}}$ are fully-awake beacon intervals. □

In what follows, we employ the *interleaving* technique such that the power consumption of the CFPP-based protocol can be further reduced. We design three types of beacon intervals: the *forward half-awake* beacon interval, the *backward half-awake* beacon interval, and the fully-sleep beacon interval. The structures of the half-awake beacon intervals are defined as follow.

- Each forward half-awake beacon interval starts with a beacon window followed by an ATIM window. After the ATIM window finishes, a PS station may enter the doze state. Importantly, we set $actW = BW + AW + DW \geq BW + BI/2$.

- Each backward half-awake beacon interval starts with an ATIM window, but the active window is terminated by a beacon window. After the active window ends, a PS station may enter the doze state. Importantly, we set $actW = AW + DW + BW \geq BW + BI/2$.

Note that we do not necessitate the assumption $AW \geq BW$ here any longer. The interleaving CFPP-based randomized power management protocol operates formally as follows. When a station switches to the PS mode, it selects a line L_i randomly from $\mathcal{L}$ as the set of half-awake beacon intervals within a pattern repetition interval $\mathcal{R}$, where the CFPP $(U, \mathcal{L})$ is a global parameter. The remaining beacon intervals are all fully-sleep beacon intervals. It is worth noticing that the sequences of pattern repetition intervals are alternatively labelled

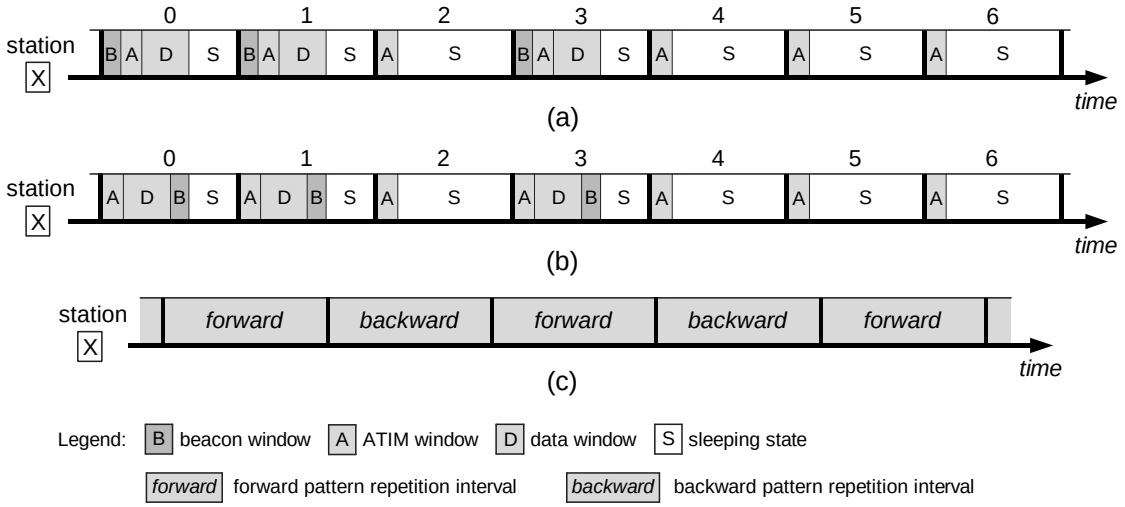

Figure 5.8: With the PS mode enabled, station X chooses the line $L_0 = \{0, 1, 3\}$ from the CFPP of order 2 as the set of its half-awake beacon intervals. (a) The awake/sleep pattern in a forward pattern repetition interval. (b) The awake/sleep pattern in a backward pattern repetition interval. (c) The sequence of pattern repetition intervals.

as *forward* and *backward* pattern repetition intervals, as illustrated in Figure 5.8(c). During the forward (backward) pattern repetition interval, all half-awake beacon intervals should be forward (backward) half-awake beacon intervals. Figure 5.8(a) and (b) depict an example where PS station X schedules its awake/sleep patterns according to the interleaving CFPP-based protocol. Via the interleaving approach, we obtain a nearly 50% reduction in the radio active ratio (which will be defined in the next subsection) as compared with the naive CFPP-based protocol. The correctness of the interleaving CFPP-based protocol is given below.

Theorem 5.3.5. The interleaving CFPP-based protocol guarantees that, if no collisions occur when receiving beacons, then any two PS neighbors, regardless of their clock difference, are able to discover each other in every other pattern repetition interval.

Proof. See Appendix B. □

5.3.3 Power Consumption Analysis

Three yardsticks (beacon transmission ratio, radio active ratio, and neighbor discovery time) have been proposed in [78] to judge the goodness of the power management protocols for

Table 5.2: Comparison of power management protocols for an asynchronous MANET.

Protocol	Beacon trans. ratio	Radio active ratio	Neighbor discovery time
IEEE 802.11 [48]	$p(m)$	$\frac{AW}{BI}$	∞
Grid quorum [78]	$\frac{2\sqrt{\mathcal{R}}-1}{\mathcal{R}}$	$\frac{2\sqrt{\mathcal{R}}-1}{\mathcal{R}} + \left(1-\frac{1}{\mathcal{R}}\right)^2\left(\frac{AW}{BI}\right)$	$\frac{\mathcal{R}\times BI}{4}$
Randomized coterie	$\frac{k}{\mathcal{R}}$	$\frac{k}{\mathcal{R}} + \frac{\mathcal{R}-k}{\mathcal{R}}\left(\frac{AW}{BI}\right)$	$\frac{\mathcal{R}\times BI}{2\times P[\mathcal{R},k]}$
Naive CFPP	$\frac{1}{\sqrt{\mathcal{R}}}$	$\frac{1}{\sqrt{\mathcal{R}}} + \frac{\mathcal{R}-\sqrt{\mathcal{R}}}{\mathcal{R}}\left(\frac{AW}{BI}\right)$	$\frac{\mathcal{R}\times BI}{2}$
Interleaving CFPP	$\frac{1}{\sqrt{\mathcal{R}}}$	$\frac{1}{2\sqrt{\mathcal{R}}} + \frac{1}{\sqrt{\mathcal{R}}}\left(\frac{BW}{BI}\right) + \frac{\mathcal{R}-\sqrt{\mathcal{R}}}{\mathcal{R}}\left(\frac{AW}{BI}\right)$	$\mathcal{R}\times BI$

ad hoc networks. *Beacon transmission ratio* indicates the average number of beacons that a station needs to transmit in a beacon interval. *Radio active ratio* is defined as the ratio of the total time that a PS station turns its radio on in a pattern repetition interval to the length of the pattern repetition interval. Namely, radio active ratio denotes the proportion of time in a beacon interval that a station needs to stay awake when operating in the PS mode. *Neighbor discovery time* signifies the average time duration that a PS station takes to detect a neighboring station. Table 5.2 summarizes the characteristics of our proposed power management protocols and compares them to IEEE 802.11 and the most power conserving protocol (grid quorum-based protocol) in [78]. The beacon transmission ratio of IEEE 802.11, $p(m)$, is equal to the probability that a station sends out its beacon frame in a beacon interval, where m is the number of contending stations in a single-hop cluster. The approximate value of $p(m)$ can be calculated as follows. $p(m) = \sum_{j=0}^{CW-1} \Pr[B=j]\big(\Pr[B \geq j]\big)^{m-1} = \sum_{j=0}^{CW-1} \left(\frac{1}{CW+1}\right)\left(\frac{CW-j+1}{CW+1}\right)^{m-1}$. The neighbor sensitivity of IEEE 802.11 is infinitely large since any two PS neighbors never discover each other when their clock difference ΔT satisfies the inequality that $h \times BI + AW < \Delta T < (h+1) \times BI - AW$, where $h \geq 0$ is an integer.

Through the formulas we derived in Table 5.2, the settings ($\mathcal{R}$, k) of our protocols can be flexibly tuned at design time, positioning the network at the predictably desired operating point in the energy-delay-accuracy design space. Moreover, Table 5.2 reveals that decreased radio active ratio generally comes with a penalty of increased neighbor sensitiv-

ity. The authors in [52] argue that a good power management protocol ought to minimize *energy* $\times$ *delay* metric. We further argue that, under about the same bounded energy-delay product, a power management protocol with a smaller ratio active ratio is more suitable for energy-limited applications, in which the stations are subject to hard constraints on available battery energy. Clearly, IEEE 802.11 performs poorly in an asynchronous MANET because of its intolerably large neighbor sensitivity. Compared with the most energy-conserving protocol (grid quorum-based protocol) in [78], the interleaving CFPP-based protocol achieves a nearly 75% reduction in radio active ratio while keeping about the same *radio active ratio* $\times$ *neighbor discovery time*.

5.4 Data Frame Transfer Procedure

This section presents how a station sends a directed data frame to a PS neighbor. Since the PS station is not always active, the sending station has to predict when the PS destination will wake up; i.e., the timings of the receiver's data windows or ATIM windows. To attain this goal, each beacon frame should contain a MAC address, a *timestamp*, *awake/sleep pattern bits*, and other management parameters. The timestamp records the current time of the sending station and is used by a neighboring station to calculate their clock difference. At most $\mathcal{R}+1$ bits are sufficient for the PS station to convey its awake/sleep pattern. Take the interleaving CFPP-based protocol for example, the first awake/sleep pattern bit can be used for judging whether the current pattern repetition interval is forward or backward, and the $(j+1)$th awake/sleep pattern bit can be used for telling whether the $(j-1)$th beacon interval is half-awake or fully-sleep, where $1 \leq j \leq \mathcal{R}$. Table 5.3 summarizes the timings of data windows and ATIM windows in the proposed power management protocols, where a, b are integers and $a \geq 0$, $1 \leq b \leq \mathcal{R}-1$. We assume that the PS station selects the set $\{\ell_1, \ldots, \ell_k\}$ ($\{\overline{\ell}_1, \ldots, \overline{\ell}_{\mathcal{R}-k}\}$) as its awake (sleep) beacon intervals in a pattern repetition interval.

Our directed data frame transfer procedure is similar to [48, 78] and operates as follows. Assume that station X is intending to send a data frame to the PS neighbor Y. Once X has already received a beacon from Y, X can correctly predict Y's awake/sleep pattern according to Y's awake/sleep pattern bits and their clock difference. If Y's current data window does not expire, X can directly transmit a data frame to Y since Y is known to be active. Otherwise,

Table 5.3: Timing of data/ATIM windows of the proposed power management protocols.

Protocol	Data windows's timing
Probability coterie-based	$[(a\mathcal{R}+\ell_i)BI+BW,(a\mathcal{R}+\ell_i+1)BI]$
Naive CFPP-based	$[(a\mathcal{R}+\ell_i)BI+BW,(a\mathcal{R}+\ell_i+1)BI]$
Interleaving CFPP-based	
Forward awake interval	$[(a\mathcal{R}+\ell_i)BI+BW+AW,(a\mathcal{R}+\ell_i)BI+actW]$
Backward awake interval	$[(a\mathcal{R}+\ell_i)BI+AW,(a\mathcal{R}+\ell_i)BI+AW+DW]$
Protocol	**ATIM windows's timing**
Randomized coterie-based	$[(a\mathcal{R}+\overline{\ell}_i)BI,(a\mathcal{R}+\overline{\ell}_i)BI+AW]$
Naive CFPP-based	$[(a\mathcal{R}+\overline{\ell}_i)BI,(a\mathcal{R}+\overline{\ell}_i)BI+AW]$
Interleaving CFPP-based	
Forward awake interval	$[(a\mathcal{R}+\ell_i)BI+BW,(a\mathcal{R}+\ell_i)BI+BW+AW]$
Backward awake interval	$[(a\mathcal{R}+\ell_i)BI,(a\mathcal{R}+\ell_i)BI+AW]$
Fully-sleep interval	$[(a\mathcal{R}+\overline{\ell}_i)BI,(a\mathcal{R}+\overline{\ell}_i)BI+AW]$

X should buffer the data frame and wait for the coming of Y's ATIM or data windows. During Y's ATIM window, X sends a unicast ATIM frame to Y. Upon reception of X's ATIM frame, Y shall reply an ATIM-ACK and remain active for the entire beacon interval. After Y's ATIM window concludes, X begins to transmit the buffered data frame and Y has to acknowledge its receipt. Note that transmission of these frames except beacons shall be done using the normal DCF access procedure. Recall that beacon frames are delivered by our scalable beacon transfer procedure. A PS station that neither transmits nor receives an ATIM frame during the ATIM window may enter the doze state after the end of the active window.

Table 5.4: Energy consumption parameters used in the simulations.

Parameter	Value
Unicast send	$420 + 1.9 \times$ frame size (μJ)
Unicast receive	$330 + 0.42 \times$ frame size (μJ)
Broadcast send	$250 + 1.9 \times$ frame size (μJ)
Broadcast receive	$56 + 0.5 \times$ frame size (μJ)
Idle	808 mW
Doze	27 mW

5.5 Performance Evaluation

5.5.1 Simulation Setup

We have developed event-driven simulators to evaluate the performance of the proposed power management protocols and compare our results to the grid quorum-based protocol. For the grid quorum-based and randomized coterie-based protocols, we set $(\mathcal{R}, k) = (16, 7)$; for the CFPP-based protocols, we set $(\mathcal{R}, k) = (13, 4)$. Each simulation run was executed for a duration of 3×10^7 μs in a single-hop ad hoc network with 30 mobile stations. Note that, in such a dense network, the out of synchronization phenomenon easily arises [38]. Hence we assume that the clock difference between any two stations ranges from 0 μs to 1000 μs. Initially, all stations are in the PS mode. However, once a PS station has data to transmit, that station will switch to the active mode and remains awake until it successfully sends out the pending frame or until it drops that frame when the DCF retry limit is reached. We assume that the arrival of data frames from higher-layer to MAC sublayer at each PS station follows the Poisson distribution with mean rate λ between $0 \sim 10$ frames/sec. The energy consumption model shown in Table 5.4 adopts the specifications suggested in [26], which are obtained by real experiments on Lucent WaveLAN IEEE 802.11b cards. Notice that, when sending a frame of the same size, unicast consumes more energy than broadcast since it requires extra cost to handle RTS, CTS, and ACK frames. The system parameter

Table 5.5: System parameters used in the simulation.

Parameter	Value
Channel bit rate	2 Mbps
Beacon window	10 ms
ATIM window	20 ms
Data frame size	2048 bytes
Beacon frame size	61 bytes
ATIM frame size	28 bytes
data/ATIM ACK frame size	14 bytes

values are summarized in Table 5.5.

5.5.2 Beacon Energy Consumption

From Table 5.4, we notice that the energy cost of beacon broadcast is relatively expensive since its fixed cost (send: $250.$ receive: $56.$) is much greater than the incremental cost of sending or receiving (send: $1.9\times61.$ receive: $0.5\times61.$) In addition, the total cost of receiving beacon is much greater than the cost of sending beacon since the simulated network is dense. Hence we first evaluate the total beacon energy consumption during the entire simulation time when using different power management protocols. We let $\lambda = 0.1$. We can see from Figure 5.9 that the beacon energy consumption decreases as the length of the beacon interval increases. This is expected since the simulation time is fixed, a longer beacon interval length means a fewer total number of fully/half-awake beacon intervals. We also observe that both grid quorum-based (naive CFPP-based) protocol and randomized coterie-based (interleaving CFPP-based) protocol have about the same beacon energy consumption. This is expected since they have the same beacon transmission ratio. Figure 5.9 concludes that CFPP-based protocols have smallest beacon energy consumption, which are subsequently followed by the randomized coterie-based and grid quorum-based protocols.

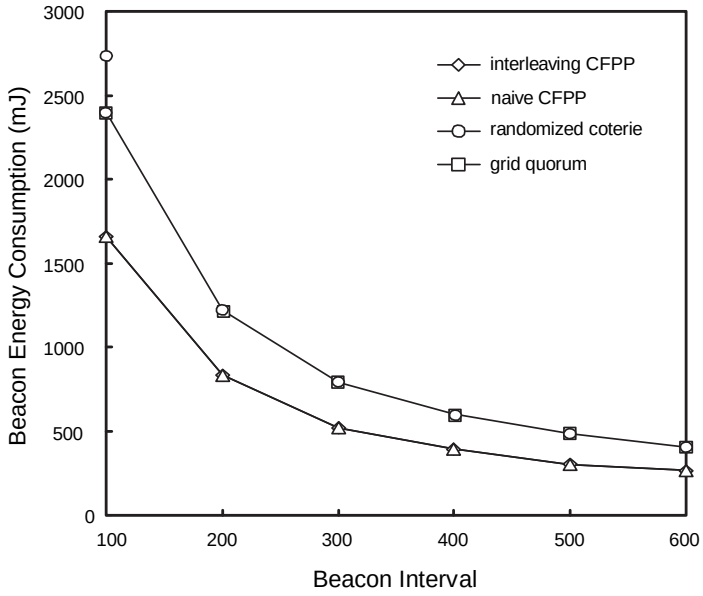

Figure 5.9: Beacon energy consumption versus the length of the beacon interval. ($\lambda = 0.1$ frames/sec/station.)

5.5.3 Neighbor Discovery Time

Figure 5.10 reports the neighbor discovery time versus the beacon interval length when data traffic load is fixed at $\lambda = 0.1$. As expected, the neighbor discovery time increases as the beacon interval enlarges. However, the grid quorum-based and randomized coterie-based protocols have smoother curves than CFPP-based protocols. Specifically, we find that the neighbor discovery time of CFPP-based protocols grows suddenly and rapidly when the beacon interval changes from 300 ms to 400 ms. The reasons are as follows. In an asynchronous MANET, a PS station may not hear neighbors' beacons because (i) beacon collisions occur, or (ii) that PS station is sleeping when the beacon frame is broadcasting. Accidentally, when beacon interval ≥ 400 ms, the latter event occurs more frequently in CFPP-based protocols. However, such events occur less frequently in the grid quorum-based and randomized coterie-based protocols. This may be because they have double radio active ratio and their fully-awake beacon intervals spread more uniformly in a pattern repetition interval. According to Figures 5.9 and 5.10, we suggest that the beacon interval could be set at around 300 ms since a longer beacon interval will gain a little more energy saving but may cause a marked increase in neighbor discovery time. Although Figure 5.10 concludes that our protocols are

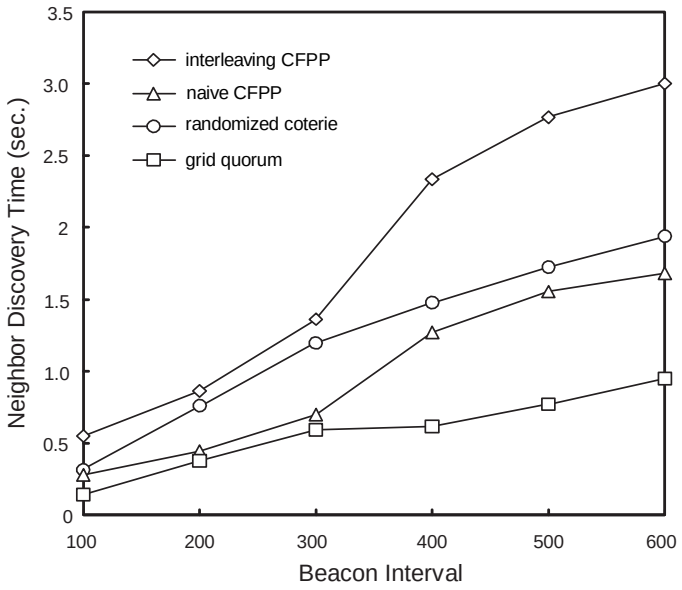

Figure 5.10: Neighbor discovery time versus beacon interval. ($\lambda = 0.1$ frames/sec/station.)

suitable in a lower mobility environment, the neighbor discovery time difference between the grid quorum-based and interleaving CFPP-based protocol is only about 0.77 sec (when beacon interval = 300 ms).

5.5.4 Throughput

Since the data frame length is fixed, the throughput could be defined as the average number of data frames successfully sent by all stations per second. Definitely, a good power management protocol ought to minimize the power consumption while not remarkably degrading the throughput. Figure 5.11 compares the throughput performances of different power management protocols under various data load when beacon interval = 300 ms. We see that, when $\lambda \leq 4$, CFPP-based protocols perform better than the randomized coterie-based protocol since the latter consumes larger overhead in beacon transmissions. However, when $\lambda > 5$, interleaving CFPP-based protocols perform worse than the randomized coterie-based protocol since the former consumes larger overhead in ATIM/ATIM-ACK transmissions.

We also observe that as the data load increases, the throughput generally increases monotonically and is finally saturated at a certain point. Compared with the grid quorum-based protocol, which saturates at about $\lambda = 4$, the naive CFPP-based protocol saturates at $\lambda = 7$.

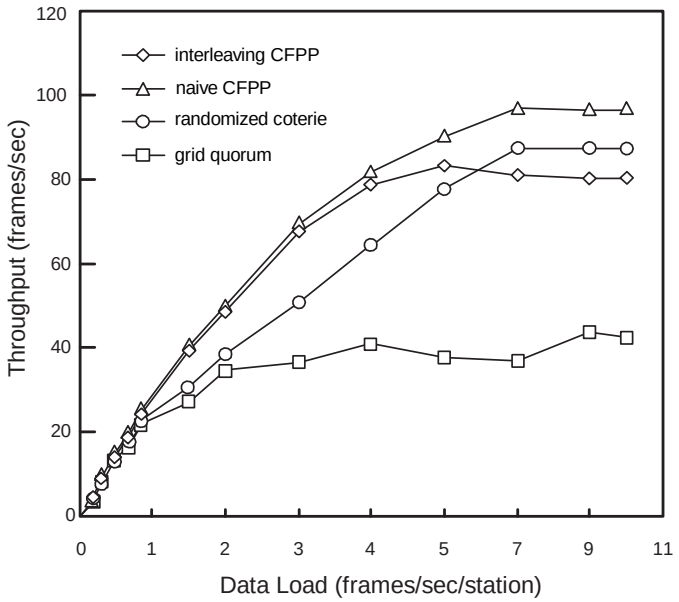

Figure 5.11: Throughput versus data traffic load. (Beacon interval = 300 ms.)

Also, the naive CFPP-based protocol can deliver a throughput at least 2 times that of the grid quorum-based protocol when $4 \leq \lambda \leq 10$. Although the grid quorum-based and randomized coterie-based protocol have the same beacon transmission ratio and radio active ratio, the gap between their throughput performances is quite large when $3 \leq \lambda \leq 10$. This is mainly because, in the grid quorum-based protocol, transmitting a data frame to a PS station requires a prior ATIM/ATIM-ACK frame exchange; however, in the randomized coterie-based protocol, if source station perceives that the PS destination is currently in the fully-awake beacon interval, then it will directly issue the data frame via DCF without first performing an ATIM/ATIM-ACK frame exchange. By this way, we can reduce a significant control frame overheads especially when data load is heavy.

5.5.5 Energy-Based Throughput

The energy-based throughput is defined as the amount of successful data delivered per Joule of energy. It is obtained by dividing the total number of data frames successfully sent by total energy consumption over all stations during the entire simulation time. Using the energy-based throughput to judge the goodness of a power management protocol is much fairer than

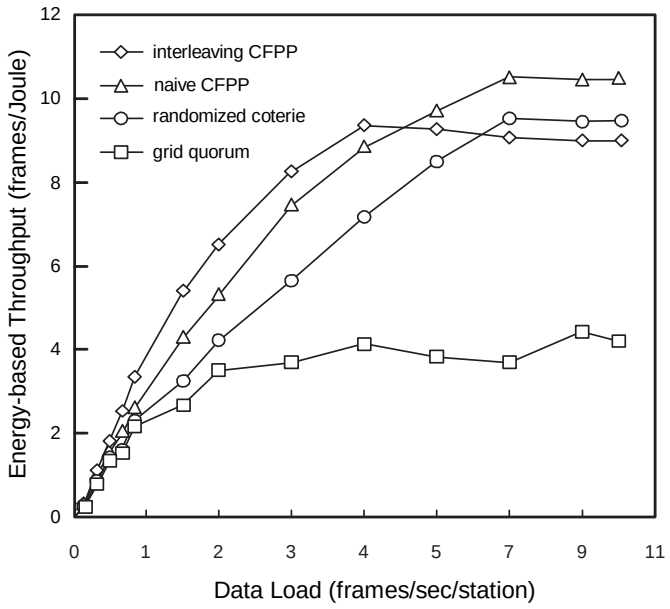

Figure 5.12: Energy-based throughput versus data traffic load. (Beacon interval = 300 ms.)

using the total energy consumption since some power management protocols may consume very little energy, but also achieve very little throughput. Figure 5.12 shows the energy-based throughput performances of different power management protocols under various data load when beacon interval = 300 ms. Comparing Figure 5.11 and Figure 5.12, we find an interesting phenomenon: the (time-based) throughput curves are very similar to the energy-based throughput curves especially for grid quorum-based, randomized coterie-based, and naive CFPP-based protocols. In Figure 5.12, we observe a 283.87% increase in the peak performance for naive CFPP-based protocol over the grid quorum-based protocol. This is because the grid quorum-based protocol consumes a great deal of energy in beacons and ATIM/ATIM-ACK traffic. We also notice that, when $\lambda \leq 4$, the interleaving CFPP-based protocol outperforms the naive CFPP-based protocol. This is because when data load is slight, almost all generated data frames can be successfully delivered both in naive and interleaving CFPP-based protocols. However, in this case, the radio active ratio of the interleaving CFPP-based protocol is only about half that of the naive CFPP-based protocol. Overall, the proposed power management protocols are superior to the grid quorum-based protocol.

5.6 Summary

Currently, IEEE 802.11 wireless LAN cards are greatly popular on the market. However, when IEEE 802.11 power management protocol operates in a large-scale ad hoc wireless network, it will face three severe challenges: beacon contention, clock synchronization, and reliable neighbor maintenance. To conquer all these challenges, we propose three novel asynchronous power management protocols, which consist of three key components: the scalable beacon transfer procedure, the energy-conserving neighbor maintenance procedure, and the data frame transfer procedure. The scalable beacon transfer procedure offer a high success probability of a beacon broadcast, regardless of the number of contending stations, thus alleviating the beacon contention problem significantly. The energy-conserving neighbor maintenance procedure ensures that any two PS neighbors are able to discover each other (via beacon frames) in finite time with high probability, no matter how much time their clocks drift away. The data frame transfer procedure specifies how a station send data to its neighbor operating in PS mode, provided that PS neighbor's beacon has already received.

Attractively, our power management protocols offer the network designers full flexibility in trading energy, latency, and accuracy versus each other by appropriately tuning system parameters. In comparison with the grid quorum-based protocol, our cyclic finite projective plane-based protocol also guarantees a 100% neighbor discovery probability while achieving a nearly 75% reduction in radio active ratio under about the same energy-delay product. Accordingly, the CFPP-based protocol is very suitable for energy-limited applications. Extensive simulation results do confirm that our schemes much outperform the grid quorum-based protocol especially in terms of time-based throughput and energy-based throughput. Above all, we believe that our protocols can be applied to the current IEEE 802.11 wireless LAN cards with only minor modifications.

Chapter 6

Conclusion and Future Work

The evolutionary advancement of radio technologies and the proliferation of portable devices has enabled the development of ubiquitous wireless networks, which can provide users in motion to easily and flexibly communicate with anyone at anytime in anywhere. However, a wireless mobile network is mainly characterized by energy-limited mobile stations, bandwidth-constrained radio links, and unpredictably dynamic topology changes; therefore, every algorithms and protocols developed on it will face many great challenges. In this dissertation, we propose several novel medium access control (MAC) protocols for infrastructure and ad hoc wireless networks. The first part (Chapter 2 $\sim$ Chapter 4) presents real-time MAC protocols. The second part (Chapter 5) presents the energy-conserving MAC designs.

In Chapter 2, on the basis of the DCB, we have proposed several different multi-channel broadcast algorithms for different network system environments. In contrast with single channel systems, the frame length is significantly reduced in multi-channel systems. With the support of GPS and the transceivers with tunable transmission power/range ability, the maximum tolerable network degree is also highly promoted. All our proposed algorithms are simple and easily implementable in a fully distributed manner. Network designers can decide which of the algorithms is preferred according to the given network resources. Most importantly, we guarantee that, for all our proposed protocols, there are no redundant transmission rounds in a frame. It implies that, in terms of bandwidth and energy consumption, our solutions reach the efficient performance.

One of the severe drawbacks of the proposed protocols is that they require priori knowl-

edge of some global network parameters, such as the maximum degree and the total number of mobile stations. However, these parameter values are extremely difficult (if not impossible) to obtain especially in a large-scale MANET. How to remove these unrealistic assumptions deserves further research.

In Chapter 3, we have proposed a hybrid MAC protocol, called the adaptive location-aware broadcast (ALAB) protocol, for link-level broadcast support in multi-channel systems. Since a MANET should operate in a physical area, it is very natural to exploit location information in such an environment. ALAB is scalable and topology-transparent since it does not maintain any link state information. Above all, in ALAB, both deadlock and hidden terminal problems are completely solved. In principle, ALAB tries to combine both of the advantages of the allocation- and contention-based protocols and overcomes their individual drawbacks. At high traffic or density, ALAB outperforms the pure TDMA because of spatial reuse and dynamic slot management. At low traffic or density, ALAB outperforms the pure CSMA/CA because of its embedded stable tree-splitting algorithms. In addition, ALAB provides deterministic access delay bounds from its base TDMA allocation protocol. Approximate throughput analyses for static ad hoc networks are provided. Simulation results do confirm the advantage of our scheme over other MAC protocols, such as IEEE 802.11, ADAPT, and ABROAD, even under the fixed-total-bandwidth model.

We believe that several future research problems can be stimulated by this work. One of the advantages of the ALAB protocol is that its success does not hinge on neighbor maintenance. On the other hand, IEEE 802.11 WLAN cards are currently popular on the market. How to tailor the IEEE 802.11 broadcast operation such that it can support MAC-level reliable broadcast without neighborhood knowledge deserves further research.

In Chapter 4, we have proposed a novel polling MAC protocol, named Q-PCF (quality-of-service PCF), which can coexist with IEEE 802.11 DCF, while providing QoS guarantees to real-time multimedia applications. Specifically, Q-PCF has the following attractive features. (i) It supports multiple priority levels and guarantees that high-priority stations always join the polling list earlier than low-priority stations. (ii) It provides fast reservation scheme such that real-time stations can get on the polling list in bounded time. (iii) It employs dynamic bandwidth allocation scheme to support CBR/VBR transportation and provide per-flow probabilistic performance assurances. (iv) It adopts the novel mobile-assisted admission

control technique such that the access point can admit as many newly flows as possible, while not violating admitted flows' guarantees. The performance of Q-PCF is evaluated via both analysis and simulations. (v) Simulation results do confirm that Q-PCF much outperforms PCF both in terms of goodput and frame delay dropped rate even under the heterogeneous traffic scenarios. Above all, we believe that the Q-PCF protocol can be easily applied to the current IEEE 802.11 products without major modifications.

We believe that several future research problems can be stimulated by this work. Recently, we witnessed the remarkably rapid installations of commercial infrastructure WLAN in entertainment or business environments, such as airports, convention centers, and fast food restaurants. Definitely, for wireless service providers, providing multiple levels of services to meet different QoS requirements of mobile customers is vital for the success of their business. How to design an appropriate pricing scheme based on the Q-PCF protocol (via parameters h, $\mathcal{G}$, or connection holding time) must be an interesting issue. For mathematical analysis, we have derived the closed-form of the throughput. How to derive the closed-form of the frame delay dropped rate is a challenging problem.

In Chapter 5, we have proposed new asynchronous power management protocols for large-scale ad hoc networks. The proposed protocols mainly contain three key components: scalable beacon transfer procedure, energy-conserving neighbor maintenance procedure, and directed data frame transfer procedure. The scalable beacon transfer procedure delivers a high success probability of beacon broadcast, thus alleviating the beacon contention problem significantly. The energy-conserving neighbor maintenance procedure allows a station to save a great deal of energy by periodically entering the doze state, while also allowing a PS station a high probability of discovering its neighbors even in a highly asynchronous MANET. The directed data frame transfer procedure specifies how a station sends a directed data frame to a PS neighbor. Since the PS station is not always active, the sending station has to predict when the PS destination will wake up and then initiates the ATIM/ATIM-ACK frame exchange or sends the data frame directly. Especially, our solutions offer the network designers full flexibility in trading energy, latency, and accuracy versus each other by appropriately tuning system parameters. As compared with the most energy-conserving protocol in [78], called the grid quorum-based protocol, our interleaving CFPP-based protocol also guarantees a 100% neighbor discovery probability while achieving a nearly 75% reduction

in radio active ratio under about the same energy-delay product. Consequently, our protocol is more suitable for energy-limited applications.

We believe that several future research problems could be stimulated by this work. Although the CFPP-based protocols perform quite well especially in terms of energy-based throughput, the length of the pattern repetition interval must be a power of a prime. How to remove this constraint while maintaining the same beacon transmission ratio or radio active ratio deserves further investigation. For mathematical analysis, we have derived the closed-form of the beacon transmission radio, radio active ratio, and neighbor discovery time. How to derive the closed-form of the energy-based throughput is a challenging problem.

Appendix

A Proof of Corollary 5.3.1

To prove Corollary 5.3.1, we claim that, when $k = \beta\sqrt{\mathcal{R}}$ and $\beta \geq 1$, the following inequality holds.

$$\frac{\binom{\mathcal{R}}{k}\binom{\mathcal{R}-k}{k} + \binom{\mathcal{R}}{1}\binom{\mathcal{R}-2}{k-1}\binom{\mathcal{R}-k-1}{k-1}}{\binom{\mathcal{R}}{k}\binom{\mathcal{R}}{k}} \leq (1+\beta^2)e^{-\beta^2}. \tag{A1}$$

For the proof, we take advantage of the following well-known results [53, 59].

Lemma A.1. For integers n, c, and i,

$$\frac{\binom{n-c}{c-i}}{\binom{n}{c}} \leq \left(\frac{c}{n}\right)^i \left(\frac{n-c}{n-i}\right)^{c-i}.$$

Lemma A.2. For every positive constant c ($0 < c < n$), the sequence $(1-\frac{c}{n})^n$ is monotonically increasing and

$$\lim_{n\to\infty}\left(1-\frac{c}{n}\right)^n = \frac{1}{e^c}.$$

Applying Lemmas A.1 and A.2 to the first term in the left hand side of (A1), we have

$$\frac{\binom{\mathcal{R}-k}{k}\binom{\mathcal{R}}{k}}{\binom{\mathcal{R}}{k}\binom{\mathcal{R}}{k}} \leq \left(\frac{\mathcal{R}-k}{\mathcal{R}}\right)^k = \left(1-\frac{\beta\sqrt{\mathcal{R}}}{\mathcal{R}}\right)^{\beta\sqrt{\mathcal{R}}} \leq e^{-\beta\sqrt{\mathcal{R}}\times\left(\frac{\beta\sqrt{\mathcal{R}}}{\mathcal{R}}\right)} = e^{-\beta^2}. \tag{A2}$$

On the other hand,

$$\begin{aligned}\frac{\binom{\mathcal{R}-k-1}{k-1}}{\binom{\mathcal{R}}{k}} = \frac{\binom{\mathcal{R}-k}{k-1}}{\binom{\mathcal{R}}{k}} \times \left(\frac{\mathcal{R}-2k+1}{\mathcal{R}-k}\right) &\leq \left(\frac{k}{\mathcal{R}}\right)\left(\frac{\mathcal{R}-k}{\mathcal{R}-1}\right)^{k-1}\left(\frac{\mathcal{R}-2k+1}{\mathcal{R}-k}\right) \\ &\leq \left(\frac{k}{\mathcal{R}}\right)\left(\frac{\mathcal{R}-k}{\mathcal{R}-1}\right)^{k}. \end{aligned} \tag{A3}$$

The first inequality in (A3) follows from Lemma A.1; the second inequality in (A3) is due to $\frac{\mathcal{R}-2k+1}{\mathcal{R}-k} \leq \frac{\mathcal{R}-2k+1+(k-1)}{\mathcal{R}-k+(k-1)} = \frac{\mathcal{R}-k}{\mathcal{R}-1}$. Combining (A3), Lemma A.2, and the fact that $\frac{\binom{\mathcal{R}-2}{k-1}}{\binom{\mathcal{R}}{k}} = \frac{k(\mathcal{R}-k)}{\mathcal{R}(\mathcal{R}-1)}$, we have

$$\frac{\binom{\mathcal{R}}{1}\binom{\mathcal{R}-2}{k-1}\binom{\mathcal{R}-k-1}{k-1}}{\binom{\mathcal{R}}{k}\binom{\mathcal{R}}{k}} \leq \frac{k^2}{\mathcal{R}} \times \left(\frac{\mathcal{R}-k}{\mathcal{R}-1}\right)^{k+1} \leq \frac{k^2}{\mathcal{R}} \times \left(e^{k-1}\right)^{\frac{k+1}{\mathcal{R}-1}} \leq \beta^2 e^{-\left(\frac{\beta^2\mathcal{R}-\beta^2}{\mathcal{R}-1}\right)} = \beta^2 e^{-\beta^2}. \tag{A4}$$

Consequently, (A2) and (A4) combined lead to the inequality (A1).

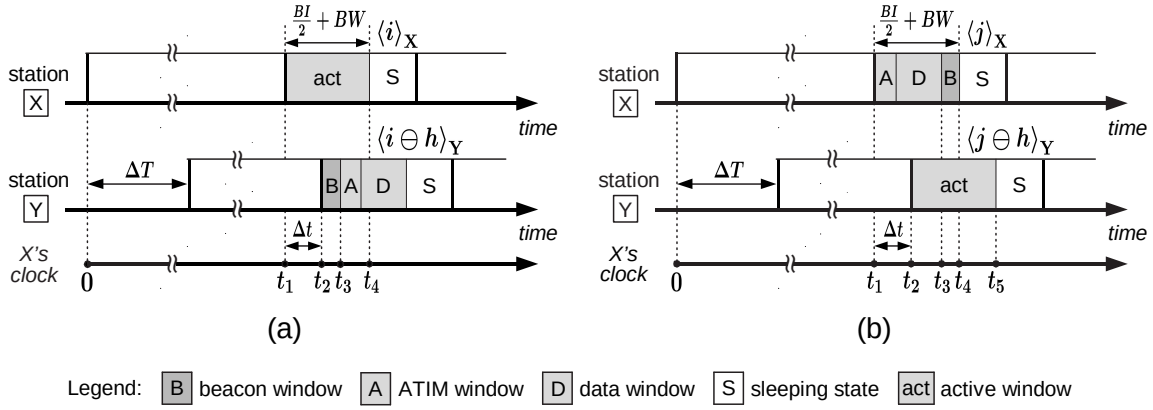

Figure B1: The case that $0 \leq \Delta t < \frac{BI}{2}$. (a) For PS station Y, one of its beacon windows in a forward pattern repetition is fully covered by the X's active window. (b) For PS station X, one of its beacon windows in a backward pattern repetition is fully covered by the Y's active window.

B Correctness of the Interleaving CFPP-based Protocol

We prove the correctness of the Interleaving CFPP-based protocol by showing that any two PS neighbors, X and Y, are able to discover each other, regardless of their clock difference. We assume that X and Y randomly choose two lines L_x and L_y respectively from the same CFPP $(U, \mathcal{L})$ as the set of their half-awake beacon intervals in a pattern repetition interval, and $\mathcal{R} = n^2 + n + 1$. Let $actW = \frac{BI}{2} + BW$. Without loss of generality, we can assume that X's clock is faster than Y's clock by $\Delta T = h \times BI + \Delta t$, where $0 \leq \Delta t < BI$ and $h \geq 0$ is an integer. In the following derivation, we use X's clock as a reference clock to derive Y's clock. We claim that at least one X's entire beacon window is fully covered by one Y's active window within two consecutive pattern repetition intervals, and vice versa. Note that other cases can be derived via the similar way. The analysis is divided into two cases.

Case 1: $0 \leq \Delta t < \frac{BI}{2}$. As illustrated in Figure B1(a), X can receive Y's beacons in Y's forward pattern repetition interval if and only if (i) both $\langle i \rangle_{\mathrm{X}}$ and $\langle i \ominus h \rangle_{\mathrm{Y}}$ are half-awake beacon intervals, for some $0 \leq i \leq \mathcal{R} - 1$, and (ii) the beacon window in $\langle i \ominus h \rangle_{\mathrm{Y}}$ begins later than the start of the active window in $\langle i \rangle_{\mathrm{X}}$, and terminates earlier than the end of the active window in $\langle i \rangle_{\mathrm{X}}$. In other words, $t_1 \leq t_2$ and $t_3 \leq t_4$. Since $L_x \cap \{-h \oplus L_y\} \neq \emptyset$, there must exist an element i such that $i \in L_x$ and $i \in \{-h \oplus L_y\}$. This implies that both $\langle i \rangle_{\mathrm{X}}$ and $\langle i \ominus h \rangle_{\mathrm{Y}}$ are half-awake beacon intervals. Without loss of generality, we can assume

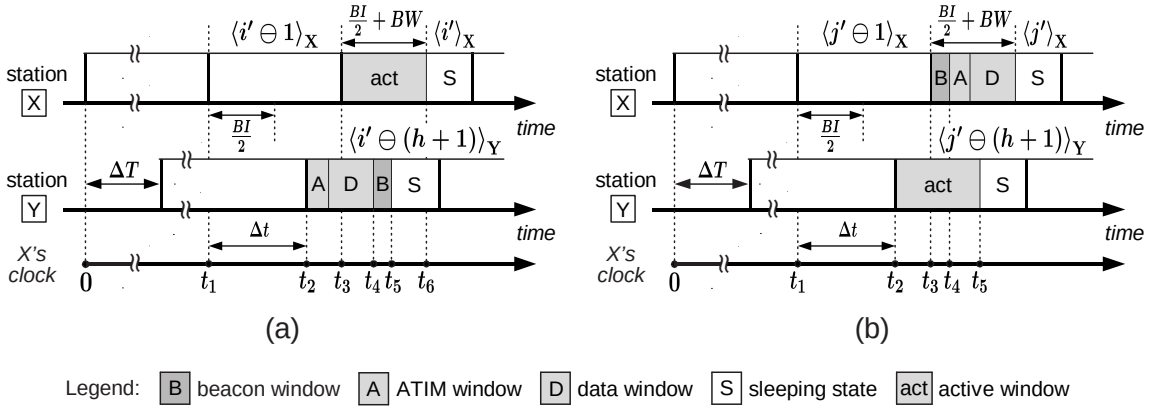

Figure B2: The case that $\frac{BI}{2} \leq \Delta t < BI$. (a) For PS station Y, one of its beacon windows in a backward pattern repetition is fully covered by the X's active window. (b) For PS station X, one of its beacon windows in a forward pattern repetition is fully covered by the Y's active window.

that $t_1 = a\mathcal{R} \times BI + (i-1) \times BI$, where $a \geq 0$ is an integer. Hence, $t_1 \leq t_1 + \Delta t = a\mathcal{R} \times BI + (i-1) \times BI + \Delta t = a\mathcal{R} \times BI + (i-h-1) \times BI + h \times BI + \Delta t = a\mathcal{R} \times BI + (i-h-1) \times BI + \Delta T = t_2$. In addition, $t_3 = t_2 + BW = a\mathcal{R} \times BI + (i-h-1) \times BI + \Delta T + BW = a\mathcal{R} \times BI + (i-h-1) \times BI + h \times BI + \Delta t + BW < a\mathcal{R} \times BI + (i-1) \times BI + (\frac{BI}{2} + BW) = t_4$.

On the other hand, as depicted in Figure B1(b), X's beacons can be received by Y in X's backward pattern repetition interval if and only if (i) both $\langle j \rangle_{\mathrm{X}}$ and $\langle j \ominus h \rangle_{\mathrm{Y}}$ are half-awake beacon intervals, for some $0 \leq j \leq \mathcal{R} - 1$, and (ii) the beacon window in $\langle j \rangle_{\mathrm{X}}$ begins later than the start of the active window in $\langle j \ominus h \rangle_{\mathrm{Y}}$, and terminates earlier than the end of the active window in $\langle j \ominus h \rangle_{\mathrm{Y}}$. That is, $t_2 \leq t_3$ and $t_4 \leq t_5$. Since $L_x \cap \{-h \oplus L_y\} \neq \emptyset$, there must exist an element j such that $j \in L_x$ and $j \in \{-h \oplus L_y\}$. This implies that both $\langle j \rangle_{\mathrm{X}}$ and $\langle j \ominus h \rangle_{\mathrm{Y}}$ are half-awake beacon intervals. Besides, $t_1 = b\mathcal{R} \times BI + (j-1) \times BI$, where $b \in \{a-1, a, a+1\}$. Hence, $t_2 = b\mathcal{R} \times BI + (j-h-1) \times BI + \Delta T = b\mathcal{R} \times BI + (j-h-1) \times BI + h \times BI + \Delta t < b\mathcal{R} \times BI + (j-1) \times BI + \frac{BI}{2} = t_3$. $t_4 = t_1 + \frac{BI}{2} + BW \leq t_1 + \frac{BI}{2} + BW + \Delta t = b\mathcal{R} \times BI + (j-1) \times BI + \frac{BI}{2} + BW + \Delta t = b\mathcal{R} \times BI + (j-h-1) \times BI + \frac{BI}{2} + BW + (h \times BI + \Delta t) = b\mathcal{R} \times BI + (j-h-1) \times BI + \frac{BI}{2} + BW + \Delta T = t_5$.

Case 2: $\frac{BI}{2} \leq \Delta t < BI$. Let $\Delta t = \frac{BI}{2} + \Delta d$ and $0 \leq \Delta d < \frac{BI}{2}$. As illustrated in Figure B2(a), X can receive Y's beacons in Y's backward pattern repetition interval if and only if

(i) both $\langle i' \rangle_{\mathrm{X}}$ and $\langle i' \ominus (h+1) \rangle_{\mathrm{Y}}$ are half-awake beacon intervals, for some $0 \leq i' \leq \mathcal{R}-1$, and (ii) the beacon window in $\langle i' \ominus (h+1) \rangle_{\mathrm{Y}}$ begins later than the start of the active window in $\langle i' \rangle_{\mathrm{X}}$, and terminates earlier than the end of the active window in $\langle i' \rangle_{\mathrm{X}}$. In other words, $t_3 \leq t_4$ and $t_5 \leq t_6$. Since $L_x \cap \{-(h+1) \oplus L_y\} \neq \emptyset$, there must exist an element i' such that $i' \in L_x$ and $i' \in \{-(h+1) \oplus L_y\}$. This implies that both $\langle i' \rangle_{\mathrm{X}}$ and $\langle i' \ominus (h+1) \rangle_{\mathrm{Y}}$ are half-awake beacon intervals. Besides, $t_1 = c\mathcal{R} \times BI + (i'-1) \times BI$, where $c \in \{a-1, a+1\}$. Hence, $t_3 = c\mathcal{R} \times BI + (i'-1) \times BI \leq c\mathcal{R} \times BI + (i'-1) \times BI + \Delta d = c\mathcal{R} \times BI + (i'-h-2) \times BI + (h \times BI + \frac{BI}{2} + \Delta d) + \frac{BI}{2} = c\mathcal{R} \times BI + (i'-1) \times BI + \Delta T + \frac{BI}{2} = t_4$. $t_5 = c\mathcal{R} \times BI + (i'-h-2) \times BI + \frac{BI}{2} + BW + \Delta T = c\mathcal{R} \times BI + (i'-h-2) \times BI + \frac{BI}{2} + BW + (h \times BI + \frac{BI}{2} + \Delta d) < c\mathcal{R} \times BI + (i'-1) \times BI + \frac{BI}{2} + BW = t_6$.

On the other hand, as depicted in Figure B2(b), X's beacons can be received by Y in X's forward pattern repetition interval if and only if (i) both $\langle j' \rangle_{\mathrm{X}}$ and $\langle j' \ominus (h+1) \rangle_{\mathrm{Y}}$ are half-awake beacon intervals, for some $0 \leq j' \leq \mathcal{R}-1$, and (ii) the beacon window in $\langle j' \rangle_{\mathrm{X}}$ begins later than the start of the active window in $\langle j' \ominus (h+1) \rangle_{\mathrm{Y}}$, and concludes earlier than the end of the active window in $\langle j' \ominus (h+1) \rangle_{\mathrm{Y}}$. That is, $t_2 \leq t_3$ and $t_4 \leq t_5$. Since $L_x \cap \{-(h+1) \oplus L_y\} \neq \emptyset$, there must exist an element j' such that $j' \in L_x$ and $j' \in \{-(h+1) \oplus L_y\}$. This implies that both $\langle j' \rangle_{\mathrm{X}}$ and $\langle j' \ominus (h+1) \rangle_{\mathrm{Y}}$ are half-awake beacon intervals. Besides, $t_1 = d\mathcal{R} \times BI + (j'-1) \times BI$, where $d \in \{a-1, a, a+1\}$. Thus, $t_2 = d\mathcal{R} \times BI + (j'-h-2) \times BI + \Delta T = d\mathcal{R} \times BI + (j'-h-2) \times BI + (h \times BI + \Delta t) < d\mathcal{R} \times BI + (j'-h-2) \times BI + h \times BI + BI = d\mathcal{R} \times BI + (j'-1) \times BI = t_3$. $t_4 = t_3 + BW \leq t_3 + BW + \Delta d = d\mathcal{R} \times BI + (j'-1) \times BI + BW + \Delta d = d\mathcal{R} \times BI + (j'-h-2) \times BI + \frac{BI}{2} + BW + (h \times BI + \frac{BI}{2} + \Delta d) = d\mathcal{R} \times BI + (j'-h-2) \times BI + \frac{BI}{2} + BW + \Delta T = t_5$.

C Derivations of Equations (4.2) and (4.3)

The authors in [1, 72, 73] assume that the bit-rate value of a VBR source in a certain holding duration is a truncated exponential random variable X with parameter γ. In this case, the probability density function of X can be written as

$$f(x) = \begin{cases} e^{\frac{\alpha - x}{\gamma}} \left[\gamma \left(1 - e^{\frac{\alpha - \beta}{\gamma}} \right) \right]^{-1} & \text{if } \alpha \leq x \leq \beta, \\ 0 & \text{otherwise.} \end{cases} \tag{C1}$$

Since (i) $f(x) \geq 0$ for all x, and (ii) $\int_{\alpha}^{\beta} f(x)dx = 1$, $f(x)$ is indeed a probability density function. Especially, when $\alpha = 0$ and $\beta = \infty$, X is reduce to the conventionally exponential random variable. Let $\mathcal{C} = \left[1 - e^{\frac{\alpha-\beta}{\gamma}}\right]^{-1}$, we obtain

$$E[X] = \mathcal{C} \int_{\alpha}^{\beta} \frac{1}{\gamma} x e^{\frac{\alpha-x}{\gamma}} dx. \tag{C2}$$

Integrating by parts yields

$$\mu = E[X] = \mathcal{C} \left(-x e^{\frac{\alpha-x}{\gamma}} \Big|_{\alpha}^{\beta} \right) + \mathcal{C} \int_{\alpha}^{\beta} e^{\frac{\alpha-x}{\gamma}} dx = \gamma + \frac{\alpha - \beta \times e^{\frac{\alpha-\beta}{\gamma}}}{1 - e^{\frac{\alpha-\beta}{\gamma}}}. \tag{C3}$$

Equation (4.3) is thus proven.

Now, given $0 \leq \varepsilon < 1$, we want to find the value g such that $\Pr[\alpha \leq X \leq g] \geq 1 - \varepsilon$. By using equation (C1), we have $\Pr[\alpha \leq X \leq g] = \int_{\alpha}^{g} f(x)dx = 1 - \varepsilon$. After simple calculus and algebraic manipulation, we can obtain

$$g = \alpha - \gamma \ln \left(\varepsilon + (1 - \varepsilon) e^{\frac{\alpha-\beta}{\gamma}} \right). \tag{C4}$$

Thus if a VBR station desires that its bandwidth demand during each CFP can be satisfied with probability at least $1 - \varepsilon$, that station shall specify $\mathcal{G} = g \times \frac{\mathrm{SF}}{\mathrm{CDR}}$ (equation (4.2)) during the registration period.

Bibliography

[1] I. F. Akyildiz, D. A. Levine, and I. Joe. A Slotted CDMA Protocol with BER Scheduling for Wireless Multimedia Networks. *IEEE Transactions on Networking*, Vol. 7, No. 2, pp. 146–158, April 1999.

[2] G. Anastasi, L. Lenzini, and E. Mingozzi. HIPERLAN/1 MAC Protocol: Stability and Performance Analysis. *IEEE Journal on Selected Areas in Communications*, Vol. 18, No. 9, pp. 1787–1798, September 2000.

[3] R. Bar-Yehuda, O. Goldreich, and A. Itai. On the Time-Complexity of Broadcast in Multihop Radio Networks: An Exponential Gap Between Determinism and Randomization. *Journal of Computer and Systems Sciences*, Vol. 45, pp. 104–126, August, 1992.

[4] S. Basagni, D. Bruschi, and I. Chlamtac. A Mobility-Transparent Deterministic Broadcast Mechanism for Ad Hoc Networks. *IEEE/ACM Transactions on Networking*, Vol. 7, No. 6, pp. 799–807, December, 1999.

[5] D. Bertsekas and R. Gallager. *Data Networks, Second Edition*, Prentice-Hall, 1992.

[6] Giuseppe Bianchi. Performance Analysis of the IEEE 802.11 Distributed Coordination Function. *IEEE Journal on Selected Areas in Communications*, Vol. 18, No. 3, pp. 535–547, March 2000.

[7] F. Cali, M. Conti, and E. Gregori. IEEE 802.11 Protocol: Design and Performance Evaluation of an Adaptive Backoff Mechanism. *IEEE Journal on Selected Areas in Communications*, Vol. 18, No. 9, pp. 1774–1786, September 2000.

[8] A. Chandra, V. Gummalla, and J. O. Limb. Wireless Medium Access Control Protocols. *IEEE Communications Surveys*, pp. 2–15, Second Quarter, 2000.

[9] C. F. Chiasserini and R. R. Rao. A Distributed Power Management Policy for Wireless Ad Hoc Networks. *IEEE Wireless Communication and Networking Conference*, pp. 1209–1213, September 2000.

[10] I. Chlamtac and A. Faragó. An Optimal Channel Access Protocol with Multiple Reception Capacity. *IEEE Transactions on Computers*, Vol. 43, No. 4, pp. 480–484, April, 1994.

[11] I. Chlamtac, A. Faragó, A. D. Myers, V. R. Syrotiuk, and G. Záruba. ADAPT: A Dynamically Self-Adjusting Media Access Control Protocol for Ad Hoc Networks. *Global Telecommunications Conference - GLOBECOM '99*, Vol. 1A, pp. 11–15, 1999.

[12] I. Chlamtac and S. Kutten. Tree-Based Broadcasting in Multihop Radio Networks. *IEEE Transactions on Computers*, Vol. C-36, pp. 1209–1223, October, 1987.

[13] I. Chlamtac, A. D. Myers, V. R. Syrotiuk, and G. Záruba. An Adaptive Medium Access Control (MAC) Protocol for Reliable Broadcast in Wireless Networks. *IEEE International Conference on Communications*, Vol. 3, pp. 1692–1696, 2000.

[14] I. Chlamtac and O. Weinstein. The Wave Expansion Approach to Broadcasting in Multihop Radio Networks. *IEEE Transactions on Communications*, Vol. 39, No. 3, pp. 426–433, March, 1991.

[15] Sunghyun Choi. Emerging IEEE 802.11e WLAN for Quality-of-Service (QoS) Provisioning. *SK Telecom Telecommunications Review*, Vol. 12, No. 6, pp. 894–906, December 2002.

[16] S. Choi and K. G. Shin. A Unified Wireless LAN Architecture for Real-Time and Non-Real-Time Communication Services. *IEEE/ACM Transactions on Networking*, Vol. 8, No. 1, pp. 44–59, February 2000.

[17] Zi-Tsan Chou, Y.-C. Deng, C.-C. Hsu, and F.-C. Lin. Bandwidth-Efficient, Mobility Transparent Deterministic Broadcasting for Multi-channel Ad-Hoc Networks. *International Conference on Wireless Networks* (ICWN'02), Las Vegas, USA., June 24–27, 2002. [Online] http://www.ece.queensu.ca/hpages/faculty/yeh/program.txt

[18] Zi-Tsan Chou, C.-C. Hsu, and F.-C. Lin. An Adaptive Location-Aware MAC Protocol for Multichannel Multihop Ad-Hoc Networks. *Networking 2002*, Lecture Notes in Computer Science, No. 2345, pp. 399–410, May 2002.

[19] Zi-Tsan Chou, C.-C. Hsu, and F.-C. Lin. Asynchronous Power Management Protocols for IEEE 802.11 Ad Hoc Wireless Networks. *Technical Report*. National Taiwan University. June 2003.

[20] Zi-Tsan Chou, C.-C. Hsu, and F.-C. Lin. A New Quality-of-Service Point Coordination Function for IEEE 802.11 Wireless Multimedia LANs. *Technical Report*. National Taiwan University. June 2003.

[21] C. Coutras, S. Gupta, and N. B. Shroff. Scheduling of Real-Time Traffic in IEEE 802.11 Wireless LANs. *ACM/Baltzer Wireless Networks*, Vol. 6, pp. 457–466, 2000.

[22] D.-J. Deng and R.-S. Chang. A Priority Scheme for IEEE 802.11 DCF Access Method. *IEICE Transactions on Communications*, pp. 96–102, January 1999.

[23] Y.-C. Deng, Zi-Tsan Chou, F.-C. Lin, and C.-C. Hsu. An Improved Mobility-Transparent Deterministic Broadcast Algorithm for Single Channel Ad-Hoc Networks. *International Symposium on Communications*, Tainan, Taiwan, Nov. 13–16, 2001.

[24] G. Dommety and R. Jain. Potential Networking Applications of Global Positioning Systems (GPS). *Techical Report. TR-24*, CS Department, The Ohio State University, April 1996.

[25] A. Faragó, I. Chlamtac, and H. Y. Ahn. Nearly Optimum Scheduling in Mobile CDMA Packet Radio Networks. *IEEE Military Communications Conference*, Vol. 2, pp. 769–773, 1992.

[26] L. M. Feeney. An Energy Consumption Model for Performance Analysis of Routing Protocols for Mobile Ad Hoc Networks. *ACM/Kluwer Mobile Networks and Applications*, Vol. 6, pp. 239–249, 2001.

[27] M. Fischer. QoS Baseline Proposal. *IEEE Document*, IEEE 802.11-00/360. [Online] http://grouper.ieee.org/groups/802/11/Documents

[28] I. Gaber and Y. Mansour. Broadcast in Radio Networks. *6th Annual ACM/SIAM Symposium on Discrete Algorithms*, pp. 577–585, January, 1995.

[29] A. Ganz, A. Phonphoem, and Z. Ganz. Robust SuperPoll with Chaining Protocol for IEEE 802.11 Wireless LANs in Support of Multimedia Applications. *ACM/Kluwer Wireless Networks*, Vol. 7, pp. 65–73, 2001.

[30] R. Garcés. Collision Avoidance and Resolution Multiple Access. *Ph.D. Dissertation*, Computer Engineering, University of California, Santa Cruz, CA 95064, March 1999.

[31] R. Garcés and J.J. Garcia-Luna-Aceves. Collision Avoidance and Resolution Multiple Access with Transmission Queues. *ACM/Kluwer Wireless Networks*, Vol. 5, pp. 95–109, 1999.

[32] R. Garcés and J.J. Garcia-Luna-Aceves. Collision Avoidance and Resolution Multiple Access for Multi-Channel Wireless Networks. *Proceedings of IEEE INFOCOM*, pp. 595–602, 2000.

[33] J.J. Garcia-Luna-Aceves and J. Raju. Distributed Assignment of Codes for Multihop Packet-Radio Networks. *IEEE Military Communications Conference*, Vol. 1, pp. 450–454, 1997.

[34] H. Garcia-Molina and D. Barbara. How to Assign Votes in a Distributed System. *Journal of the ACM*, Vol. 32, No. 4, pp. 841–860, October 1985.

[35] Matthew S. Gast. *802.11 Wireless Networks: The Definitive Guide*, O'Reilly & Associates, Inc., 2002.

[36] Z. J. Haas and M. R. Perlman. ZRP: A Hybrid Framework for Routing in Ad Hoc Networks. *Ad Hoc Networking*, editor C. E. Perkins, Chapter 7, Addison-Wesley Inc., pp. 221–253, 2001.

[37] T.-C. Hou and T.-J. Tsai. An Access-Based Clustering Protocol for Multihop Wireless Ad Hoc Networks. *IEEE Journal on Selected Areas in Communications*, Vol. 19, No. 7, pp. 1201–1210, July, 2001.

[38] L. Huang and T-.H. Lai. On the Scalability of IEEE 802.11 Ad Hoc Networks. *ACM International Symposium on Mobile Ad Hoc Networking and Computing (MobiHoc 2002)*, pp. 173–182, June 2001.

[39] J. Jiang, T.-H. Lai, and N. Soundarajan. On Distributed Dynamic Channel Allocation in Mobile Cellular Networks. *IEEE Transactions on Parallel and Distributed Systems*, Vol. 13, No. 10, pp. 1024–1037, October, 2002.

[40] M. Joa-Ng and I-T. Lu. A Peer-to-Peer Zone-Based Two-Level Link State Routing for Mobile Ad Hoc Networks. *IEEE Journal on Selected Areas in Communications*, Vol. 7, No. 8, pp. 1415–1425, August, 1999.

[41] J.-H. Ju and V. O. K. Li. TDMA Scheduling Design of Multihop Packet Radio Networks Based on Latin Squares. *IEEE Journal on Selected Areas in Communications*, Vol. 7, No. 8, pp. 1345–1352, August, 1999.

[42] J. Y. Juang and B. W. Wah. Unified Window Protocols for Contention Resolution in Local Multiaccess Networks. *IEEE INFOCOM*, pp. 97–104, April 1984.

[43] E.-S. Jung and N. Vaidya. An Energy Efficient MAC Protocol for Wireless LANs. *IEEE INFOCOM*, 2002.

[44] S. Keshav. *An Engineering Approach to Computer Networking: ATM Networks, the Internet, and the Telephone Network*. Addison-Wesley Publishing Company, 1997.

[45] I. Koutsopoulos, D. Connors, A. Savvides, and S. K. Dao. Intra-Team Multi-Hop Broadcasting (ITMB): A MAC Layer Protocol for Efficient Control Signaling in Wire-

less Ad-Hoc Networks. *IEEE International Conference on Communications*, Vol. 3, pp. 1723–1727, December, 2000.

[46] J. Kuri and S. K. Kasera. Reliable Multicast in Multi-Access Wireless LANs. *ACM/Kluwer Wireless Networks*, Vol. 7, pp. 359–369, 2001.

[47] E. Kushilevitz and Y. Mansour. An $\Omega(D \log(N/D))$ Lower Bound for Broadcast in Radio Networks. *SIAM Journal on Computing*, Vol. 27, pp. 702–712, June, 1998.

[48] LAN MAN Standards Committee of the IEEE Computer Society. *IEEE Standard 802.11-1999 Wireless LAN Medium Access Control (MAC) and Physical Layer (PHY) Specifications.* IEEE, November 1999.

[49] LAN MAN Standards Committee of the IEEE Computer Society. *IEEE 802.11e/D3.2, Draft Supplement to Part 11: Wireless Medium Access Control (MAC) and physical layer (PHY) specifications: Medium Access Control (MAC) Enhancements for Quality of Service (QoS).* IEEE, August 2002.

[50] Averill M. Law and W. David Kelton. *Simulation Modeling and Analysis, Third Edition*, McGrraw-Hill Book Company Inc., 2000.

[51] C. Lee, J. E. Burns, and M. H. Ammar. Improved Randomized Broadcast Protocols in Multi-Hop Radio Networks. *IEEE International Conference on Network Protocols*, pp. 234–241, October, 1993.

[52] S. Lindsey, C. Raghavendra, and K. M. Sivalingam. Data Gathering Algorithms in Sensor Networks Using Energy Metrics. *IEEE Transactions on Parallel and Distributed Systems*, Vol. 13, No. 9, pp. 924–935, September 2002.

[53] D. Malkhi, M. Reiter, A. Wool, and R. N. Wright. Probabilistic Quorum Systems. *Information and Computation*, Vol. 170, No. 2, pp. 184–206, November 2001.

[54] M. K. Marina, G. D. Kondylis, and U. C. Kozat. RBRP: A Robust Broadcast Reservation Protocol for Mobile Ad Hoc Networks. *IEEE International Conference on Communications*, Vol. 3, pp. 878–885, 2001.

[55] Marshall Hall, Jr. *Combinatorial Theory, Second Edition*. A Wiley-Interscience Publication, John Wiley & Sons, Inc., 1998.

[56] Jiři Matoušek and Jaroslav Nešetřil. *Invitation to Discrete Mathematics*. Oxford University Press Inc., New York, 1998.

[57] M. J. McGlynn and S. A. Borbash. Birthday Protocols for Low Energy Deployment and Flexible Neighbor Discovery in Ad Hoc Wireless Networks. *ACM/IEEE International Conference on Mobile Computing and Networking (MobiCom 2001)*, pp. 137–145, July 2001.

[58] P. Merlin and A.Segall. A Failsafe Distributed Routing Protocol. *IEEE Transactions on Communications*, Vol. COM-27, pp. 1280–1287, September, 1979.

[59] K. Nakano and S. Olariu. Randomized Initialization Protocols for Ad Hoc Networks. *IEEE Transactions on Parallel and Distributed Systems*, Vol. 11, No. 7, pp. 749–759, July, 2000.

[60] S. Ni, Y.-C. Tseng, and J.-P. Sheu. The Broadcast Storm Problem in a Mobile Ad Hoc Network. *ACM/IEEE International Conference on Mobile Computing and Networking*, pp. 151–162, 1999.

[61] Charles E. Perkins. *Ad Hoc Networking*, Addison-Wesley Publishing Company, Inc., 2001.

[62] V. Rodoplu and T. H. Meng. Position Based CDMA with Multiuser Detection (P-CDMA/MUD) for Wireless Ad Hoc Networks. *IEEE 6th Symposium on Spread-Spectrum Techniques and Applications*, 2000.

[63] S. Ross. *A First Course in Probability, Fifth Edition*. Prentice-Hall, Inc., 1998.

[64] A. K. Salkintzis and C. Chamzas. An In-Band Power-Saving Protocol for Mobile Data Networks. *IEEE Transactions on Communications*, Vol. 46, pp. 1194–1205, September 1999.

[65] Jochen Schiller. *Mobile Communications*. Addison-Wesley, Inc., 2000.

[66] O. Sharon and E. Altman. An Efficient Polling MAC for Wireless LANs. *IEEE/ACM Transactions on Networking*, Vol. 9, No. 4, pp. 439–451, August 2001.

[67] C. Schurgers, V. Tsiatsis, S. Ganeriwal, and M. Srivastava. Optimizing Sensor Networks in the Energy-Latency-Density Design Space. *IEEE Transactions on Mobile Computing*, Vol. 1, No. 1, pp. 70–80, Janunary–March 2002.

[68] C. Schurgers, V. Tsiatsis, and M. Srivastava. STEM: Topology Management for Energy Efficient Sensor Networks. *IEEE Aerospace Conference 2002*, pp. 10–15, March 2002.

[69] A. Segall and M. Sidi. A Failsafe Distributed Routing Protocol for Minimum Delay Routing. *IEEE Transactions on Communications*, Vol. COM-29, pp. 689–695, May, 1981.

[70] A. Sen and M. L. Huson, A New Model for Scheduling Packet Radio Networks. *ACM/Kluwer Wireless Networks*, Vol. 3, pp. 71–82, 1997.

[71] Ching-Kuang Shene. *Selections of 100 Famous Algorithms: Problem Solving Using C*, Chinese Version, Scholars Books, Inc., 1990.

[72] J.-P. Sheu, C.-H. Liu, S.-L. Wu, and Y.-C. Tseng. A Priority MAC Protocol to Support Real-Time Multimedia Traffic in Ad Hoc Networks. *ACM/Kluwer Wireless Networks*, to appear, 2003.

[73] S.-T. Sheu and T.-F. Sheu. A Bandwidth Allocation/Sharing/Extension Protocol for Multimedia Over IEEE 802.11 Ad Hoc Wireless LANs. *IEEE Journal on Selected Areas in Communications*, Vol. 19, No. 10, pp. 2065–2080, October 2001.

[74] A. Silberschatz and P. B. Galvin. *Operating System Concepts, Fourth Edition*. Addison-Wesley Publishing Company, 1994.

[75] J. L. Sobrinho and A. S. Krishnakumar. Quality-of-Service in Ad Hoc Carrier Sense Multiple Access Wireless Networks. *IEEE Journal on Selected Areas in Communications*, Vol. 17, No. 8, pp. 1353–1368, August 1999.

[76] Z. Tang and J.J. Garcia-Luna-Aceves. A Protocol for Topology-Dependent Transmission Scheduling in Wireless Networks. *IEEE Wireless Communications and Networking Conference*, Vol. 3, pp. 1333–1337, 1999.

[77] Y. C. Tay and K. C. Chua. A Capacity Analysis for the IEEE 802.11 MAC Protocol. *ACM/Kluwer Wireless Networks*, Vol. 7, pp. 159–171, 2001.

[78] Y.-C. Tseng, C.-S. Hsu, and T.-Y. Hsieh. Power-Saving Protocols for IEEE 802.11-Based Multi-Hop Ad Hoc Networks. *IEEE INFOCOM*, pp. 200–209, 2002.

[79] Y.-C. Tseng, S.-Y. Ni, and E.-Y. Shih. Adaptive Approaches to Relieving Broadcast Storms in a Wireless Multihop Mobile Ad Hoc Network. *International Conference on Distributed Computing Systems*, pp. 481–488, 2001.

[80] Y.-C. Tseng, S.-L. Wu, C.-M. Chao, and J.-P. Sheu. Location-Aware Channel Assignment for a Multi-Channel Mobile Ad Hoc Network. *ICS2000 Workshop on Computer Networks, Internet, and Multimedia*, 2000.

[81] H. Woesner, J.P. Ebert, M. Schlager, and A. Wolisz. Power-Saving Mechanisms in Emerging Standards for Wireless LANs: the MAC Level Perspective. *IEEE Personal Communications*, pp. 40–48, June 1998.

[82] S.-L. Wu, C.-Y. Lin, Y.-C. Tseng, and J.-P. Sheu. A New Multi-Channel MAC Protocol with On-Demand Channel Assignment for Mobile Ad Hoc Networks. *International Symposium on Parallel Architectures, Algorithms and Networks*, pp. 232–237, 2000.

[83] C. Zhu and M. Corson. A Five-Phase Reservation Protocol (FPRP) for Mobile Ad Hoc Networks. *ACM/Kluwer Wireless Networks*, Vol. 7, pp. 371–384, 2001.